

# Higgs Phases and Boundary Criticality

Kristian Tyn Kai Chung<sup>1\*</sup>, Rafael Flores-Calderón<sup>1,2</sup>, Rafael C. Torres<sup>3</sup>, Pedro Ribeiro<sup>3</sup>  
Sergej Moroz<sup>4,5</sup> Paul McClarty<sup>1,6</sup>

<sup>1</sup> Max Planck Institute for the Physics of Complex Systems, Dresden, Germany

<sup>2</sup> Max Planck Institute for Chemical Physics of Solids, Dresden, Germany

<sup>3</sup> CeFEMA, LaPMET, Instituto Superior Técnico, Universidade de Lisboa, Lisboa, Portugal

<sup>4</sup> Department of Engineering and Physics, Karlstad University, Karlstad, Sweden

<sup>5</sup> Nordita, KTH Royal Institute of Technology and Stockholm University, Stockholm, Sweden

<sup>6</sup> Laboratoire Léon Brillouin, CEA, CNRS, Université Paris-Saclay, CEA Saclay, Gif-sur-Yvette, France

\* [ktchung@pks.mpg.de](mailto:ktchung@pks.mpg.de)

## Abstract

Motivated by recent work connecting Higgs phases to symmetry protected topological (SPT) phases, we investigate the interplay of gauge redundancy and global symmetry in lattice gauge theories with Higgs fields in the presence of a boundary. The core conceptual point is that a global symmetry associated to a Higgs field, which is pure-gauge in a closed system, acts physically at the boundary under boundary conditions which allow electric flux to escape the system. We demonstrate in both Abelian and non-Abelian models that this symmetry is spontaneously broken in the Higgs regime, implying the presence of gapless edge modes. Starting with the U(1) Abelian Higgs model in 4D, we demonstrate a boundary phase transition in the 3D XY universality class separating the bulk Higgs and confining regimes. Varying the boundary coupling while preserving the symmetries shifts the location of the boundary phase transition. We then consider non-Abelian gauge theories with fundamental and group-valued Higgs matter, and identify the analogous non-Abelian global symmetry acting on the boundary generated by the total color charge. For SU( $N$ ) gauge theory with fundamental Higgs matter we argue for a boundary phase transition in the O( $2N$ ) universality class, verified numerically for  $N = 2, 3$ . For group-valued Higgs matter, the boundary theory is a principal chiral model exhibiting chiral symmetry breaking. We further demonstrate this mechanism in theories with higher-form Higgs fields. We show how the higher-form matter symmetry acts at the boundary and can spontaneously break, exhibiting a boundary confinement-deconfinement transition. We also study the electric-magnetic dual theory, demonstrating a dual magnetic defect condensation transition at the boundary. We discuss some implications and extensions of these findings and what they may imply for the relation between Higgs and SPT phases.

Copyright attribution to authors.

This work is a submission to SciPost Physics.

License information to appear upon publication.

Publication information to appear upon publication.

Received Date

Accepted Date

Published Date

1

## 2 Contents

### 3 1 Introduction

3

4	<b>2</b>	<b>Boundary Symmetry Breaking in Abelian Higgs Models</b>	<b>5</b>
5	2.1	Preliminaries: Lattice Formulation	6
6	2.1.1	Action Formulation	6
7	2.1.2	Hamiltonian Formulation and Gauss Law	7
8	2.1.3	Magnetic Monopoles	8
9	2.2	Open Boundaries and Global Symmetry	8
10	2.3	Boundary Symmetry Breaking in the Abelian Higgs Model	10
11	2.3.1	Boundary XY Model at Infinite $\kappa$	11
12	2.3.2	Boundary Phase Transition at Finite $\kappa$	11
13	2.3.3	Tuning the Boundary Coupling	12
14	2.4	Summary and Discussion: Abelian Case	13
15	<b>3</b>	<b>Boundary Symmetry Breaking in Non-Abelian Higgs Models</b>	<b>14</b>
16	3.1	Preliminaries: Lattice Formulation	14
17	3.1.1	Higgs Fields	15
18	3.1.2	Hamiltonian Formulation and Gauss Law	15
19	3.1.3	Open Boundaries and Global Symmetry	17
20	3.2	Boundary Symmetry Breaking in the SU(2) Higgs Model	19
21	3.2.1	Bulk Phase Diagram	19
22	3.2.2	Boundary Symmetry Breaking	20
23	3.2.3	Tuning the Boundary Coupling	22
24	3.3	Boundary Symmetry Breaking in Non-Abelian Group-Valued Higgs Models	23
25	3.4	Boundary Symmetry Breaking in Non-Abelian Fundamental-Higgs Models	24
26	3.4.1	Gauge-Invariant Resolution of the Infinite Kappa Limit	24
27	3.4.2	Formulation for General Gauge Groups	26
28	3.4.3	Hamiltonian Perspective	26
29	3.5	Boundary Phase Transition Order and Universality Class	27
30	3.5.1	Group-Valued Higgs	27
31	3.5.2	Fundamental Higgs	27
32	3.5.3	Fate of the Un-Higgsed Subgroup: SU(3) Numerical Results	28
33	3.6	Summary and Discussion: Non-Abelian Case	29
34	<b>4</b>	<b>Boundary Symmetry Breaking in Higher-Form Abelian Higgs Models</b>	<b>31</b>
35	4.1	Higher-Form Abelian Higgs Models	31
36	4.1.1	Gauss Law and Matter Symmetry	32
37	4.1.2	Open Boundaries and Global Matter Symmetry	34
38	4.1.3	Boundary Symmetry Breaking	35
39	4.2	Electric-Magnetic Dual Picture	38
40	4.2.1	Open Boundary Duality Transformation	38
41	4.2.2	Dual Boundary Symmetry Breaking	41
42	4.3	Summary and Discussion: Higher-Form Case	42
43	<b>5</b>	<b>Discussion and Conclusion</b>	<b>44</b>
44	5.1	Summary and Outlook	44
45	5.2	Higgs = SPT	45
46	5.2.1	Review of Higgs=SPT	45
47	5.2.2	Insights, Challenges, and Future Directions	47
48	<b>A</b>	<b>Discrete Differential Calculus for Abelian Fields</b>	<b>48</b>
49	<b>B</b>	<b>U(1) Bulk Phase Diagram: Limits, Symmetries and Monte Carlo</b>	<b>51</b>

51

52

53 **1 Introduction**

54 Gauge fields and gauge invariance have a long and complex history in theoretical physics,  
55 deeply interwoven with the advent of quantum field theory, the formulation of the Standard  
56 Model of particle physics, and firmly embedded in the modern theory of quantum many body  
57 systems. In fundamental physics, gauge theories arise naturally in Lorentz covariant theories  
58 of massless particles where they resolve a mismatch between the physical degrees of freedom  
59 admitted by the Wigner little group—such as photon polarizations—and the vector potential  
60 used to describe the particle states. This is accomplished by rendering the surplus degrees of  
61 freedom redundant. As such they arise naturally in field theories of gravity, nuclear forces and  
62 electromagnetism. In condensed matter physics, gauge fields play a key role in describing a  
63 plethora of physical phenomena including highly-entangled emergent states of matter such as  
64 spin liquids and fractional quantum Hall fluids.

65 The redundancy inherent to gauge theories leads to important subtleties. In particular,  
66 while the theories are local, the physical gauge-invariant objects are non-local Wegner-Wilson  
67 string loops [1,2]. This implies a tension in describing the spontaneous breaking of symmetries  
68 in the presence of dynamical gauge fields. Whereas many condensed matter systems demon-  
69 strate symmetry lowering phase transitions governed by spontaneous breaking of a global sym-  
70 metry, gauge redundancy, being unphysical, cannot be broken. This fact, enshrined in Elitzur’s  
71 theorem [3], belies a rich landscape of different phases separated by phase transitions whose  
72 study began systematically in the 1970s—confined, deconfined, Higgs, topologically ordered,  
73 etc. While Landau theory successfully accounts for a broad range of phase transitions in cor-  
74 related many-body systems, the order parameters for theories with dynamical gauge fields  
75 are necessarily non-local, raising the question of how to understand the nature of the phase  
76 transitions in such theories. Recent advances generalizing notions of symmetries to higher-  
77 dimensional charged objects [4] allowed to extend the Landau paradigm to describe such  
78 phase transitions [5–7], for a review see [8].

79 The Anderson-Higgs mechanism [9–12], i.e. the condensation of charged scalar matter  
80 in gauge theories, is a cornerstone of physics. It plays a key role in our understanding of  
81 superconductivity phenomena and the nature of electroweak interactions within the Standard  
82 Model of particle physics. Two closely related questions about this mechanism have stood the  
83 test of time and continue to generate significant interest: First, what is the gauge-invariant  
84 order parameter characterizing Higgs phases [13]? Second, what is the distinction between  
85 the Higgs and confined phases [14]? Let us illustrate this with the 4D compact U(1) gauge  
86 theory, i.e. Maxwell theory with magnetic monopoles. In the pure gauge theory there is a  
87 deconfined phase at weak coupling in which static electric charges interact via a  $1/r$  Coulomb  
88 potential mediated by a gapless photon. At strong coupling, the proliferation of magnetic  
89 monopoles drives the system into the gapped confined phase, where static electric charges  
90 interact via a linearly rising potential. On the other hand, if we couple the gauge field to  
91 a charged scalar Higgs field, then the Higgs field may condense, driving a transition from  
92 the gapless deconfined phase to a gapped Higgs phase via the Anderson-Higgs mechanism.  
93 Can these two gapped regimes be distinguished, and if so by what order parameter? For a  
94 Higgs field in the fundamental representation of the gauge group, i.e. one carrying elementary  
95 charge, it is generally understood that the Higgs and confined regimes are actually the same

96 phase, i.e. they are not separated by any thermodynamic bulk phase transition [14, 15]. This  
97 Higgs-confinement continuity is believed to be true in generic models with a gauge group  $\mathcal{G}$   
98 coupled to a scalar Higgs field in the fundamental representation, including both discrete and  
99 continuous Abelian and non-Abelian gauge groups [14].

100 The question of whether there is a qualitative difference between these two regimes has  
101 been revisited time after time from many different perspectives [16]. To survey briefly the  
102 history of the endeavor to delineate these two regimes, one approach has been to perform  
103 a partial gauge fixing and observe symmetry breaking in an unfixed global subgroup, which  
104 shows a phase transition separating them, though the location of the transition line is gauge-  
105 dependent and thus lacks a clear physical meaning [17]. Other proposals seek to delineate  
106 them in the presence of global symmetries (whose realization is unaltered between the two  
107 regimes), see e.g. [18–20]. Yet another approach, advanced partially by one of the authors,  
108 emphasizes that (in a certain limit) Abelian Higgs phases with fundamental matter exhibit  
109 symmetry-protected topological (SPT) order [21–23]. This observation motivates the inves-  
110 tigation of the Higgs mechanism in open geometries, and zooms in on low-energy excita-  
111 tions localized near boundaries. In contrast to the confined regime, where the ground state is  
112 unique, in the Higgs regime previous studies uncovered energy spectrum degeneracies, see for  
113 example [21–23]. The robustness of these degeneracies originating from boundary-localized  
114 modes arises from the interplay of the protecting (generalized) symmetries that depends on  
115 the gauge group and dimensionality of the problem. In summary, the presence of a boundary  
116 introduces a criterion by which one can delineate the Higgs and confined regimes of Abelian  
117 gauge theories with fundamental matter—they are separated by a boundary phase transition.

118 In this paper we explore in detail boundary symmetry breaking in Wilson lattice gauge  
119 theories. We find that the Higgs-confinement boundary criticality mechanism is in fact ubiq-  
120 uitous. We begin in Section 2 by showing the presence of a boundary phase transition in the  
121 4D  $U(1)$  Abelian Higgs model, where the magnetic one-form symmetry is broken explicitly.  
122 We discuss how, in the presence of boundaries which allow flux but not charge to exit the  
123 system, there is a bulk  $U(1)$  global matter symmetry which, by the Gauss law, is equivalent to  
124 an electric flux symmetry acting on the boundary. We show that in a particular limit of the  
125 theory, in which the action reduces to a 3D XY model on the boundary, this boundary  $U(1)$   
126 symmetry can be broken spontaneously. We provide numerical evidence that there is a cor-  
127 responding boundary phase transition in the presence of bulk fluctuations, and we trace the  
128 phase boundary in the bulk phase diagram. Next we turn to non-Abelian Higgs theories in  
129 Section 3. We consider two types of Higgs models, those with group-valued Higgs fields and  
130 those with fundamental representation (vector-valued) Higgs fields, which coincide for gauge  
131 group  $SU(2)$  but differ for other gauge groups. We demonstrate that these models also have  
132 a global charge symmetry which is realized at the boundary. Using large-scale lattice simula-  
133 tion, we first show that 4D  $SU(2)$  Higgs theory has a boundary phase transition in the 3D  $O(4)$   
134 universality class, verifying our theoretical prediction. We show that this boundary symmetry  
135 breaking is expected to be generic in group-valued Higgs models, and provide a general argu-  
136 ment that fundamental-Higgs models with gauge group  $SU(N)$  and  $SO(N)$  exhibit  $O(2N)$  and  
137  $O(N)$  boundary criticalities, respectively. We verify this prediction numerically for the case  
138 of the 4D  $SU(3)$  fundamental-Higgs. Lastly, in Section 4, we consider generalizing to higher-  
139 form Abelian-Higgs models, with a  $k$ -form gauge field coupled to a  $(k-1)$ -form Higgs field. We  
140 discuss how the higher-form matter symmetry is realized at the boundary through the Gauss  
141 law, and show that the action reduces in a limiting case to a boundary  $(k-1)$ -form gauge  
142 theory which may exhibit a confinement-deconfinement phase transition in which the matter  
143  $(k-1)$ -form symmetry is spontaneously broken. In the same section, we perform a duality  
144 transformation and discuss how this symmetry breaking can be viewed from the perspective  
145 of magnetic defects which live at the boundary. Finally, we provide an overview of our find-

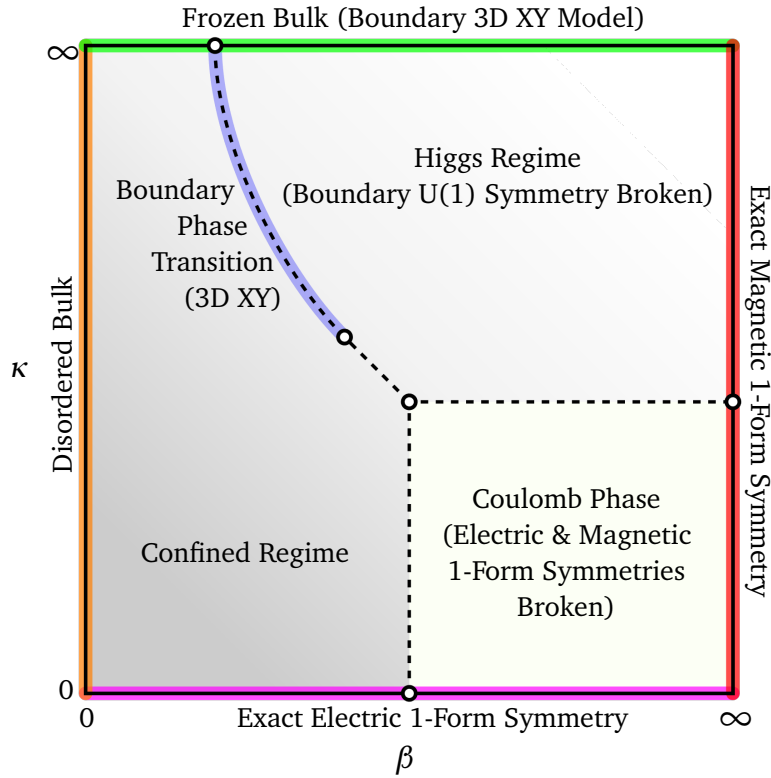


Figure 1: A sketch of the phase diagram of the 4D U(1) lattice Abelian-Higgs phase diagram discussed in Section 2. The confined and Higgs regimes belong to the same thermodynamic phase, though we demonstrate that in presence of symmetry-preserving boundary they are sharply separated by a second order boundary phase transition in the 3D XY universality class. Along the line  $\kappa = 0$  the model has an exact electric 1-form symmetry, while along the line with  $\beta = \infty$  the model has an exact magnetic 1-form symmetry. The confined regime is smoothly connected to the  $\beta = 0$  limit where the gauge field is maximally disordered. Along the  $\kappa = \infty$  line, the bulk is completely frozen, and the boundary reduces to a 3D XY model. The boundary U(1) symmetry is spontaneously broken on the Higgs side of the transition line. A review of the structure of this phase diagram is provided in Appendix B.

146 ings and discuss how our work gives rise to new insights and challenges for the Higgs=SPT  
147 proposal.

## 148 2 Boundary Symmetry Breaking in Abelian Higgs Models

149 The prototypical theory for the interaction of charges with a gauge field is the U(1) Abelian-  
150 Higgs model—i.e. scalar QED, electrodynamics in (3+1)D Lorentzian or 4D Euclidean dimen-  
151 sions coupled to scalar matter. The continuum action for this theory is

$$S = \underbrace{-\frac{1}{4g^2} \int d^4x F_{\mu\nu} F^{\mu\nu}}_{\text{Dynamical U(1) Gauge Field}} + \underbrace{\frac{1}{2} \int d^4x (|D_\mu \phi|^2 - V(|\phi|^2))}_{\text{Minimally Coupled Complex Scalar}}, \quad (1)$$

152 where  $F = dA$  is the field strength tensor,  $A$  is the vector potential,  $\phi$  is a complex scalar  
153 Higgs field,  $D = d - iA$  is the covariant derivative, and  $V(\phi)$  is a potential for the Higgs

154 field. This theory is known to exhibit two phases: a deconfined or Coulomb phase, where  
 155 charged particles interact via a  $1/r$  Coulomb potential mediated by massless photons and a  
 156 gapped confinement-Higgs phase. The latter phase has two distinct regimes, a confined regime  
 157 at strong coupling and a Higgs regime at weak coupling, which are continuously connected  
 158 without any thermodynamic phase transition between them [14].

159 This theory is invariant under local  $U(1)$  gauge transformations of the form

$$\phi(x) \rightarrow \phi(x)e^{i\lambda(x)}, \quad A \rightarrow A + d\lambda, \quad (2)$$

160 where  $\lambda$  is an arbitrary 0-form. By construction, gauge-non-invariant operators cannot exhibit  
 161 a non-zero vacuum expectation which is formalized by Elitzur's theorem [3]. Thus, while it is  
 162 commonly stated that this theory exhibits spontaneous breaking of the  $U(1)$  gauge symmetry  
 163 leading to the Higgs phase,  $\langle \phi(x) \rangle = 0$  and thus cannot serve as a local order parameter for  
 164 such a phase transition. Rather, the gauge-invariant observables are non-local string operators,  
 165 such as an open Wilson line

$$W_C = \phi(x)^\dagger \exp\left(i \int_C A\right) \phi(y), \quad (3)$$

166 where  $C$  is a curve from  $y$  to  $x$ , which creates electric charges attached to their concomitant  
 167 electric field lines [2, 24]. When properly normalized, such observables allow one to quanti-  
 168 tatively distinguish the deconfined phase from the Higgs-confined phase [25–28].

169 We demonstrate that, in the presence of open boundaries of certain type, there is a second-  
 170 order *boundary phase transition* distinguishing the Higgs and confined phases. We derive an  
 171 explicit boundary theory in a limit where the bulk is completely frozen, which we show is a  
 172 3D XY model, and demonstrate with Monte Carlo that the critical exponents of the boundary  
 173 transition do not change when we restore bulk fluctuations. Surprisingly, the line of boundary  
 174 transitions appears to merge with the bulk critical endpoint, see Fig. 1. We then discuss  
 175 deformations of the model which tune the location of the boundary transition.

## 176 2.1 Preliminaries: Lattice Formulation

177 We begin our discussion with a quick summary of the formulation of the discretized lattice  
 178 theory, the importance of the Gauss law, the role of magnetic monopoles, before introducing  
 179 the open boundary problem and presenting our numerical results.

### 180 2.1.1 Action Formulation

181 To study this theory in more depth we consider regulating it by imposing a UV lattice cutoff.  
 182 We undertake our exploration of Higgs phases in gauge theories within the Wilson-Fradkin-  
 183 Shenker lattice formulation. We work on a 4D hypercubic lattice with linear dimension  $L$  and  
 184 periodic boundaries, a discretization of four-dimensional Euclidean spacetime. We consider  
 185 a complex 0-form Higgs field taking values  $\phi_i$  at each vertex  $i$ . Expanding the Higgs field  
 186 at site  $i$  as  $\phi_i = \rho_i \exp(i\theta_i)$ , we freeze the radial mode by fixing the radius  $\rho_i$ , which does  
 187 not affect the qualitative physics.<sup>1</sup> Thus we work with the compact  $\mathbb{R}/2\pi\mathbb{Z}$ -valued 0-form  
 188  $\theta$ , i.e. the phase of the Higgs field, which is minimally coupled to the dynamical  $U(1)$  gauge  
 189 field. We consider a compact 1-form gauge potential  $A$  taking values on each oriented link  $\ell$ ,  
 190  $A_\ell \in \mathbb{R}/2\pi\mathbb{Z}$ . Denoting the reversed orientation by  $-\ell$ , the gauge potential satisfies  $A_{-\ell} = -A_\ell$ .

<sup>1</sup>This freezing corresponds to the limit of infinite bare Higgs self-coupling [14, 26], and the radial mode will be restored upon coarse-graining. Equivalently it may be regarded as a Stückelberg field, and the model can be viewed as a lattice discretization of a gauged nonlinear  $\sigma$ -model with target space  $U(1)$ . We use these two perspectives to give two different generalizations to non-Abelian gauge groups in Section 3.

191 We will often denote link variables by their endpoints, i.e.  $A_{ij} = -A_{ji}$ . See Appendix A for a  
 192 more detailed explanation of lattice differential forms and the notation used here.

193 We demand the theory to be invariant under gauge transformations of the form of Eq. (2),  
 194 which on the lattice become

$$\theta \rightarrow \theta + \lambda, \quad A \rightarrow A + d\lambda, \quad (4)$$

195 where  $\lambda$  is an arbitrary  $\mathbb{R}/2\pi\mathbb{Z}$ -valued 0-form, and  $d$  is the discrete exterior derivative, defined  
 196 so that  $(d\lambda)_{ij} \equiv \lambda_j - \lambda_i$ . The minimal gauge-invariant building blocks are the Wilson links  $\Lambda_\ell$ ,  
 197 defined on oriented links  $\ell$ ,

$$\Lambda_\ell = \exp[i(d\theta - A)_\ell], \quad (5)$$

198 and the minimal Wilson loops  $W_p$ , defined on oriented plaquettes  $p$ ,

$$W_p = \exp[i(dA)_p], \quad (6)$$

199 where  $(dA)_p = \sum_{\ell \in \partial p} A_\ell$ . The minimal gauge-invariant Euclidean lattice theory is the gov-  
 200 erned by what we will refer to as the Fradkin-Shenker action,

$$S_{\text{FS}} = -\beta \sum_p \text{Re } W_p - \kappa \sum_\ell \text{Re } \Lambda_\ell, \quad (7)$$

201 which reduces upon substituting in Eqs. (5) and (6) to the Abelian-Higgs model, the lattice  
 202 equivalent of Eq. (1) in the limit where the radial mode of the Higgs field is frozen,

$$S_{\text{AH}} = -\beta \sum_p \cos(dA)_p - \kappa \sum_\ell \cos(d\theta - A)_\ell. \quad (8)$$

203 Note that  $\kappa$  may be interpreted as the squared length of the Higgs field. The generating func-  
 204 tion of the model is

$$Z_{\text{AH}} = \int \prod_i d\theta_i \prod_\ell dA_\ell \exp[-S]. \quad (9)$$

### 205 2.1.2 Hamiltonian Formulation and Gauss Law

206 It will also serve us to consider the Hamiltonian formulation of the model on a 3D cubic lat-  
 207 tice with continuous time. This may be obtained from the action by fixing to temporal gauge  
 208 ( $A_\ell = 0$  on all timelike links) and taking the continuum limit in the time direction, expressing  
 209 the partition sum in terms of transfer matrices [29]. The Higgs field phase and gauge connec-  
 210 tion become operators, denoted  $\hat{\theta}_i$  and  $\hat{A}_\ell$  respectively, acting on a local Hilbert space on each  
 211 vertex or link. They each have a canonically conjugate operator, denoted  $\hat{n}_i$  and  $\hat{E}_\ell$  respec-  
 212 tively, both with integer eigenvalues, satisfying  $[\hat{\theta}_i, \hat{n}_i] = i$  and  $[\hat{A}_\ell, \hat{E}_\ell] = i$ . Thus  $\exp(\pm i\hat{\theta}_i)$  is  
 213 the raising/lowering operator for  $\hat{n}_i$ , while  $\exp(\pm i\hat{A}_\ell)$  is the raising/lowering operator for  $\hat{E}_\ell$ .  
 214 The Hamiltonian may then be expressed as<sup>2</sup>

$$H_{\text{AH}} = \sum_\ell \hat{E}_\ell^2 - \beta \sum_p \cos(d\hat{A})_p + \sum_i \hat{n}_i^2 - \kappa \sum_\ell \cos(d\hat{\theta} - \hat{A})_\ell. \quad (10)$$

215 The operator  $\hat{n}_i$  counts the amount of charge on site  $i$ , while  $\hat{E}_\ell$  counts the number of electric  
 216 field lines on oriented link  $\ell$ .

<sup>2</sup>Note that the  $\beta$  and  $\kappa$  couplings in the Hamiltonian formulation cannot be quantitatively compared to their values in the Lagrangian formulation, as they are renormalized when taking the continuum limit in the timelike direction [30].

217 Gauge transformations, Eq. (4), are implemented by the operators

$$\begin{aligned}\hat{G}[\lambda] &= \exp\left(i \sum_i \lambda_i \hat{n}_i + i \sum_\ell (d\lambda)_\ell \hat{E}_\ell\right) \\ &\equiv \exp\left(i \sum_i \lambda_i \hat{n}_i + i \sum_i \lambda_i (d^\dagger \hat{E})_i\right).\end{aligned}\quad (11)$$

218 Here we have used the coexterior derivative (see Appendix A)

$$(d^\dagger \hat{E})_i = \sum_{\ell \in \partial^\dagger i} \hat{E}_\ell \quad (12)$$

219 where  $\partial^\dagger$  indicates the coboundary, the set of oriented links *ending* at site  $i$ . Demanding that  
220  $\hat{G}[\lambda]$  acts as the identity on physical states for arbitrary  $\lambda_i$  implies that physical states satisfy  
221 the Gauss law constraint

$$-(d^\dagger \hat{E})_i = (\nabla \cdot \hat{E})_i = \hat{n}_i, \quad (13)$$

222 at each site  $i$ , where we used  $\hat{E}_{-\ell} = -\hat{E}_\ell$  to rewrite the constraint in terms of the lattice  
223 divergence. Gauge invariant states satisfying the Gauss law are then created by Wilson line  
224 operators,

$$\hat{W}[\gamma] = \exp\left(i \sum_{\ell \in \gamma} (d\hat{\theta} - \hat{A})_\ell\right), \quad (14)$$

225 where  $\gamma$  is a 1-dimensional contour in the lattice. Acting on the trivial vacuum state with  
226  $n_i = E_\ell = 0$  everywhere, this operator creates a unit electric charge/anti-charge pair at the  
227 ends of the contour connected by a string of unit electric flux. If  $\gamma$  is a closed contour, this  
228 inserts a closed string of electric flux.

### 229 2.1.3 Magnetic Monopoles

230 In addition to the electric sector, there is also the magnetic sector, though it is not readily seen in  
231 this formulation, instead being exposed by duality transformations [31–35] (see Section 4.2.  
232 In the Hamiltonian formulation, the magnetic excitations are sources of divergence of the  
233 magnetic field,  $\hat{B} = d\hat{A}$ , i.e. magnetic monopoles. In the action formulation, they may be  
234 viewed as U(1) vortex defects of the gauge field, characterized by  $d^2 A \neq 0$ , which are allowed  
235 because the identity  $d^2 = 0$  is only enforced modulo  $2\pi$ . In 4D, these homotopy defects  
236 form 1-dimensional closed strings in the dual lattice, which we refer to as 't Hooft loops, the  
237 worldlines of magnetic monopoles. They are necessarily included in the Euclidean lattice  
238 gauge theory partition sum due to the compactness of the U(1) link variables. In the limit  
239  $\beta \rightarrow \infty$  of Eq. (8), fluctuations of the gauge field are completely suppressed and no monopoles  
240 are present. Correspondingly, we may equate this absence of monopoles (equivalently, the  
241 closure of magnetic flux lines) to the presence of an exact magnetic 1-form symmetry, indicated  
242 in Fig. 1.

## 243 2.2 Open Boundaries and Global Symmetry

244 We address now a well-known, but subtle point: by taking  $\lambda$  in Eq. (4) to be a constant  
245 function, it appears at first sight that this theory has a *global* 0-form U(1) symmetry, shifting  
246  $\theta_i \rightarrow \theta_i + \lambda$ , leaving  $A$  unchanged since  $d\lambda = 0$ . In the Hamiltonian picture, this transformation  
247 is generated by the total charge,

$$\hat{Q}_{\text{bulk}} = \sum_i \hat{n}_i, \quad (15)$$



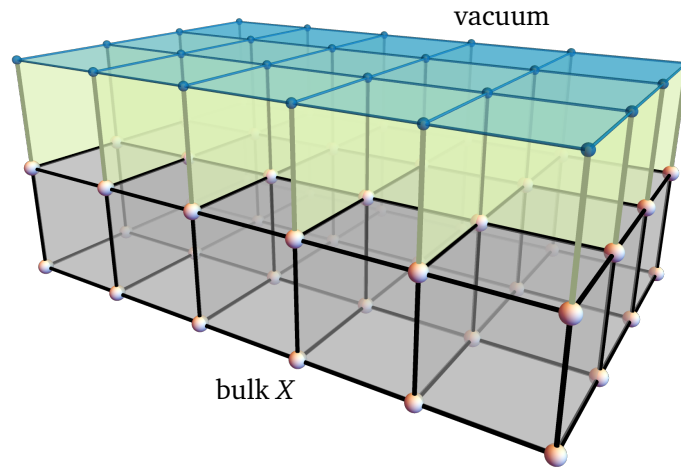


Figure 2: A demonstration of the boundary conditions considered in this work. The gauge field takes values on the bulk links (black) as well as a set of links extending out of the bulk (green). The holonomy of the gauge field is defined on all bulk plaquettes (gray), as well as on the set of plaquettes extending out of the bulk (green). The matter field takes values only in the bulk of the system (white spheres), with the Gauss law satisfied at all bulk vertices. The outside vacuum (blue sites, links, plaquettes) has no dynamical fields. With these boundary conditions electric flux is capable of passing through the boundary, allowing for non-trivial charge sectors in the bulk. We denote the bulk cells (white, black, gray) by  $X$  and the boundary layer cells (green) by  $\partial X$ .

248 thus such a symmetry corresponds to global conservation of electric charge. Note, however,  
 249 that in the absence of boundaries this “global symmetry” is pure gauge, because all physical  
 250 quantum states belong to the zero-charge sector and thus carry the same quantum number. By  
 251 the Gauss law, Eq. (13),  $\hat{Q}_{\text{bulk}}$  is *exactly zero* for a system with periodic boundary conditions.  
 252 In other words, since all electric flux lines must end somewhere inside the system, the system  
 253 must be globally charge neutral. By construction, such a “symmetry” is therefore trivial and  
 254 cannot be explicitly or spontaneously broken. However, in presence of specific boundary condi-  
 255 tions, these global  $U(1)$  transformations actually generate a physical global symmetry that  
 256 acts on the boundaries which can be spontaneously broken [22, 23].

257 We consider a lattice with open boundaries in the form illustrated in Fig. 2. The bulk of  
 258 the system is a (hyper)cubic lattice with sites indicated by white spheres, links by black lines,  
 259 and plaquettes by gray faces. At the boundary, we include a layer of cubic cells (green) which  
 260 separate the bulk from the vacuum (blue sites, edges, and plaquettes). In particular, there is a  
 261 set of links bridging between the bulk and the vacuum which carry dynamical gauge degrees  
 262 of freedom and can therefore support electric flux lines which effectively exit the system. The  
 263 vacuum side (blue) does not contain any dynamical degrees of freedom.

264 Key to our choice of boundary conditions is that we demand that the Gauss law, Eq. (13), is  
 265 respected at every bulk site (white sphere), including those at the ends of the boundary links.  
 266 No Gauss law constraints are imposed at vacuum sites. Let  $A_i$  denote the gauge potential on  
 267 the boundary link touching site  $i$ , oriented “in” from the vacuum to the bulk. For the Gauss law  
 268 to be respected at  $i$ , we must have that under the gauge transformation Eq. (4),  $A_i \rightarrow A_i + \lambda_i$ ,  
 269 i.e. it is “uncompensated” at the vacuum end of the link.

270 With this choice of boundary conditions, the global part of the gauge symmetry becomes  
 271 physical—charge can pass in and out of the system, meaning there are different gauge-invariant  
 272 charge sectors. More precisely, there are gauge-invariant half-open Wilson string operators

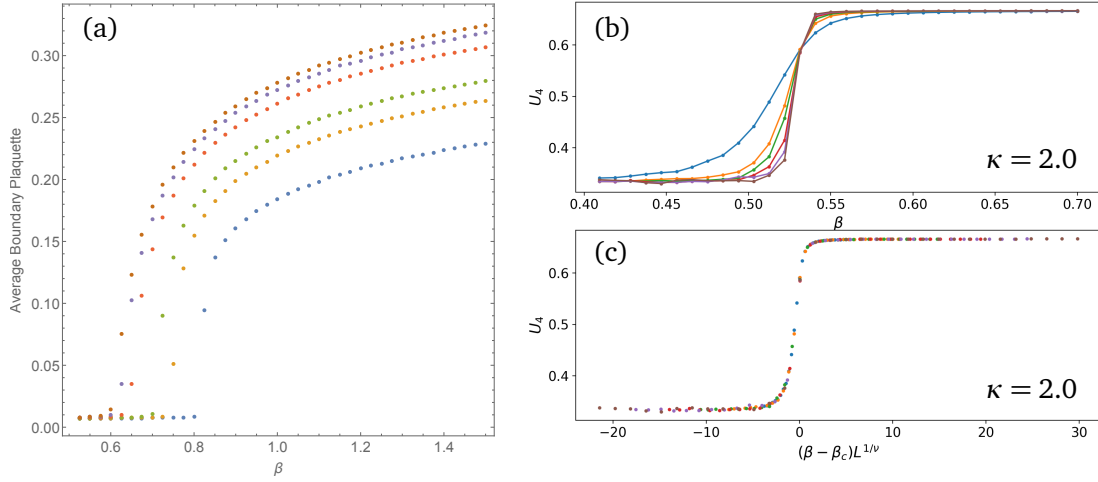


Figure 3: Boundary criticality for the 4D  $U(1)$  Higgs phase: (a) Average boundary plaquette for  $\kappa = 0.55, 0.64, 0.85, 0.94, 1.0$  for  $L = 16$ . The transition shifts towards smaller  $\beta$  for larger values of  $\kappa$ . (b) The Binder ratio  $U_4$  for the magnetization at the boundary as a function of  $\beta$  for  $\kappa = 2.0$  and  $L = 16, 20, 24, 28, 32$ . (c) Rescaled Binder ratio for  $\kappa = 2.0$  showing collapse for  $\nu = 0.67$  corresponding to the 3D XY universality class.

273 with one end in the bulk and the other passing through the boundary,

$$\hat{W}[\gamma_{\text{open}}] = \exp \left( i \left[ \hat{\theta}_i - \sum_{\ell \in \gamma_{\text{open}}} \hat{A}_\ell \right] \right), \quad (16)$$

274 where  $\gamma_{\text{open}}$  is a contour starting in the vacuum and ending at bulk site  $i$ . These operators  
 275 create an isolated charge in the bulk, attached to an electric flux line that exits through the  
 276 boundary, which is not possible in a closed system. These half-open string operators are *charged*  
 277 under the global transformations generated by  $\hat{Q}_{\text{bulk}}$ , Eq. (15). By the Gauss law,  $\hat{Q}_{\text{bulk}}$  is  
 278 equivalent to the *net electric flux through the boundary*,

$$\hat{Q}_{\text{bulk}} = \sum_{\ell \in \partial X} \hat{E}_\ell \equiv \hat{Q}_{\text{bdry}}, \quad (17)$$

279 where the sum is over all boundary links (green in Fig. 2) oriented *out*. If the Hamiltonian  
 280 contains no half-open string operators, then the bulk charge is conserved, and there is a global  
 281  $U(1)$  symmetry. Eq. (17) defines a “bulk-boundary correspondence” between charge and flux,  
 282 and generates a global symmetry which may either be seen as acting on the bulk matter degrees  
 283 of freedom or on the boundary gauge degrees of freedom.

### 284 2.3 Boundary Symmetry Breaking in the Abelian Higgs Model

285 The theory can now be chosen such that the Hamiltonian commutes with the charge  $\hat{Q}_{\text{bulk}}$ . This  
 286 now-physical global  $U(1)$  symmetry corresponds to global charge conservation or, equivalently,  
 287 conservation of flux through the boundary. Since the open system has a global symmetry on  
 288 the boundary, it may be spontaneously broken, a scenario we now study. With the boundary  
 289 conditions shown in Fig. 2, the Euclidean action that we will study is given by

$$S = S_{\text{AH}}^{\text{bulk}} + S^{\text{bdry}}, \quad (18)$$

290 with the boundary portion given by the Wilson plaquette loops on the boundary plaquettes  
 291 (light green in Fig. 2),

$$S^{\text{bdry}} = -\beta \sum_{p \in \partial X} \cos(dA)_p. \quad (19)$$

292 The absent links on the vacuum side are excluded, so that

$$(dA)_{p \in \partial X} = A_i + A_{ij} - A_j, \quad (20)$$

293 where  $A_i$  indicates the value of  $A$  on the boundary link touching site  $i$ , oriented inwards from  
 294 the vacuum to the bulk.<sup>3</sup>

### 295 2.3.1 Boundary XY Model at Infinite $\kappa$

296 To begin, we consider the behavior of this theory in the  $\kappa \rightarrow \infty$  limit, i.e. deep in the Higgs  
 297 regime. From the bulk action, Eq. (8), in this limit the bulk satisfies the constraint  $A = d\theta$ ,  
 298 i.e. the bulk gauge field is exact and thus pure gauge. Indeed there are no physical degrees  
 299 of freedom left in the bulk—rotating to unitary gauge,  $\theta = \text{const.}$ , we end up with  $A = 0$  on  
 300 all bulk links and a vanishing matter field. However, no such constraint is enforced on the  
 301 boundary links bridging between the bulk and vacuum, and the gauge field on these links  
 302 is free to fluctuate. Thus we obtain a dynamical 3D theory on the boundary of the system  
 303 governed by the boundary action in Eq. (19).

304 In this limit, referring to Fig. 2, each boundary plaquette (green) has one edge in the bulk  
 305 (black) with  $A_{ij} = \theta_j - \theta_i$ , and two edges straddling between the bulk and vacuum (green)  
 306 which remain dynamical degrees of freedom. Substituting this into Eq. (20), we can recombine  
 307 terms into the gauge-invariant variables

$$\vartheta_i = A_i - \theta_i, \quad (21)$$

308 corresponding to a half-open Wilson line coming from the vacuum and ending at site  $i$ . The  
 309 boundary action can then be written in the gauge-invariant form

$$S_{\kappa \rightarrow \infty}^{\text{bdry}} = -\beta \sum_{\langle ij \rangle \in \partial X} \cos(\vartheta_j - \vartheta_i), \quad (22)$$

310 which is a 3D XY model at inverse temperature  $\beta$ . This must exhibit a continuous phase  
 311 transition from a paramagnet at small  $\beta$  to a spontaneously broken phase at large  $\beta$ . Thus we  
 312 infer that along the  $\kappa = \infty$  line in the phase diagram there is a boundary phase transition in  
 313 the 3D XY universality class indicated at the top of Fig. 1. We note that in the case of the  $\mathbb{Z}_2$   
 314 Abelian-Higgs model, the same mechanism generates a boundary Ising model at  $\kappa = \infty$  [22].

### 315 2.3.2 Boundary Phase Transition at Finite $\kappa$

316 Next we consider  $\kappa$  to be large,  $\kappa \gg 1$ , but finite. The constraint  $A = d\theta$  is no longer enforced  
 317 exactly, so we expand in small fluctuations as  $A = d\theta + \delta A$ . Assuming that the bulk action can  
 318 be expanded in terms of  $\delta A \ll 1$  (i.e. that topological defects are negligible), the bulk action  
 319 becomes a Proca-type action,

$$S_{\kappa \gg 1}^{\text{bulk}} \approx \frac{\beta}{2} \sum_p F_p^2 + \frac{\kappa}{2} \sum_\ell (\delta A)_\ell^2 \quad (\kappa \gg 1), \quad (23)$$

<sup>3</sup>We may equivalently consider the exterior vacuum (blue in Fig. 2) to have trivial gauge field  $A_\ell = 0$  on all vacuum links and zero Higgs field  $\phi_i = 0$  on all vacuum sites.

320 where  $F_p = d(\delta A)$ , which describes a massive 1-form field. The boundary action is then

$$S_{\kappa \gg 1}^{\text{bdry}} \sim -\beta \sum_{\langle ij \rangle \in \partial X} \cos(\vartheta_j - \vartheta_i + \delta A_{ij}). \quad (24)$$

321 While at infinite  $\kappa$  the theory reduces to an XY model on the boundary, at finite  $\kappa$  the XY model  
 322 is minimally coupled to the weakly fluctuating massive bulk gauge field. While the bulk field  
 323 lives in a higher dimension, the boundary remains quasi-3D, exponentially localized with a  
 324 length scale determined by the mass of the bulk photon,  $m^2 \sim \kappa$ . We therefore expect the  
 325 symmetry breaking phase transition at the boundary to persist at large but finite  $\kappa$ .

326 We may ask where the boundary transition line may run from  $\kappa \rightarrow \infty$ , finite  $\beta$ . As it  
 327 is a spontaneously broken symmetry it must end either on a boundary of the phase diagram  
 328 or on a bulk transition line. The former case is ruled out as follows: It cannot end on the  
 329  $\beta = 0$  line because this is trivial from the point of view of both bulk and boundary variables. It  
 330 also cannot end on the  $\kappa = 0$  line because matter decouples on this line. The only remaining  
 331 possibility is that the line ends at  $\beta \rightarrow \infty$  but there we understand the bulk theory as being  
 332 pure gauge and an XY model so the physical degrees of freedom on the boundary drop out.  
 333 We conclude that the boundary transition line must end on a bulk transition line.

334 These arguments are suggestive of the picture illustrated in Fig. 1, with a boundary phase  
 335 transition between the Higgs and confinement regimes of the bulk phase diagram. To test this  
 336 assertion, we have carried out Monte Carlo simulations of the full 4D lattice gauge theory with  
 337 boundary. We compute the local XY order parameter  $\langle \vartheta_i \rangle$  on the boundary as well as gauge  
 338 invariant bulk observables  $\langle \Lambda_\ell \rangle$  and  $\langle W_p \rangle$ . The results are summarized in Fig. 3. We find clear  
 339 signs of a boundary phase transition, with Fig. 3(a) showing the boundary order parameter  
 340 behavior as a function of  $\beta$  while holding  $\kappa$  fixed showing behavior consistent with a continu-  
 341 ous boundary phase transition. Fig. 3(b) shows the Binder cumulant for the order parameter  
 342 taken along a cut at  $\kappa = 2$  for different system sizes ranging from  $L = 16$  to  $L = 32$ , showing  
 343 crossing behavior consistent with a second-order transition. Lastly, Fig. 3(c) shows the Binder  
 344 parameter with  $\beta$  scaled by  $L^{1/\nu}$  using the 3D XY critical exponent  $\nu \approx 0.67$  [36], showing  
 345 excellent scaling collapse, confirming a second-order phase transition on the boundary even  
 346 for only moderately large  $\kappa$ .

347 Monte Carlo simulations of the 3D XY model in the literature put the critical point at  
 348  $\beta_c = 0.45420(2)$  [36]. We find that  $\beta_c$  tends towards this value in the large  $\kappa$  limit. On general  
 349 grounds we should expect that bulk fluctuations will serve to disorder the boundary. Therefore,  
 350 by lowering  $\kappa$  we expect the transition shifts to larger  $\beta$  (lower effective temperature in the  
 351 statistical model). This is indeed what we observe numerically. For even smaller  $\kappa$  we find  
 352 that the boundary transition line appears to intercept the bulk critical endpoint, as shown in  
 353 Fig. 1.

### 354 2.3.3 Tuning the Boundary Coupling

355 We now consider tuning the boundary coupling in Eq. (19) relative to the bulk, parameterized  
 356 by the dimensionless ratio

$$\alpha = \beta_{\text{bdry}} / \beta_{\text{bulk}}. \quad (25)$$

357 Such a change is allowed by gauge symmetry and does not affect either the electric or magnetic  
 358 1-form symmetries. The reason for this modification is that by tuning  $\alpha$  we can shift the  
 359 location of the critical  $\beta$  in the  $\kappa = \infty$  limit, as  $\beta_{\text{bdry},c}^{\kappa \rightarrow \infty}(\alpha) = \beta_{\text{bdry},c}^{\kappa \rightarrow \infty}(\alpha = 1) / \alpha$ . This implies  
 360 that the location of the boundary transition line must shift in the phase diagram in order to  
 361 meet the location of the transition in the  $\kappa \rightarrow \infty$  limit.

362 Indeed, this is precisely what we find numerically with the resulting transition lines shown  
 363 in Fig. 4. We find, for all  $\alpha$ , that the transition is present and that it drifts to larger  $\beta$  as  $\kappa$

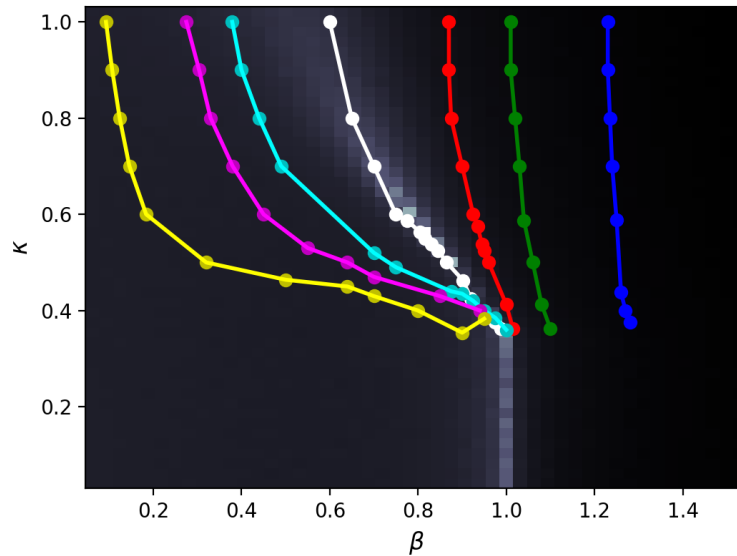


Figure 4: Boundary phase transition lines for the U(1) Abelian Higgs model, for different  $\alpha = \beta_{\text{bdry}}/\beta_{\text{bulk}}$ , overlaid on the bulk plaquette susceptibility. From right to left,  $\alpha = 0.4, 0.5, 0.6, 1.0, 2.0, 3.0, 10.0$  for system size  $L = 16$ .

364 is reduced, consistent with having to lower the temperature more to suppress the enhanced  
 365 matter field fluctuations. For  $\alpha < 1$  the line shifts to larger values of  $\beta$ , and appears to separate  
 366 from the tricritical point, instead terminating on the first order transition line separating the  
 367 Higgs phase from the deconfined phase. For  $\alpha > 1$ , the boundary transition line shifts to  
 368 smaller values of  $\beta$ , and appears to continue to terminate on the tricritical point.

## 369 2.4 Summary and Discussion: Abelian Case

370 In this section we have explored the case of the U(1) Abelian-Higgs model in  $D$  spacetime  
 371 dimensions with open boundary conditions of the form shown in Fig. 2, governed by the action  
 372 defined by Eqs. (8), (18) and (19). In the case of open boundaries there is a global bulk  
 373 charge symmetry for this model, because charge is not allowed to enter or leave the system.  
 374 By the Gauss law, this is physically equivalent to a symmetry acting on the boundary of the  
 375 system, yielding conservation of total electric flux through the boundary. We investigated the  
 376 possibility of spontaneously breaking this symmetry.

377 In the  $\kappa \rightarrow \infty$  limit, the bulk degrees of freedom are fully frozen while the boundary de-  
 378 grees of freedom remain fluctuating. The boundary theory in this limit can be written in the  
 379 gauge-invariant form of a  $(D-1)$ -dimensional 0-form U(1) model, i.e. an XY model, Eq. (22),  
 380 which therefore exhibits a boundary phase transition at a critical value of  $\beta$  in the appropriate  
 381 XY universality class. By performing explicit numerical simulation in  $D = 4$  Euclidean space-  
 382 time dimensions and measuring the gauge-invariant order parameter, Fig. 3, we found that  
 383 this boundary phase transition persists away from the  $\kappa \rightarrow \infty$  limit, and appears to stay in  
 384 the 3D XY universality class. The transition line appears to terminate at a critical point in the  
 385 bulk phase diagram and can be tuned by adjusting the boundary coupling relative to the bulk  
 386 coupling, as shown in Fig. 4.

387 This boundary transition line appears to delineate between the Higgs and confining regimes  
 388 of the phase diagram. The idea that the Higgs phase can be characterized by boundary symme-  
 389 try breaking was first raised in [22,23]. This gives physical meaning to the non-gauge-invariant  
 390 adage that the Higgs regime is a charge condensate by imposing open boundaries that make  
 391 the symmetry physical. We note, however, that by tuning the boundary coupling relative to

392 the bulk coupling, the location of the transition line in the phase diagram can be moved. This  
 393 raises questions as to what the boundary phase transition implies as a probe of bulk physics,  
 394 which we defer to the discussion at the end of the paper (Section 5.2). First we broaden  
 395 our perspective by studying more complex non-Abelian models exhibiting similar physics in  
 396 Section 3.

397 A few comments on extensions and exceptional cases are in order before we proceed. These  
 398 results naturally carry over to the discrete Abelian gauge groups  $\mathbb{Z}_N$  by restricting the Higgs  
 399 field  $\theta_i$  and gauge field  $A_{ij}$  to take discrete values in multiples of  $2\pi/N$ . The boundary theory  
 400 Eq. (22) then becomes an  $N$ -state clock model. The  $\mathbb{Z}_2$  case was discussed in [22] where the  
 401 boundary theory was shown to be an Ising model. They also can be generalized to higher-form  
 402 extensions of the Abelian-Higgs model, which we discuss further in Section 4.

403 The  $D = 3$   $U(1)$  Abelian-Higgs model is interesting because it reduces in the  $\kappa \rightarrow \infty$  limit  
 404 to the  $D = 2$  XY model on the boundary, which exhibits a BKT transition. It would be interest-  
 405 ing to know if this BKT transition persists to finite  $\kappa$ . We complete our discussion of special  
 406 cases by highlighting here  $U(1)$  gauge theory in four dimensions coupled to a charge  $q = 2$   
 407 Higgs field. For this case, a sharp distinction can be made in the bulk between confining and  
 408 Higgs phases with a transition between them. The distinguishing feature of this theory is the  
 409 partial Higgsing of the  $U(1)$  gauge group down to  $\mathbb{Z}_2$  [37]. For sufficiently large  $\kappa$  the bulk  
 410 transition is the confinement-deconfinement transition of the residual  $\mathbb{Z}_2$  gauge theory. On  
 411 the boundary, however, one still expects the emergence of the XY model we identified for the  
 412  $q = 1$  case. It would be quite interesting to investigate the interplay of boundary  $U(1)$  0-form  
 413 symmetry breaking with the bulk  $\mathbb{Z}_2$  1-form symmetry breaking and the resulting topological  
 414 order present at large  $\beta$  and  $\kappa$ .

### 415 3 Boundary Symmetry Breaking in Non-Abelian Higgs Models

416 We now turn to extend the results of the previous section regarding Abelian Higgs models  
 417 and boundary criticality to non-Abelian Higgs models. We will show that the general pic-  
 418 ture of boundary symmetry breaking persists, albeit with a richer structure owing to a set of  
 419 non-commuting gauge transformations. We discuss two types of non-Abelian Higgs models:  
 420 those with group-valued Higgs fields and those with fundamental representation vector-valued  
 421 Higgs fields with fixed length. The two classes of models are equivalent for gauge group  $SU(2)$ ,  
 422 and are distinct for other gauge groups. The group-valued case is a relatively straightforward  
 423 extension of the Abelian case, because the fixed-length XY-rotor Higgs field considered previ-  
 424 ously is naturally a  $U(1)$  group element. The vector-valued case is more subtle because the  
 425  $\kappa \rightarrow \infty$  limit does not trivialize all bulk degrees of freedom. We present numerical results for  
 426 both  $SU(2)$  and vector-valued  $SU(3)$  cases and extract corresponding boundary criticalities.

#### 427 3.1 Preliminaries: Lattice Formulation

428 Let  $\mathcal{G}$  be a compact connected Lie group, e.g.  $SU(N)$  or  $SO(N)$ . The lattice action is formulated  
 429 in terms of group-valued link variables  $U_\ell \in \mathcal{G}$  satisfying  $U_{-\ell} = U_\ell^{-1}$ , which may be viewed as  
 430 the exponentiated Lie-algebra-valued gauge field,  $U_\ell = P \exp(i \int_\ell A)$ , where  $P$  indicates path-  
 431 ordering. Under a gauge transformation, these transform as

$$U_{ij} \rightarrow g_i U_{ij} g_j^{-1} \quad (26)$$

432 where  $g_i \in \mathcal{G}$  are arbitrary group elements associated to each site  $i$ . The minimal gauge-  
433 invariant quantity is the Wilson plaquette-loop (compare to Eq. (6)),

$$W_p = \frac{1}{\dim(r)} \text{Tr}_r \left[ \prod_{\ell \in \partial p}^P U_\ell \right] \quad (27)$$

434 where the superscript  $P$  on the product indicates path-ordering, and the trace may be taken  
435 in a representation  $r$ . Normalizing by the dimension of the representation ensures that the  
436 trivial Wilson loop has unit magnitude. We focus primarily on the cases  $SU(N)$  and  $SO(N)$ ,  
437 taking the trace in the fundamental representation as  $N \times N$  matrices.

### 438 3.1.1 Higgs Fields

439 For the Higgs field, many different models can be considered by putting the Higgs field in  
440 different representations of the gauge group. We consider two different types here for con-  
441 creteness: vector-valued (fundamental representation) Higgs, and group-valued Higgs. These  
442 are both possible extensions of the Abelian  $U(1)$  rotor model considered in Section 2, since a  
443 rotor may be viewed either as a fixed-length vector, or as a  $U(1)$  group element. In either case,  
444 the action is given by the Fradkin-Shenker form, Eq. (7), the only difference being the defi-  
445 nition of the Wilson link  $\Lambda_\ell$ . The generating function for the quantum theory is given by the  
446 Euclidean path integral, where the integration over the group-valued variables is performed  
447 with respect to the Haar measure.

448 The familiar model is the fundamental-Higgs, where the Higgs field is an  $N$ -component  
449 vector, as in the Standard Model and analogous to Eq. (1). Denoting the Higgs vector at site  
450  $i$  by  $\phi_i \in V_i$ , we freeze the radial mode as in the Abelian Fradkin-Shenker model. Gauge  
451 transformations rotate the Higgs field as  $\phi_i \rightarrow g_i^f \phi_i$  where  $g_i^f$  is a group element in the funda-  
452 mental matrix representation. The group-valued link variables define parallel-transport maps  
453 for the Higgs field,  $U_{ij} : V_j \rightarrow V_i$ , i.e. they related the color frames at neighboring sites, and  
454 the generalization of the gauge-invariant Wilson link observable, Eq. (5), is

$$\Lambda_\ell = \langle \phi_i, U_{ij}^f \phi_j \rangle_i \equiv \sum_{\alpha, \beta=1}^N \phi_i^{\alpha*} (U_{ij}^f)^{\alpha\beta} \phi_j^\beta, \quad (28)$$

455 where  $\langle -, - \rangle_i$  is the canonical inner product on  $V_i$ ,  $*$  indicates complex conjugation, and we  
456 enforce the fixed-length constraint  $\langle \phi_i, \phi_i \rangle = 1$ .

457 The second type of model we consider takes the Higgs field to be *group-valued*, like the  
458 link variables, denoted  $\varphi_i \in \mathcal{G}$ . In this case, the Higgs field transforms as  $\varphi_i \rightarrow g_i \varphi_i$  under  
459 gauge transformations, and we can define a gauge-invariant Wilson link by

$$\Lambda_\ell = \frac{1}{N} \text{Tr}_f [\varphi_i^{-1} U_{ij} \varphi_j], \quad (29)$$

460 where we take the trace in the fundamental representation. This is a lattice regularization of  
461 a gauged principal chiral model [38], a non-linear  $\sigma$ -model whose target space is the group  
462 manifold.

### 463 3.1.2 Hamiltonian Formulation and Gauss Law

464 The Hamiltonian formulation of the non-Abelian lattice gauge theory has a similar form to  
465 the Abelian case, but the electric field of the non-Abelian theory carries color indices and  
466 the different components do not commute. Fixing to temporal gauge and reformulating the  
467 partition function using transfer matrices, taking the continuum limit in the time direction one

468 obtains a Hamiltonian for the time evolution [30, 39]. The basic ingredients are the group-  
 469 valued link operators  $\hat{U}_\ell$  with eigenstates  $|U\rangle$ , such that  $\hat{U}_\ell|U\rangle = U|U\rangle$  and  $\hat{U}_{-\ell}|U\rangle = U^{-1}|U\rangle$ ,  
 470 along with a set of translation operators

$$\hat{T}_\ell(g)|U\rangle = |gU\rangle, \quad \hat{T}_{-\ell}(g)|U\rangle = |Ug^{-1}\rangle, \quad (30)$$

471 where left and right translations correspond to the two orientations of the link. Each group  
 472 element may be expressed as  $U = \exp(i\theta^a t^a)$ , where  $\theta^a$  are real numbers and  $t^a$  a basis for  
 473 the Lie algebra of gauge group  $\mathcal{G}$ . The  $\theta^a$  serve as coordinates on the group manifold, and  
 474 may be thought of as generalized Euler angles. The link operators can then be expressed as

$$\hat{U}_\ell = \exp(i\hat{\theta}_\ell^a t^a), \quad \hat{T}_\ell(e^{i\lambda^a t^a}) = \exp(i\lambda^a \hat{E}_\ell^a). \quad (31)$$

475 The operators  $\hat{\theta}_\ell^a$  are position operators on the group manifold, while  $\hat{E}_\ell^a$  are the color-electric  
 476 fields, which serve as the conjugate momenta and can be expressed as derivatives with respect  
 477 to the  $\theta^a$ . The electric fields satisfy the same commutation relations as the group generators,

$$[\hat{E}_\ell^a, \hat{E}_\ell^b] = if^{abc} \hat{E}_\ell^c, \quad (32)$$

478 where  $f^{abc}$  are the structure constants of  $\mathcal{G}$ .

479 For the Higgs field in the group-valued representation, we define the group-valued oper-  
 480 ators  $\hat{\varphi}_i$  (analogous to  $\hat{U}$ ) and left- and right-translation generators  $\hat{t}_{i,L}^a$  and  $\hat{t}_{i,R}^a$  (analogous  
 481 to  $\hat{E}$ ). For the Higgs field in the fundamental vector representation with frozen radial mode,  
 482 the classical configuration space is that of a rigid rotor, and we define corresponding angular  
 483 momentum operators  $\hat{J}_i^\mu$ . The Hamiltonian is then given by the Kogut-Susskind form [39, 40]

$$H = \sum_\ell |\hat{E}_\ell|^2 - \beta \sum_p (\hat{W}_p + \hat{W}_p^\dagger) + \sum_i |\hat{Q}_i^m|^2 - \kappa \sum_\ell (\hat{\Lambda}_\ell + \hat{\Lambda}_\ell^\dagger), \quad (33)$$

484 where all sites, links, and plaquettes are purely spatial. Here,  $\hat{Q}_i^m$  are the matter charge oper-  
 485 ators,

$$\hat{Q}_i^m = \begin{cases} \hat{t}_{i,L} & \text{group-valued Higgs,} \\ \hat{J}_i & \text{fundamental Higgs,} \end{cases} \quad (34)$$

486 and  $|\hat{E}_\ell|^2$  and  $|\hat{Q}_i^m|^2$  are the corresponding quadratic Casimir operators, which do not depend  
 487 on whether we use left- or right-generators. The operator  $\hat{W}_p$  is the operator analog of Eq. (27),  
 488 the trace of the oriented product of  $\hat{U}_\ell$  on the links of spatial plaquette  $p$ . Similarly,  $\hat{\Lambda}_\ell$  is the  
 489 operator analog of Eq. (29).

490 The eigenstates of  $|\hat{E}_\ell|^2$  correspond to the irreducible representations of the gauge group,  
 491 with the  $\hat{U}_\ell$  acting as raising and lowering operators [39–41]. The same is true for the group-  
 492 valued Higgs, with  $\hat{\varphi}_i$  acting as the raising and lowering operators, while for the fundamental  
 493 vector-valued Higgs, the charge eigenstates are angular momentum eigenstates of a rigid rotor.

494 Gauge transformations are performed by the operators

$$\begin{aligned} \hat{G}[\lambda] &= \exp\left(i \sum_i \lambda_i^a \hat{Q}_i^{m,a} + i \sum_{\langle ij \rangle} (\lambda_i^a \hat{E}_{ij}^a + \lambda_j^a \hat{E}_{ji}^a)\right) \\ &= \exp\left(i \sum_i \lambda_i^a \hat{Q}_i^{m,a} + i \sum_i \lambda_i^a (\nabla \cdot \hat{E}^a)_i\right), \end{aligned} \quad (35)$$

495 where the lattice divergence is defined as

$$(\nabla \cdot \hat{E}^a)_i = \sum_{-\ell \in \partial^\dagger i} \hat{E}_\ell^a, \quad (36)$$



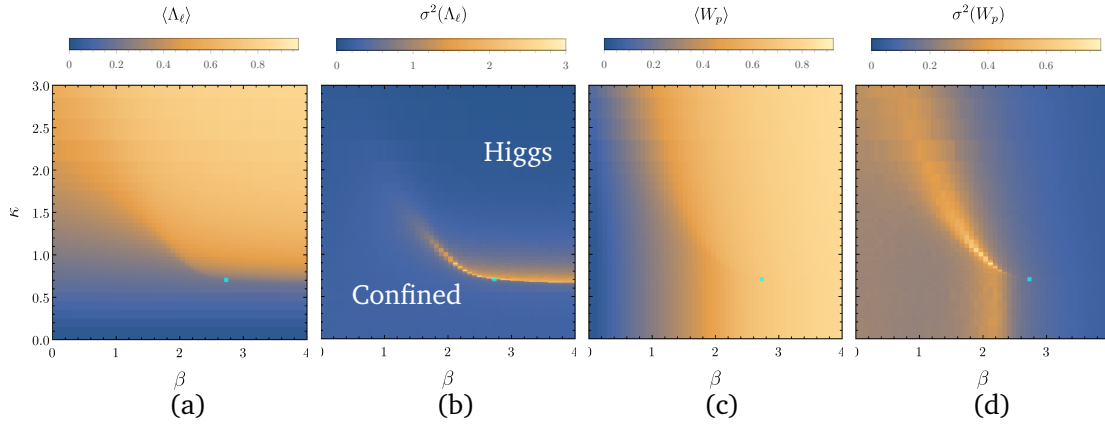


Figure 5: Bulk phase diagram of the SU(2) Higgs model, showing (a) the link expectation value  $\langle \Lambda_\ell \rangle$ , (b) the link variance  $\sigma^2(\text{Re } \Lambda_\ell)$ , (c) the Wilson plaquette average  $\langle \text{Re } W_p \rangle$ , and the plaquette variance  $\sigma^2(\text{Re } W_p)$ . The small cyan-colored point is the location of the critical endpoint identified in Ref. [42],  $(\beta_c, \kappa_c) \approx (2.73, 0.70)$ . From the critical endpoint there is a first-order transition line extending to larger  $\beta$  with nearly-constant  $\kappa$ , which is clearly seen in (b). A rapid-crossover region extends from the critical point to smaller  $\beta$  and larger  $\kappa$ , signaled in both (b) and (d) by strong bulk fluctuations, indicating the “supercritical” region which roughly delineates the Higgs and confined regimes.

496 with the sum taken over the links emanating from site  $i$  oriented *out*.  $\hat{G}[\lambda]$  acts as the identity  
 497 on physical, gauge-invariant states, which therefore satisfy the color-electric Gauss laws,

$$(\nabla \cdot \hat{E})_i^a = -\hat{Q}_i^{m,a}, \quad (37)$$

498 one for each color index.

499 Note that this is similar but subtly distinct from the Abelian case, Eqs. (11) to (13), where  
 500 we used  $\hat{E}_\ell^{\text{Abelian}} = -\hat{E}_{-\ell}^{\text{Abelian}}$ . This relationship is not true in non-Abelian gauge theory. Instead,  
 501 left- and right-translations of the gauge field are related by

$$T_{-\ell}(g)|U_\ell\rangle = |U_\ell g^{-1}\rangle = T_\ell(U_\ell g^{-1} U_\ell^{-1})|U_\ell\rangle, \quad (38)$$

502 which implies that the electric field in the two directions along a link are related by

$$\hat{E}_{-\ell}^a |U\rangle = -U_\ell^{a,ab} \hat{E}_\ell^b |U\rangle, \quad (39)$$

503 where  $U_\ell^a$  is the adjoint representation of  $U_\ell$ . As such the gauge field itself is charged in the  
 504 adjoint representation with respect to color rotations, generated by the charge operators

$$\hat{Q}_\ell^{g,a} = \hat{E}_\ell^a + \hat{E}_{-\ell}^a, \quad (40)$$

505 which are manifestly orientation-independent. The classic (though heuristic) way to think  
 506 of this is that the gauge bosons (gluons) carry a distinct charge and anti-charge in the two  
 507 directions along the link. In the Abelian case,  $U_\ell^a = 1$  in Eq. (39), and the link charge Eq. (40)  
 508 is exactly zero.

### 509 3.1.3 Open Boundaries and Global Symmetry

510 We introduce electric open boundary conditions as in Fig. 2, with dynamical links extending  
 511 from the bulk to the vacuum which allow electric flux to pass through the boundary. We denote  
 512 the link variables on the boundary link touching site  $i$  by  $U_i$ , with the convention that the link

513 is oriented “in” from the vacuum to site  $i$ . We have minimal open Wilson strings going around  
 514 the boundary plaquettes, which we can write as

$$W_{p \in \partial X} = \frac{1}{N} \text{Tr}_f[U_i U_{ij} U_j^{-1}] \quad (41)$$

515 Using these, we define the boundary action for our theory directly analogous to the Abelian  
 516 case as

$$S^{\text{bdry}} = -\beta \sum_{p \in \partial X} \text{Re } W_p \quad (42)$$

517 Electric flux can thus enter and leave the system, but matter charges cannot. Under gauge  
 518 transformations the fields transform as

$$\mathcal{G}_{\text{gauge}} : \begin{cases} \phi_i \rightarrow g_i^f \phi_i & \text{or } \varphi_i \rightarrow g_i \varphi_i, \\ U_{ij} \rightarrow g_i U_{ij} g_j^{-1}, \\ U_i \rightarrow U_i g_i^{-1}. \end{cases} \quad (43)$$

519 Notice that each boundary link only receives a transformation from the *inside* end, where it  
 520 terminates on a matter field. In addition to this gauge symmetry, the boundary action Eq. (42)  
 521 has a *physical global*  $\mathcal{G}$  symmetry acting on the boundary,

$$\mathcal{G}_{\text{bdry}} : U_i \rightarrow g U_i \quad (44)$$

522 where every boundary link is translated from the *outside* end.

523 This boundary symmetry is similar to the Abelian case, but with a subtle distinction. The  
 524 total color charge of the system, including boundary links, is

$$\hat{Q}_{\text{total}}^a = \sum_i \hat{Q}_i^{m,a} + \sum_{\ell} \hat{Q}_{\ell}^{g,a}, \quad (45)$$

525 which rotates all matter fields in the fundamental representation and all gauge fields, including  
 526 boundary links, in the adjoint representation. But this is *not* the generator of global gauge  
 527 transformations, Eq. (43), under which the boundary links only rotate from the *inside*. The  
 528 generator of global gauge transformations is the “bulk charge”

$$\hat{Q}_{\text{bulk}}^a = \sum_i \hat{Q}_i^{m,a} + \sum_{\ell \in X} \hat{Q}_{\ell}^{g,a} + \sum_{\ell \in \partial X} \hat{E}_{-\ell}^a, \quad (46)$$

529 where the second sum contains only the bulk links, and in the last sum the boundary links are  
 530 oriented inwards. By the Gauss law, this operator must be *zero* on the physical gauge-invariant  
 531 Hilbert space. On the other hand, the generator of the global symmetry is the “boundary  
 532 charge”

$$\hat{Q}_{\text{bdry}}^a = \sum_{\ell \in \partial X} \hat{E}_{\ell}^a, \quad (47)$$

533 again with inward orientation. Together these make up the total charge of the system,

$$\hat{Q}_{\text{total}}^a = \hat{Q}_{\text{bulk}}^a + \hat{Q}_{\text{bdry}}^a = \hat{Q}_{\text{bdry}}^a, \quad (48)$$

534 where we have assumed global gauge invariance to identify  $\hat{Q}_{\text{bulk}}^a = 0$ . Thus the boundary  
 535 symmetry Eq. (44) may be viewed, by the Gauss law constraint, as being generated by the  
 536 total color charge of the system. This is analogous to the Abelian case, where the total charge  
 537 of the system is just the matter charge, Eq. (15), since the links do not carry any charge. Note,  
 538 however, that in the non-Abelian case the charge of the boundary links is “fractionalized” into  
 539 a piece that contributes to the bulk charge and a piece that contributes to the boundary charge.

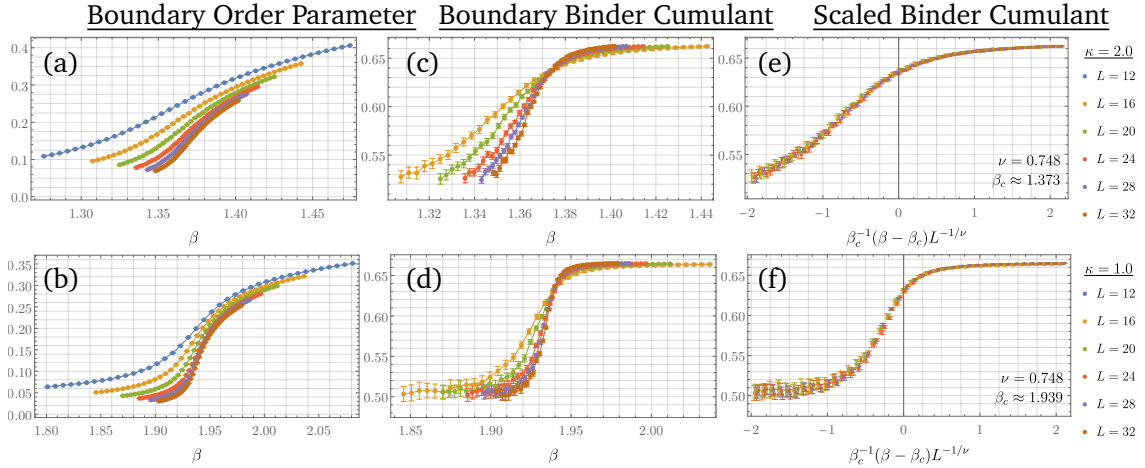


Figure 6: Boundary criticality in the SU(2) Higgs model. (a,b) Boundary order parameter, (c,d) Binder cumulant, and (e,f) scaled Binder cumulant for the SU(2) Higgs model at (a,c,e)  $\kappa = 2.0$  and (b,d,f)  $\kappa = 1.0$ , each shown for system sizes ranging from  $L = 12$  to  $L = 32$ . Each data point is averaged over  $10^5$  samples. The Binder cumulants for different system sizes collapse when scaled with the 3D O(4) universality critical exponent  $\nu \approx 0.748$  [43], indicating that the boundary phase transition remains second order all the way to the bulk critical endpoint (with  $\kappa_c \approx 0.7$  [42]).

### 540 3.2 Boundary Symmetry Breaking in the SU(2) Higgs Model

541 We focus first on the case where the gauge group is SU(2). In this case the fundamental and  
 542 group-valued representations are equivalent. In the fundamental representation, each  $\phi_i$  is  
 543 a  $\mathbb{C}^2$  vector with unit length, and the configuration space is a 3-sphere. Notice that SU(2) is  
 544 also topologically the 3-sphere, meaning that every configuration of the Higgs vector  $\phi_i$  can be  
 545 written as a unique fundamental-representation SU(2) matrix times a fixed vector, for example  
 546 as

$$\phi_i = \begin{pmatrix} \phi_1 \\ \phi_2 \end{pmatrix} = \begin{pmatrix} \phi_1 & -\phi_2^* \\ \phi_2 & \phi_1^* \end{pmatrix} \begin{pmatrix} 1 \\ 0 \end{pmatrix} \equiv \varphi_i^f \phi_0, \quad (49)$$

547 where  $\phi_1$  and  $\phi_2$  are complex numbers. Note that the determinant of  $\varphi_i^f$  is the length of the  
 548 rotor. The Wilson link for the vector Higgs model, Eq. (28), can then be written as

$$\Lambda_{ij} = \langle \phi_0, (\varphi_i^f)^{-1} U_{ij}^f \varphi_j^f \phi_0 \rangle = \frac{1}{2} \text{Tr}_f[\varphi_i^{-1} U_{ij} \varphi_j] \quad (50)$$

549 which is exactly equivalent to the group-valued Higgs definition, Eq. (29). This makes the  
 550 SU(2) Higgs rotors special, since they may be viewed as either vector-valued or group-valued  
 551 (which is also the case for U(1) rotor).

#### 552 3.2.1 Bulk Phase Diagram

553 To map the phase diagram, we perform classical Monte Carlo simulations for the 4D SU(2)  
 554 model defined by the Fradkin-Shenker action, Eq. (7), with periodic boundary conditions on  
 555 an  $L^4$  hypercubic lattice [30, 44, 45]. The phase diagram can be mapped out by measuring the  
 556 Wilson plaquette and link observables along with their variances (i.e. susceptibilities), which  
 557 are shown in Fig. 5. There is a roughly horizontal first-order transition line extending from  
 558 a critical endpoint at  $(\beta_c, \kappa_c) \approx (2.73, 0.70)$  [42] (cyan box) towards  $\beta \rightarrow \infty$ . This line is  
 559 clearly visible in the link susceptibility, Fig. 5(b).

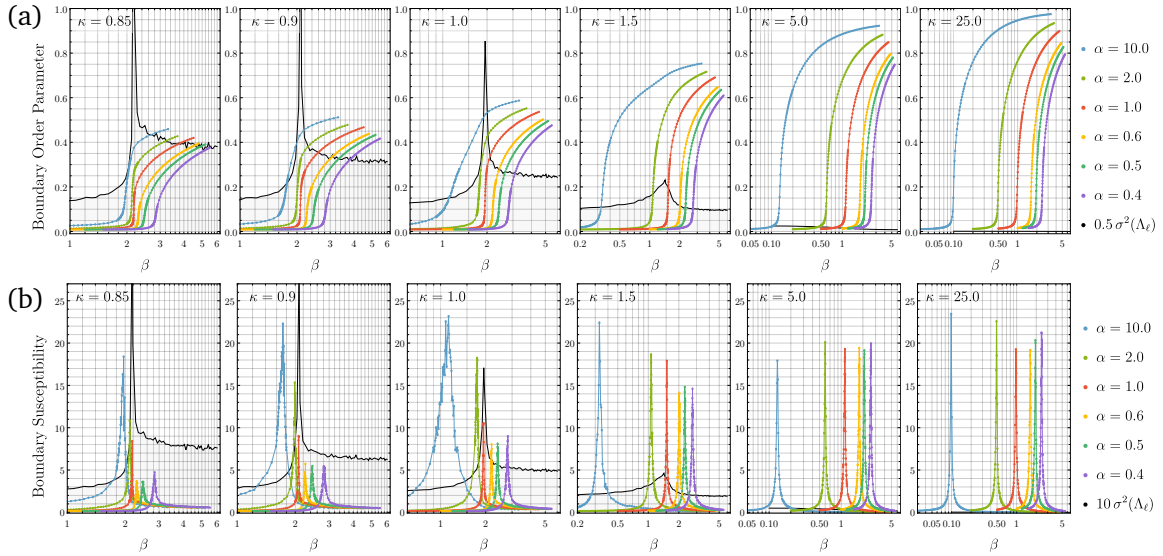


Figure 7: Results for varying  $\alpha$  in the SU(2) Higgs model. Behavior of (a) the boundary order parameter and (b) the boundary order parameter variance, cut along  $\beta$  with  $\kappa$  fixed, for different values of  $\alpha$ . The variance of  $\Lambda_\ell$  in the bulk is shown behind (black curves, scaled for visibility), as an indication of the magnitude of bulk fluctuations and how they influence the boundary transition in a finite-size system. Data taken at  $L = 24$  with  $10^4$  samples averaged for each data point.

560 The phase diagram exhibits only one clearly distinct bulk phase—the confined-Higgs phase—  
 561 a deconfined phase being absent in non-Abelian theories. The phase diagram is, however,  
 562 roughly separated into two regions indicated by the behavior of the Wilson link expectation  
 563 value, shown in Fig. 5(a), with  $\langle \text{Re} \Lambda_\ell \rangle \sim 0$  indicating the confining regime and  $\langle \text{Re} \Lambda_\ell \rangle \sim 1$   
 564 indicating the Higgs regime. To the left of this critical endpoint is a supercritical region (a  
 565 Widom line [46]) extending to smaller  $\beta$  and larger  $\kappa$ , a rapid crossover from the Higgs to the  
 566 confined regimes. The location of this supercritical region is most evident in the Wilson plaquette  
 567 susceptibility, Fig. 5(d), which shows a pronounced intensity emanating from the critical  
 568 endpoint. We expect this phase diagram to be qualitatively consistent with those for general  
 569 non-Abelian Higgs models with either fundamental vector- or group-valued Higgs fields. In  
 570 the group-valued case the continuity of the Higgs and confined regimes was proven by Fradkin  
 571 and Shenker [14].

### 572 3.2.2 Boundary Symmetry Breaking

573 We now consider open boundaries, with boundary action Eq. (42) in a slab geometry. As in  
 574 Section 2.3, we start by considering the limiting behavior when  $\kappa \rightarrow \infty$ . In this limit every bulk  
 575 link satisfies the constraint  $\text{Re} \Lambda_\ell = 1$ . In this section we will resolve this constraint by fixing  
 576 a gauge. Gauge-invariant formulations for the group-valued representation are presented in  
 577 Section 3.3, and for the fundamental representation in Section 3.4.

578 From Eq. (50), if we fix to unitary gauge where all the Higgs rotors are aligned globally,  
 579  $\phi_i = \phi_0$  or  $\varphi_i = \mathbb{1}$ , the bulk constraint becomes  $(U_\ell^f)^{11} = 1$ , or  $\text{Tr}_f[U_\ell]/2 = 1$ , which can only  
 580 be satisfied if  $U_\ell = \mathbb{1}$  on every bulk link. Thus in the  $\kappa \rightarrow \infty$  limit of the SU(2) Higgs model,  
 581 the bulk is completely frozen and has no remaining degrees of freedom, as in the Abelian case.  
 582 The boundary links, however, have no constraint and remain fluctuating. In unitary gauge

583 where the bulk links are set to the identity, the boundary action becomes

$$S_{\kappa \rightarrow \infty}^{\text{bdry}} = -\beta \sum_{\langle ij \rangle \in \partial X} \frac{1}{2} \text{Tr}_i[U_i U_j^\dagger] \quad (\text{unitary gauge}). \quad (51)$$

584 This boundary action may be viewed as a lattice discretization of a nonlinear  $\sigma$ -model with  
585 target space the  $SU(2)$  group manifold, i.e. a principal chiral model [38].

586 The boundary model, Eq. (51), has an  $SU(2) \times SU(2) \simeq O(4)$  symmetry. To see this, we  
587 can re-express it as an  $O(4)$  Heisenberg model by representing the  $SU(2)$  group-valued link  
588 variables as unit quaternions,

$$U_i \equiv \sum_{\mu=1}^4 S_i^\mu \sigma^\mu \quad \text{with} \quad \sum_{\mu=1}^4 S_i^\mu S_i^\mu = 1 \quad (\text{unitary gauge}), \quad (52)$$

589 where the  $S_i^\mu$  are real numbers,  $\sigma^0 = \mathbb{1}$  and  $\sigma^1, \sigma^2$ , and  $\sigma^3$  are Pauli matrices. The boundary  
590 action then becomes an  $O(4)$  Heisenberg model,

$$S_{\kappa \rightarrow \infty}^{\text{bdry}} = -\beta \sum_{\langle ij \rangle \in \partial X} S_i^\mu S_j^\mu \quad (\text{unitary gauge}). \quad (53)$$

591 Therefore, in the limit  $\kappa \rightarrow \infty$ , the system exhibits a boundary phase transition in the 3D  $O(4)$   
592 universality class, at a critical coupling  $\beta_{\text{bdry},c} \approx 0.9360$  [43], with order parameter,

$$\mathcal{O}_{SU(2)} = \left\langle \left| \frac{1}{L^3} \sum_{i \in \partial X} \mathbf{s}_i \right| \right\rangle \quad (\text{unitary gauge}). \quad (54)$$

593 The gauge-invariant object which reduces to  $U_i$  in the unitary gauge is

$$U_i \varphi_i \quad \text{or} \quad U_i \phi_i, \quad (55)$$

594 where the former is an  $SU(2)$  matrix which decomposes according to Eq. (52), and the latter  
595 is explicitly a 4-component unit-length vector. For large but finite  $\kappa$ , the bulk fluctuations are  
596 strongly gapped and the boundary should behave as quasi- $(D-1)$ -dimensional, and we expect  
597 the boundary phase transition to persist as in the Abelian case.

598 To test this prediction, we perform Monte Carlo simulations with open boundaries and  
599 measure the order parameter, Eq. (54) (defined in terms of gauge invariant observables Eq. (55)),  
600 at finite values of  $\kappa$ . In Fig. 6 we show the evolution of the boundary order parameter as a  
601 function of  $\beta$ , for  $\kappa = 2.0$  in (a) and  $\kappa = 1.0$  in (b), for different system sizes. These reveal  
602 a transition from a disordered, symmetric boundary on the confined side (small  $\beta$ ) to an or-  
603 dered, symmetry-broken boundary on the Higgs side (large  $\beta$ ). This value of  $\kappa$  is quite close  
604 to the bulk critical point ( $\kappa_c \sim 0.7$ ), demonstrating that the boundary phase transition persists  
605 far into the phase diagram where the bulk is quite strongly fluctuating. In Fig. 6(c) and (d),  
606 we show the Binder cumulant for the same cuts, showing crossing behavior at a  $\kappa$ -dependent  
607 critical coupling. In (e) and (f) we have rescaled  $\beta - \beta_c(\kappa)$  using the 3D  $O(4)$  critical expo-  
608 nent  $\nu \approx 0.748$  [43], demonstrating a clean scaling collapse, thus verifying that the transition  
609 remains second order and in the same universality class even for relatively small values of  $\kappa$ .  
610 The transition line appears to terminate at the bulk critical point, which can be seen in the red  
611 line in Fig. 7, though verifying this numerically is difficult as the bulk correlation length grows  
612 larger than the finite width of the open boundaries as the system approaches bulk criticality.

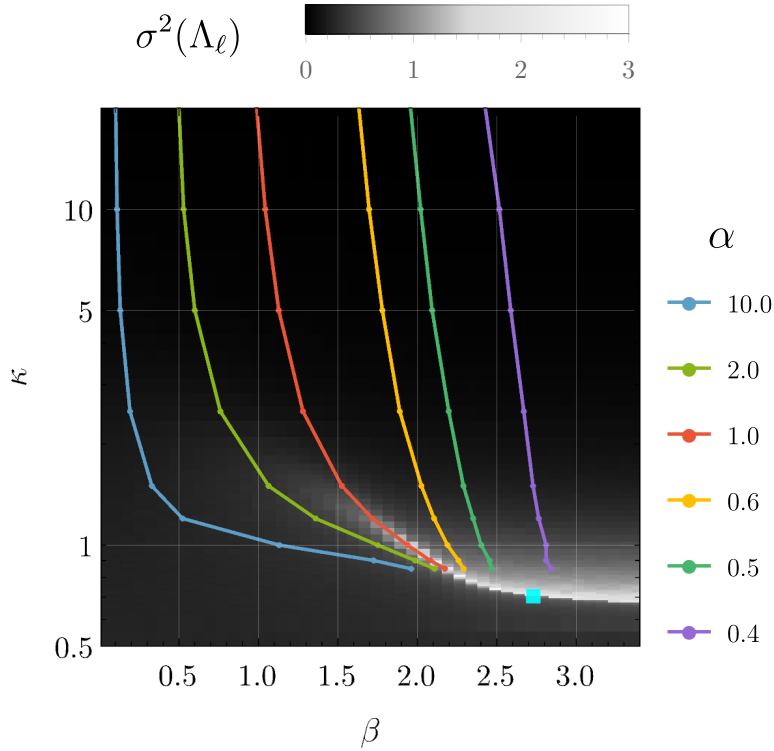


Figure 8: Location of the boundary phase transition for the SU(2) Higgs model for different values of  $\alpha = \beta_{\text{bdry}}/\beta_{\text{bulk}}$ , determined by the location of the peak in the boundary order parameter susceptibility (cf. Fig. 7). Large values of  $\alpha$  push the transition line to smaller  $\beta_{\text{bulk}}$ , while small values of  $\alpha$  push the phase boundary to larger  $\beta_{\text{bulk}}$ . The cyan square indicates the location of the bulk critical endpoint. For  $\alpha = 1$  (red), the boundary transition line appears to terminate at the bulk critical point, and closely follows the bulk rapid-crossover (super critical) region that extends beyond the critical endpoint. This remains true for  $\alpha > 1$ , while for sufficiently small  $\alpha < 1$  the boundary transition line appears to terminate on the bulk first-order transition line.

### 613 3.2.3 Tuning the Boundary Coupling

614 We now consider varying the parameter  $\alpha = \beta_{\text{bdry}}/\beta_{\text{bulk}}$ , which shifts the location of the  $\kappa \rightarrow \infty$   
615 transition. Figure 7 shows the behavior of the boundary order parameter and its susceptibility  
616 for different values of  $\alpha$ , along different constant- $\kappa$  cuts at fixed system size. The correspond-  
617 ing behavior of the bulk link susceptibility is shown in black in the background for reference.  
618 The bulk transition line moves as  $\alpha$  is varied, but appears to remain second-order through-  
619 out. Figure 8 summarizes the results by showing the approximate location of the boundary  
620 transition line for different values of  $\alpha$ , with results very similar to the Abelian case (Fig. 4).  
621 For  $\alpha > 1$  the transition moves to smaller values of  $\beta_{\text{bulk}}$  and appears to terminate at the bulk  
622 critical endpoint (cyan box). No boundary transition is detected for small values of  $\kappa$  below  
623 the bulk first-order line. For  $\alpha < 1$  the location of the boundary transition line moves to larger  
624 values of  $\beta$ , and appears to terminate on the line of bulk first-order transitions, at least for  
625 sufficiently small  $\alpha$ .

### 626 3.3 Boundary Symmetry Breaking in Non-Abelian Group-Valued Higgs Models

627 Having verified the existence of a boundary phase transition in the SU(2) Higgs model, which  
 628 is both a fixed-length-rotor Higgs model and a group-valued Higgs model, we now consider  
 629 how these results generalize to these two types of models separately for a general gauge group  
 630  $\mathcal{G}$ . From the point of view of the boundary action, the group-valued Higgs is the simpler case,  
 631 so we consider it first. The action (up to an overall normalization convention for the trace) is

$$S_{\text{bulk}} = -\beta \sum_{p \in X} \text{Tr} \prod_{\ell \in \partial p} U_\ell - \kappa \sum_{\langle ij \rangle \in X} \text{Tr} [\varphi_i^{-1} U_{ij} \varphi_j]. \quad (56)$$

632 The boundary action is given by Eq. (42). In addition to the global color charge symmetry  
 633 acting on the boundary, Eq. (44), it also has a global  $\mathcal{G}$  symmetry given by right multiplication  
 634 of the Higgs field

$$\mathcal{G}_{\text{bulk}} : \varphi_i \rightarrow \varphi_i g. \quad (57)$$

635 The global symmetry group is therefore  $\mathcal{G}_{\text{bdry}} \times \mathcal{G}_{\text{bulk}}$ . We expect the bulk phase diagram to  
 636 be qualitatively similar to the SU(2) case, Fig. 5, with a single thermodynamic phase, a first-  
 637 order line terminating at a critical endpoint. These models were considered by Fradkin and  
 638 Shenker [14], who showed that the Higgs and confining regimes are contiguous, as in the  
 639 Abelian models.

640 We now consider taking the  $\kappa \rightarrow \infty$  limit. Maximizing the trace in Eq. (56) yields the  
 641 constraint  $\varphi_i^{-1} U_{ij} \varphi_j = \mathbb{1}$ , which implies that the bulk links can be expressed in terms of the  
 642 matter field as

$$U_{ij} \xrightarrow{\kappa \rightarrow \infty} \varphi_i \varphi_j^{-1}. \quad (58)$$

643 The bulk of the system is completely frozen in this limit, which can be most easily seen in  
 644 unitary gauge where  $\varphi_i = \mathbb{1}$ . Substituting Eq. (58) into Eq. (41), the boundary action can  
 645 then be expressed in terms of the gauge-invariant observables

$$\Theta_i = U_i \varphi_i, \quad (59)$$

646 where  $U_i$  was defined with the boundary link oriented “in”, which are short half-open Wilson  
 647 strings coming from the vacuum and ending at site  $i$ . The boundary action becomes

$$S_{\kappa \rightarrow \infty}^{\text{bdry}} = -\beta \sum_{\langle ij \rangle \in \partial X} \text{Re Tr} [\Theta_i \Theta_j^{-1}], \quad (60)$$

648 which is a lattice chiral model. Compare this to the equivalent results for the Abelian case,  
 649 Eq. (22) and Eq. (51), to which it reduces when  $\mathcal{G} = \text{U}(1)$ . The  $\mathcal{G}_{\text{bdry}} \times \mathcal{G}_{\text{bulk}}$  symmetry acts  
 650 on this chiral model by left and right multiplication of the  $\Theta_i$ , respectively. Such a model is  
 651 known to exhibit chiral symmetry breaking, i.e. breaking to the diagonal  $\mathcal{G}$  subgroup [47]. We  
 652 discuss boundary phase transitions in these models further in Section 3.5

653 Note that if  $\mathcal{G}$  is Abelian there is no distinction between left and right group multiplication,  
 654 therefore  $\mathcal{G}_{\text{bulk}}$  and  $\mathcal{G}_{\text{bdry}}$  are not independent symmetries of the system.  $\mathcal{G}_{\text{bulk}}$  corresponds to  
 655 global rotation of the Higgs field generated by the total matter charge, Eq. (15), while  $\mathcal{G}_{\text{bdry}}$  is  
 656 generated by the net electric flux through the boundary links, Eq. (17). These two generators  
 657 are the same operator on the physical gauge-invariant Hilbert space by the Gauss law. In  
 658 contrast, in the group-valued non-Abelian Higgs models these are really distinct symmetries  
 659 generated by different physical operators.

### 660 3.4 Boundary Symmetry Breaking in Non-Abelian Fundamental-Higgs Models

661 We now consider non-Abelian gauge groups  $SU(N)$  (and by trivial generalization  $SO(N)$ ) with  
 662 fundamental Higgs fields. As a convenient shorthand, in this section we will represent the  
 663 Higgs vectors as kets,  $\phi_i \equiv |\phi_i\rangle$ , which should not be confused with quantum states. Fur-  
 664 thermore, we suppress the subscript “f” on the fundamental representation matrices  $U_\ell$ . The  
 665 action we write as

$$S_{\text{bulk}} = -\beta \sum_{p \in X} \frac{1}{N} \text{Tr} \prod_{\ell \in \partial p} U_\ell - \kappa \sum_{\langle ij \rangle \in X} \text{Re} \langle \phi_i | U_{ij} | \phi_j \rangle. \quad (61)$$

666 The boundary action is given by Eq. (42). For  $N > 2$  the Higgs rotors can no longer be identified  
 667 as group elements. Because of this, the  $\kappa \rightarrow \infty$  constraint,

$$\text{Re} \langle \phi_i | U_{ij} | \phi_j \rangle = 1, \quad (62)$$

668 does not completely trivialize the bulk. To see this, note that the constraint enforces that  
 669 nearest-neighbor Higgs rotors are parallel relative to the gauge field. However, since there is  
 670 still freedom to perform rotations about the colinear axis of the remaining  $N - 1$  components  
 671 of the Higgs field, the gauge field can continue to fluctuate so long as it does not rotate the  
 672 Higgs field away from the parallel axis. This is explicitly seen by rotation to unitary gauge  
 673 where the Higgs field is parallel in a global frame, which then fixes one diagonal element of  
 674 the gauge field to unity, i.e.

$$\phi_i = \begin{pmatrix} 1 \\ 0 \\ \vdots \end{pmatrix} \xrightarrow{\kappa \rightarrow \infty} (U_{ij})^{11} = 1 \quad (\text{unitary gauge}). \quad (63)$$

675 This constraint forces the link matrices to take the form

$$U_{ij}^{\text{SU}(N)} \xrightarrow{\kappa \rightarrow \infty} \begin{pmatrix} 1 & 0 \\ 0 & U_{ij}^{\text{SU}(N-1)} \end{pmatrix} \quad (\text{unitary gauge}). \quad (64)$$

676 Thus in this limit the bulk theory becomes (gauge-equivalent to) an  $SU(N - 1)$  gauge theory.  
 677 Note that  $SU(1)$  is trivial, making the  $SU(2)$  case special, as discussed in Section 3.2.

#### 678 3.4.1 Gauge-Invariant Resolution of the Infinite Kappa Limit

679 To resolve the constraint in a fully gauge-invariant fashion analogous to Eqs. (22) and (60),  
 680 we first note that the constraint Eq. (62) actually implies that

$$\langle \phi_i | U_{ij} | \phi_j \rangle = 1, \quad (65)$$

681 which follows from the fact that real part of a Hermitian inner product on  $\mathbb{C}^N$  is the Euclidean  
 682 product when the vector space is viewed as  $\mathbb{R}^{2N}$ . In other words,  $|\phi_i\rangle$  and  $U_{ij}|\phi_j\rangle$  have the  
 683 same real and imaginary components, and so are the same complex vector. We can think  
 684 of  $|\phi_i\rangle$  and  $|\phi_j\rangle$  as unit vectors spanning a two-dimensional complex vector space, in which  
 685 case  $U_{ij}$  must act within this subspace as the unique  $SU(2)$  rotation  $\tilde{U}_{ij}$  rotating  $|\phi_j\rangle$  to  $|\phi_i\rangle$ .<sup>4</sup>  
 686 Therefore we can resolve the constraint as

$$U_{ij} = u_i \tilde{U}_{ij} u_j, \quad (66)$$

<sup>4</sup>Within the two-dimensional subspace this rotation is given by  $\varphi_i^f(\varphi_j^f)^{-1}$ , using the notation of Eq. (49). That this rotation is unique follows from the fact that the two vectors have unit norm within this  $\mathbb{C}^2$  subspace, thus they live on a 3-sphere, and  $SU(2)$  is isomorphic to the 3-sphere, so each point on the 3-sphere corresponds to a unique  $SU(2)$  rotation.



687 where  $u_i$  is an  $SU(N)$  matrix which preserves  $|\phi_i\rangle$ , i.e. an  $SU(N-1)$  rotation in the subspace  
 688 orthogonal to  $|\phi_i\rangle$ . Note that the  $u_i$ 's are independent for every link, i.e. they are associated to  
 689 the ends of the links and are independent on different links touching the same site. Further-  
 690 more, there is only one independent  $SU(N-1)$  degree of freedom on each link, because  $\tilde{U}_\ell u$   
 691 is equivalent to  $(\tilde{U}_\ell u \tilde{U}_{-\ell}) \tilde{U}_\ell$ . Thus the constraint reduces each link variable to an  $SU(N-1)$   
 692 degree of freedom, and the whole theory reduces to an  $SU(N-1)$  gauge theory.

693 While Eq. (66) demonstrates the reduction of the gauge group, it is not that useful for  
 694 formulating the boundary theory. A more useful way is to decompose each  $U_{ij}$  by sandwiching  
 695 it between two resolutions of the identity decomposed into the parallel and perpendicular  
 696 subspace of  $|\phi_i\rangle$  and  $|\phi_j\rangle$ . Namely, for site  $i$

$$\mathbb{1} = P_i + |\phi_i\rangle\langle\phi_i|, \quad (67)$$

697 where  $P_i$  is the projector to the orthogonal complement of  $|\phi_i\rangle$ . Note that under a gauge trans-  
 698 formation  $P_i \rightarrow g_i P_i g_i^{-1}$ . Inserting this identity on either side of a link variable decomposes it  
 699 into four pieces,

$$\begin{aligned} (P_i + |\phi_i\rangle\langle\phi_i|) U_{ij} (P_j + |\phi_j\rangle\langle\phi_j|) = \\ P_i U_{ij} P_j + |\phi_i\rangle\langle\phi_i| U_{ij} |\phi_j\rangle\langle\phi_j| \\ + |\phi_i\rangle\langle\phi_i| U_{ij} P_j + P_i U_{ij} |\phi_j\rangle\langle\phi_j|. \end{aligned} \quad (68)$$

700 In the limit  $\kappa \rightarrow \infty$ , this simplifies significantly. Firstly, the two cross terms (the last line)  
 701 are exactly zero by Eq. (66), i.e. because  $P_i U_{ij} |\phi_j\rangle = P_i |\phi_i\rangle = 0$ . Second, in the second term,  
 702 Eq. (65) reduces it to  $|\phi_i\rangle\langle\phi_j|$ . In summary, in the limit  $\kappa \rightarrow \infty$  every link variable in the bulk  
 703 can be expressed as

$$U_{ij} \rightarrow P_i U_{ij} P_j + |\phi_i\rangle\langle\phi_j|. \quad (69)$$

704 It follows that a product of two consecutive link variables is

$$U_{ij} U_{jk} \rightarrow P_i U_{ij} P_j U_{jk} P_k + |\phi_i\rangle\langle\phi_k| \quad (70)$$

705 where we used that  $P_i^2 = P_i$  and  $\langle\phi_j|\phi_j\rangle = 1$ . Therefore gauge-invariant closed Wilson loops  
 706 have a projector to the orthogonal subspace inserted between each consecutive link,

$$\text{Tr}[U_{ij} U_{jk} U_{kl} U_{li}] \rightarrow 1 + \text{Tr}[P_i U_{ij} P_j U_{jk} P_k U_{kl} P_l U_{li}], \quad (71)$$

707 which is another manifestation of the Higgsing down to an  $SU(N-1)$  gauge theory.

708 Now consider the three-legged plaquettes appearing in the boundary action, Eq. (42).  
 709 Inserting the identities at the two bulk sites, we obtain

$$\begin{aligned} \text{Tr}[U_i U_{ij} U_j^{-1}] \xrightarrow{\kappa \rightarrow \infty} \text{Tr}[U_i (P_i U_{ij} P_j + |\phi_i\rangle\langle\phi_j|) U_j^{-1}] \\ = \text{Tr}[U_i P_i U_{ij} P_j U_j^{-1}] + \langle\Phi_i|\Phi_j\rangle \end{aligned} \quad (72)$$

710 where we have defined the gauge-invariant variables

$$|\Phi_i\rangle \equiv U_i |\phi_i\rangle, \quad (73)$$

711 which are  $\mathbb{C}^N$  unit vectors corresponding to the short half-open Wilson strings at the boundary.  
 712 This highlights an important distinction for fundamental Higgs compared to group-valued  
 713 Higgs models—here the half-open Wilson string is a vector degree of freedom, not group-  
 714 valued. The  $\kappa \rightarrow \infty$  theory then can be expressed in the gauge-invariant form

$$\begin{aligned} S_{\text{bulk}} &\rightarrow -\frac{\beta}{N} \sum_{p \in X} (1 + \text{Re} \text{Tr}[U_{ij} P_j U_{jk} P_k U_{kl} P_l U_{li} P_i]), \\ S_{\text{bdry}} &\rightarrow -\frac{\beta}{N} \sum_{\langle ij \rangle \in \partial X} (\text{Re} \text{Tr}[U_i P_i U_{ij} P_j U_j^{-1}] + \text{Re} \langle\Phi_i|\Phi_j\rangle). \end{aligned} \quad (74)$$

715 Thus the bulk Higgses down to an  $SU(N - 1)$  gauge theory while the boundary decomposes  
 716 into a pure  $SU(N - 1)$  part plus a part which may be viewed as an  $SU(N)$  ferromagnet. The  
 717 global  $SU(N)$  boundary symmetry acts as  $U_i \rightarrow gU_i$ , under which  $|\Phi_i\rangle \rightarrow g|\Phi_i\rangle$ . The three-  
 718 leg projected Wilson loop which appears in the boundary action in Eq. (74) is not charged  
 719 under this symmetry since the trace cancels the contribution from the two ends. We therefore  
 720 generically expect the boundary  $SU(N)$  symmetry to spontaneously break above a critical  $\beta$   
 721 down to  $SU(N - 1)$ , and the short Wilson string rotors  $|\Phi_i\rangle$  on the boundary to exhibit long  
 722 range order and Goldstone modes. We discuss the nature of this phase transition further and  
 723 provide numerical support for this statement in Section 3.5.

### 724 3.4.2 Formulation for General Gauge Groups

725 For a general gauge group  $\mathcal{G}$  with fundamental Higgs, the large- $\kappa$  limit Higgses it down to a  
 726 subgroup  $\mathcal{H}$ . We consider here cases where the residual gauge group  $\mathcal{H}$  is non-Abelian. In  
 727 the limit  $\kappa \rightarrow \infty$  the bulk fluctuates as a pure gauge theory with gauge group  $\mathcal{H}$  governed by  
 728 the Wilson action, while the boundary links continue to explore the full gauge group  $\mathcal{G}$ . The  
 729 generic picture (which can be obtained in unitary gauge) is that the action Higgses down to

$$S_{\kappa \rightarrow \infty} = -\beta \sum_{p \in X} \text{Re Tr } W_p^{\mathcal{H}} - \beta \sum_{(ij) \in \partial X} \text{Re Tr} \left[ U_i^{\mathcal{G}} U_{ij}^{\mathcal{H}} (U_j^{\mathcal{G}})^{-1} \right], \quad (75)$$

730 where  $U^{\mathcal{H}}$  is the  $\mathcal{G}$  link variable restricted to the  $\mathcal{H}$  subgroup, and  $W^{\mathcal{H}}$  is the corresponding  
 731 Wilson plaquette for these  $\mathcal{H}$ -valued bulk links. Taking the traces in any faithful representation  
 732 of the group should yield the same physics.

733 Assuming the bulk is gapped with a finite correlation length, as it must be if  $\mathcal{H}$  is non-  
 734 Abelian, the boundary is quasi- $(D - 1)$ -dimensional with some finite correlation length ex-  
 735 tending into the bulk. The system retains a  $\mathcal{G}$  global symmetry rotating all of the boundary  
 736 links, together with the bulk  $\mathcal{H}$  gauge symmetry. The appropriate boundary theory is there-  
 737 fore expected to be a gauged nonlinear  $\sigma$ -model with target space  $\mathcal{G}$  with subgroup  $\mathcal{H}$  gauged,  
 738 or equivalently, a nonlinear  $\sigma$ -model with target space the quotient space  $\mathcal{G}/\mathcal{H}$ . For example,  
 739  $SU(N)$  Higgses down to  $SU(N - 1)$  and the quotient space is  $SU(N - 1)/SU(N) \simeq S^{2N-1}$ , which  
 740 agrees with the finding in Eq. (74) of a boundary theory of  $SU(N)$  rotors, whose configuration  
 741 space is a sphere in  $2N$  dimensions. Similarly,  $SO(N)$  Higgses to  $SO(N - 1)$ , with quotient  
 742 space  $S^{N-1}$ .

### 743 3.4.3 Hamiltonian Perspective

744 Similar considerations apply to the Hamiltonian formulation of the non-Abelian Higgs theory  
 745 described in Section 3.1.2. The analog of the large  $\kappa$  limit in the Hamiltonian formulation  
 746 (Eq. (33)) is first of all to drop the conjugate variables  $\hat{Q}_i^m$  leaving only the  $\hat{\Lambda}$  variables in the  
 747 matter sector. This essentially renders the Higgs fields classical and they may be gauge fixed  
 748 without loss of generality along some fixed direction  $\phi^\alpha = \delta^{\alpha 1}$ . There is now a Hamiltonian  
 749 constraint

$$-\kappa \sum_{\ell} \hat{U}_{\ell}^{11} \quad (76)$$

750 that breaks gauge fluctuations from  $SU(N)$  down to  $SU(N - 1)$ .

751 Now if we consider only the boundary plaquettes, this constraint acts only on the bulk links  
 752 parallel to the boundary while those extending out of the boundary have no such constraint.  
 753 Therefore the boundary theory of the four dimensional bulk in the large  $\kappa$  limit is a three  
 754 dimensional  $SU(N)$  chiral model that is partially gauged by an  $SU(N - 1)$  gauge group where  
 755 the  $SU(N - 1)$  gauge theory permeates the bulk.

### 756 3.5 Boundary Phase Transition Order and Universality Class

757 So far we have demonstrated that Higgs models with group-valued or fundamental Higgs fields  
 758 have large- $\kappa$  limits with well-defined boundary degrees of freedom that may exhibit symme-  
 759 try breaking. Having discussed the  $\kappa \rightarrow \infty$  boundary actions for the family of fundamental  
 760 Higgs  $SU(N)$  models we are in a position to say something about the phase transitions at the  
 761 boundary. As the bulk is gapped for finite  $\kappa$  we should expect that the boundary theory has a  
 762 finite correlation length into the bulk making it a quasi- $(D - 1)$ -dimensional boundary theory  
 763 so that statements at  $\kappa \rightarrow \infty$  hold also for finite  $\kappa$ .

764 In the light of Refs. [22, 23] and our analysis above, the quasi- $(D - 1)$ -dimensional bound-  
 765 ary theory typically should have a symmetry breaking phase transition as the boundary cou-  
 766 pling is tuned. But what is the nature of the phase transition? When there are only global  
 767 symmetries, the symmetry group and the spacetime dimension determine the type of the tran-  
 768 sition. When some symmetries are gauged, the full set of global symmetries (including higher-  
 769 form symmetries originating from the gauging [4]) are expected to determine the nature of  
 770 the phase transition, while the gauge redundancy only serves to reduce to the quotient space.  
 771 For the coupled bulk-boundary models considered here, the bulk gap ensures the integrity of  
 772 the boundary model across the phase diagram well away from bulk critical points. Having  
 773 identified the physical gauge-invariant boundary variables on the lattice that can go critical,  
 774 in this part we write down the corresponding Landau boundary theories.

#### 775 3.5.1 Group-Valued Higgs

776 The boundary degrees of freedom, Eq. (59), are gauge-invariant composites transforming under  
 777 the global  $\mathcal{G}_L \times \mathcal{G}_R$  symmetry. Considering the case  $\mathcal{G} = SU(N)$ , the coarse-grained (generally  
 778 complex) matrix-valued fields are denoted  $X_i^{ab}$  [48], where  $a, b$  are color indices, which  
 779 transform as  $\mathbf{X} \rightarrow \mathbf{g}_L \mathbf{X} \mathbf{g}_R^\dagger$  under the symmetry. The Landau theory is

$$\mathcal{L} = \text{Re Tr} [\partial^\mu \mathbf{X} \partial_\mu \mathbf{X}^\dagger] + a \text{Re Tr} [\mathbf{X}^\dagger \mathbf{X}] + b \text{Re Det} [\mathbf{X}] + \dots \quad (77)$$

780 The  $SU(N) \times SU(N)$  symmetry is susceptible to breaking down to the diagonal subgroup. This  
 781 set of models has been studied in Ref. [48] to which we refer for more details. One finds, in  
 782 the case  $N = 2$ , that the determinant contributes to the quadratic term. Numerically one finds  
 783 a continuous transition consistent with a quartic term stabilizing the free energy. In the case  
 784  $N = 3$ , the determinant is cubic implying that the transition is first order. In the case  $N = 4$ ,  
 785 the determinant contributes a quartic term but with a negative sign that is expected to drive  
 786 the transition first order. We therefore expect a continuous transition for  $N = 2$  and first order  
 787 for  $N = 3$  and for  $N = 4$ .

788 Chiral models on a lattice, such as the one in Eq. (60), have been studied for many years  
 789 especially in two dimensions at large  $N$ , where they are integrable [49]. If one is interested  
 790 in boundaries of four dimensional gauge theories, the three dimensional analogs of such  
 791 models are of interest. One early work on  $\mathcal{G} = SU(N)$  in three dimensions, Ref. [48], con-  
 792 tains Monte Carlo results for  $N = 2, 3, 4$ . For  $N = 2$  (Section 3.2) the symmetry group is  
 793  $SU(2) \times SU(2) \simeq O(4)$  and the transition is continuous, consistent with  $O(4)$  criticality. For  
 794  $N = 3, 4$  the numerical results reveal the transition to be first order in agreement with the  
 795 mean field theory predictions.

#### 796 3.5.2 Fundamental Higgs

797 The boundary model in the case of a fundamental Higgs has gauge-invariant degrees of free-  
 798 dom of the form  $\Phi_i^a \equiv U_i^{ab} \phi_i^b$  where  $a, b$  are the color indices, Eq. (73). There is a single global  
 799  $\mathcal{G}$  symmetry that acts from the left  $\Phi \rightarrow g \Phi$ . This will be broken spontaneously for sufficiently

800 large  $\beta$  (modulo Mermin-Wagner restrictions). The coarse-grained version of  $\Phi^a$  is denoted  
 801  $\Psi^a$  and the Landau theory for  $SU(N)$  is

$$\mathcal{L} = \partial^\mu \Psi^\dagger \partial_\mu \Psi + a \Psi^\dagger \Psi + b (\Psi^\dagger \Psi)^2 + \dots \quad (78)$$

802 which is invariant under  $U(N)$  transformations. This may instead be viewed as a theory of  
 803  $2N$  real variables invariant under the enlarged  $O(2N)$  symmetry group. This Landau theory  
 804 gives the impression that, for the three dimensional boundary of a four dimensional  $SU(N)$   
 805 gauge theory, there is a phase transition in the  $O(2N)$  universality class. In the case of  $SU(2)$   
 806 this is  $O(4)$  criticality as shown above at the level of the microscopic model both analytically  
 807 and numerically. Note that the coupling of the  $\Phi_i$  rotors in Eq. (74) is invariant under  $O(2N)$   
 808 rotations, even though the microscopic action manifestly only has a global  $SU(N)$  symmetry.

809 It may seem surprising that the  $SU(N)$  invariant model exhibits  $O(2N)$  criticality. One  
 810 simple check is that  $SU(N)$  has  $N^2 - 1$  generators and that  $SU(N) \rightarrow SU(N - 1)$  symmetry  
 811 breaking therefore has  $2N - 1$  broken generators (corresponding to the number of Goldstone  
 812 modes) which matches the count for  $O(2N) \rightarrow O(2N - 1)$  symmetry breaking where  $O(N)$  has  
 813  $N(N - 1)/2$  generators. But what about the terms that are  $SU(N)$  invariant but not  $O(2N)$   
 814 invariant? These terms are certainly present. An example is given by taking an operator  
 815  $\Xi_{ab} \equiv \Psi_a \Psi_b^\dagger$  which transforms as  $g \Xi g^\dagger$  and considering its determinant. This is only  $U(N)$   
 816 invariant, but it is also an irrelevant operator for  $N > 2$  in  $D = 4$ . More precisely, the couplings  
 817 in the action originating from the determinant have mass dimension  $[g_{\det}] = D + N(2 - D)$   
 818 which, in dimensions higher than two, is negative for all but  $N = 2, 3$  in three dimensions  
 819 and  $N = 2$  in four dimensions. As we have seen, the case of  $SU(2)$  is special because it is  
 820 identical to a problem with a group valued Higgs. So we have treated it separately. Therefore  
 821 the remaining puzzle relates to  $SU(3)$  in three dimensions where the determinant coupling  
 822 goes like  $|\Psi^\dagger \Psi|^3$  and is marginal by power counting. As with the problem of scalar field theory  
 823 in three dimensions [50], among other cases, we expect this sixth order term to be marginally  
 824 irrelevant. Taking this together with our results for  $SU(2)$  we surmise that the  $SU(N)$  boundary  
 825 theory phase transition is in the  $O(2N)$  universality class since terms breaking  $O(2N)$  down to  
 826  $SU(N)$  are irrelevant or marginally irrelevant.

### 827 3.5.3 Fate of the Un-Higgsed Subgroup: $SU(3)$ Numerical Results

828 The discussion above for the fundamental Higgs assumed that the relevant critical degrees of  
 829 freedom on the boundary are the  $\Phi_i$ , Eq. (73). One may be concerned, however, about the  
 830 residual fluctuations from the un-Higgsed  $SU(N - 1)$  part of the gauge group. In particular,  
 831 the  $\Phi_i$  are composite degrees of freedom between a boundary link and its attached Higgs field,  
 832 and that the boundary link also appears in the second term in the boundary action, Eq. (74),  
 833 a three-leg Wilson loop with projectors at the two bulk sites. However, since this term is not  
 834 charged under the global  $SU(N)$  symmetry acting on the boundary links from the outside, we  
 835 expect it to be irrelevant to the boundary criticality.

836 To verify this and our prediction of  $O(2N)$  criticality, we have performed simulations of 4D  
 837  $SU(3)$  gauge theory with fundamental Higgs. The Higgs field  $\phi_i$  is a 3-component complex  
 838 unit vector at each site, and we measure the average of the Higgs field measured from the  
 839 vacuum end of the boundary links, Eq. (73), along with the boundary Wilson loops,

$$\Phi = \frac{1}{L^3} \sum_{i \in \partial X} (U_i \phi_i) \in \mathbb{C}^3 \quad (79)$$

$$W_p = \frac{1}{3L^3} \sum_{(ij) \in \partial X} \frac{1}{3} \text{Re} \text{Tr} [U_i P_i U_{ij} P_j U_j^{-1}]. \quad (80)$$

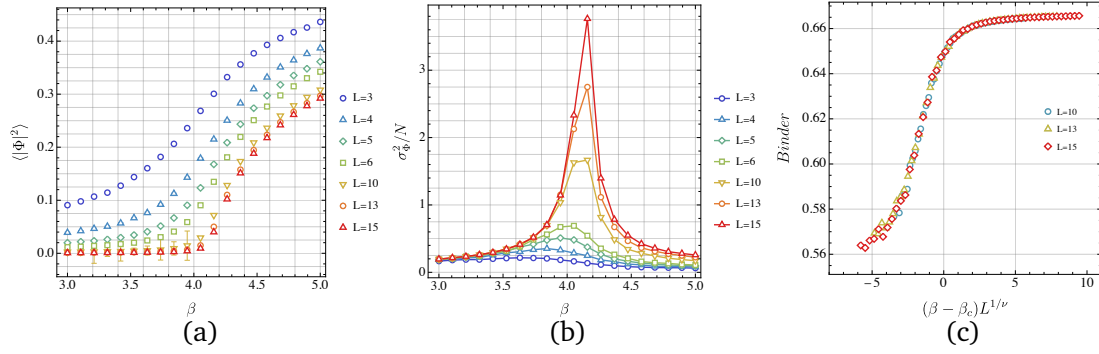


Figure 9: Monte Carlo results for the boundary phase transition for the SU(3) fundamental-Higgs model. (a) Boundary order parameter as a function of  $\beta$  at  $\kappa = 3.0$ . (b) Boundary susceptibility for the same  $\kappa$  showing a critical  $\beta$  of  $\beta_c \approx 4.19$ . (c) We use the previous  $\beta_c$  together with the 3D O(6) critical exponent  $\nu = 0.789$  from Ref. [51] to plot the Binder cumulant, showing a clear scaling collapse.

840 The numerical results for the average Higgs field are presented in Fig. 9 for  $\kappa = 3.0$ . Fig-  
 841 9(a) shows its behavior for various system sizes, while Fig. 9(b) shows the behavior of its  
 842 variance. The behavior is consistent with that of an order parameter at a second order phase  
 843 transition, approaching zero at small  $\beta$  and continuously increasing from  $\beta > \beta_c \approx 4.19$ , with  
 844 a diverging susceptibility. Figure 9 shows the Binder cumulant scaled by the 3D O(6) criti-  
 845 cal exponent  $\nu \approx 0.789$  [51], which shows a clear collapse to a universal scaling function.  
 846 Furthermore, Fig. 10 shows the behavior of  $W_p$ , which shows no system-size dependence and  
 847 smooth behavior, verifying that this term is irrelevant at the transition. We therefore conclude  
 848 that the SU(3) Higgs model in  $D = 4$  indeed demonstrates a boundary phase transition in  
 849 the 3D O(6) universality class, even though a single fundamental Higgs field does not remove  
 850 all bulk degrees of freedom when  $\kappa \rightarrow \infty$ , in agreement to the general picture of boundary  
 851 O(2N) criticality on the boundary of SU(N) fundamental Higgs models.

### 852 3.6 Summary and Discussion: Non-Abelian Case

853 In this section we have discussed global boundary symmetries in non-Abelian Higgs models  
 854 and their spontaneous symmetry breaking with both fundamental Higgs fields and group-  
 855 valued Higgs fields. For general non-Abelian gauge group  $\mathcal{G}$  there is a global  $\mathcal{G}$  symmetry  
 856 acting on the boundary of the system, which is equivalent by the Gauss law to the total color  
 857 charge of the system, Eq. (48). For the group-valued case, there is an additional bulk matter  
 858 symmetry given by right multiplication of the matter field. If  $\mathcal{G}$  is an Abelian group, these two  
 859 symmetries exactly coincide, since there is no distinction between left and right multiplication.  
 860 For  $\mathcal{G} = \text{SU}(2)$ , the two types of models are equivalent due to fact that SU(2) is equivalent to  
 861 the unit quaternions. For other gauge groups the two types of models are inequivalent. In  
 862 all cases, the location of the boundary transition that we identify can be shifted by tuning the  
 863 boundary coupling.

864 In the group-valued case, the infinite  $\kappa$  limit freezes the bulk of the system. The resulting  
 865 boundary theory can be expressed in terms of gauge-invariant half-open Wilson strings at the  
 866 boundary, Eq. (60). This may be viewed as a lattice discretization of a principal chiral model,  
 867 with  $\mathcal{G} \times \mathcal{G}$  symmetry coming from the boundary color flux and bulk matter symmetries. This  
 868 global symmetry is expected to be broken to the diagonal subgroup at large  $\beta$ . Since the  
 869 boundary is frozen in the  $\kappa \rightarrow \infty$  limit and should remain strongly gapped at large  $\kappa$ , the  
 870 boundary transition is expected to persist also for finite  $\kappa$ . Our SU(2) Monte Carlo simulations  
 871 verify this, and the boundary transition line appears to terminate at the bulk critical endpoint.

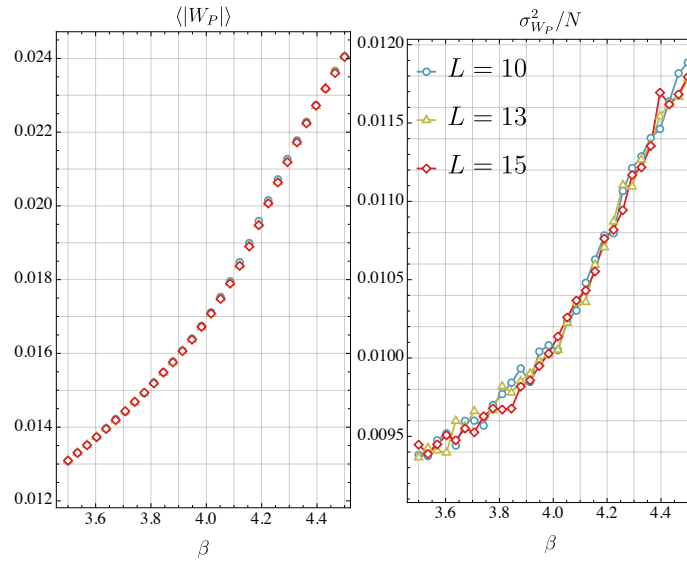


Figure 10: The expectation and variance of the boundary  $SU(N - 1)$  Wilson loop, Eq. (80), which appears as one of the two terms in the  $\kappa \rightarrow \infty$  limit of the fundamental-Higgs  $SU(N)$  boundary action in Eq. (74). This quantity shows no system-size dependence, indicating it plays no role in the boundary phase transition (cf. the boundary order parameter in Fig. 9).

872 For Higgs fields in the fundamental representation, there is only a single global  $\mathcal{G}$  symmetry,  
 873 generated by the total color charge of the system and acting on the boundary. The general  
 874 picture is that the bulk  $\mathcal{G}$  gauge symmetry is Higgsed down to a subgroup  $\mathcal{H}$ . If  $\mathcal{H}$  is trivial, then  
 875 the bulk is completely frozen in the  $\kappa \rightarrow \infty$  limit. If  $\mathcal{H}$  is Abelian, there may be a bulk phase  
 876 transition even at infinite  $\kappa$  (though that does not preclude a boundary symmetry breaking). If  
 877  $\mathcal{H}$  is non-Abelian then the bulk reduces to a gapped  $\mathcal{H}$  gauge theory as  $\kappa \rightarrow \infty$ . The boundary  
 878 theory is expected to be a gauged nonlinear  $\sigma$ -model with target space  $\mathcal{G}/\mathcal{H}$ , Eq. (75). Note  
 879 that by placing the Higgs in other representations (e.g. adjoint) or adding additional Higgs fields,  
 880 one may target different subgroups  $\mathcal{H}$  [52] and thus obtain different boundary theories. For  
 881 example, by starting from an  $SO(N)$  gauge theory with  $M$  Higgs fields in the fundamental  
 882 representation, the general expectation is that it reduces to an  $SO(N - M)$  gauge theory in the  
 883 bulk, and the boundary target space is the Stiefel manifold  $SO(N)/SO(N - M)$ , which have  
 884 recently attracted significant interest [53]

885 We considered in particular the case  $SU(N)$  (and by direct extension  $SO(N)$ ). In the  
 886  $\kappa \rightarrow \infty$  limit, the bulk Higgses down to a  $SU(N - 1)$  gauge theory, while the boundary de-  
 887 composes into a pure  $SU(N - 1)$  part and an  $SU(N)$  rotor part. The global symmetry, under  
 888 most circumstances, will be broken spontaneously at large  $\beta$ . We argued that this  $SU(N)$  fun-  
 889 damental Higgs boundary phase transition lies in the  $O(2N)$  universality class, since there are  
 890 no relevant operators differentiating  $SU(N)$  from  $O(2N)$ . We tested this prediction numeri-  
 891 cally for the  $SU(3)$  lattice gauge theory with fundamental Higgs, demonstrating a clean scaling  
 892 collapse with  $O(6)$  critical exponents.

893 One interesting exceptional case is  $SO(3)$  gauge theory with fundamental Higgs. This is  
 894 equivalent to the Georgi-Glashow electroweak theory, with gauge group  $SU(2)$  and the Higgs  
 895 field in the adjoint representation. In the  $\kappa \rightarrow \infty$  limit we can fix to unitary gauge which  
 896 Higgses the bulk gauge group down to  $SO(2) \simeq U(1)$ . In  $D = 4$  and  $\kappa \rightarrow \infty$ , the bulk has a  
 897 confinement-deconfinement transition as a function of  $\beta$ , while we predict an additional  $O(3)$   
 898 boundary critical point in the Higgs regime. This may have implications for the physics of

899 domain walls or cosmic strings formed in the early universe.

## 900 4 Boundary Symmetry Breaking in Higher-Form Abelian Higgs Mod- 901 els

902 Thus far we have discussed boundary symmetry breaking in Higgs phases of both Abelian and  
903 non-Abelian gauge theories with 1-form gauge fields, drawing a general picture of a global  
904 charge symmetry realized on the boundary due to the Gauss law constraint of a gauge-invariant  
905 system. Here we consider a further extension, to higher-form gauge fields. A  $k$ -form gauge  
906 field describes the parallel transport of charged  $(k - 1)$ -dimensional objects [54–57]. Two-  
907 form gauge fields are often called Kalb-Ramond fields in string theory literature [58], they  
908 appear in the dual descriptions of superfluids and superconductors [59, 60] and may be real-  
909 ized in certain spin models on frustrated lattices [61]. The gauge group for  $k > 1$  is generically  
910 Abelian, because a unique path ordering only exists on 1-dimensional contours [54, 55].

### 911 4.1 Higher-Form Abelian Higgs Models

912 Here we consider the case of  $k$ -form  $U(1)$  gauge theory, though restriction to  $\mathbb{Z}_N$  subgroups  
913 follows. Let  $A$  be a  $k$ -form field and  $\theta$  a  $(k - 1)$ -form field, each taking values in  $\mathbb{R}/2\pi\mathbb{Z}$  in  
914  $D$  Euclidean spacetime dimensions, with  $1 \leq k \leq D - 2$ .<sup>5</sup> By a  $k$ -form we mean a function  $\omega$   
915 on oriented  $k$ -dimensional cells  $c$  of the lattice, such that  $\omega(-c) = -\omega(c)$ , where  $-c$  denotes  
916 the cell  $c$  with the opposite orientation. See Appendix A for a more detailed discussion of the  
917 discrete differential forms notation used throughout this section. Let  $X_k$  denote the collection  
918 of  $k$ -cells of the lattice, each with a fixed orientation. The fields are governed by the generalized  
919 Fradkin-Shenker action

$$S_{\text{bulk}} = -\beta \sum_{c \in X_{k+1}} \cos(dA)_c - \kappa \sum_{c' \in X_k} \cos(d\theta - A)_{c'}. \quad (81)$$

920 The exterior derivative of a  $k$ -form  $\omega$  is a  $(k + 1)$ -form  $d\omega$  whose value is defined by the discrete  
921 Stoke’s theorem,

$$d\omega_c = \sum_{c' \in \partial c} \omega_{c'}, \quad (82)$$

922 where the sum is over the  $k$ -cells forming the oriented boundary of the  $(k + 1)$ -cell  $c$ . This is  
923 a straightforward generalization of the Abelian Higgs model, Eq. (8), to a theory of extended  
924  $(k - 1)$ -dimensional charged objects attached to  $k$ -dimensional electric flux branes [54].

925 The action is invariant under higher-form gauge transformations,

$$\theta \rightarrow \theta + \lambda, \quad A \rightarrow A + d\lambda, \quad (83)$$

926 for an arbitrary  $(k - 1)$ -form  $\lambda$ . We will see that this enforces the Gauss law attaching electric  
927 branes to the charged objects. When  $k > 1$ , this gauge invariance includes “gauge-of-gauge”  
928 transformations

$$\theta \rightarrow \theta + d\alpha, \quad (84)$$

929 for arbitrary  $(k - 2)$ -form  $\alpha$ . This yields an additional Gauss-type constraint which enforces  
930 that the  $(k - 1)$ -dimensional electrically charged objects are closed.<sup>6</sup>

<sup>5</sup>If  $k = 0$  there is no gauge field. If  $k = D - 1$  then the gauge field is not dynamical and can be completely integrated out using the Gauss law, yielding long-range interactions for the Higgs field. If  $k = D$  then  $dA = 0$  identically.

<sup>6</sup>In the continuum formulation these extra constraints are the pure-spatial components of the conserved higher-form Noether current [23].

931 When  $\kappa = 0$ , Eq. (81) reduces to a pure  $k$ -form U(1) gauge theory, which has a global  
 932 electric  $k$ -form symmetry given by

$$A \rightarrow A + \lambda \quad \text{with} \quad d\lambda = 0, \quad (85)$$

933 corresponding to conservation of global electric flux. In  $D$  spacetime dimensions, it also ad-  
 934 mits magnetic homotopy defects, whose cores trace out  $k_m$ -dimensional worldsheets in space-  
 935 time [54, 55, 62], where

$$k_m = D - (k + 2). \quad (86)$$

936 In the limit  $\beta \rightarrow \infty$  it has a  $k_m$ -form magnetic symmetry, discussed further in Section 4.2.

937 The phase diagram of this model is expected to be similar to that of the 1-form U(1) gauge  
 938 theory, sketched in Fig. 1, as long as  $D > k + 2$  ( $k_m > 0$ ). In the marginal case  $D = k + 2$   
 939 ( $k_m = 0$ ), the magnetic defect is an instanton (zero dimensional in spacetime) and is expected  
 940 to destabilize the deconfined phase [63–65]—a generalization of the Polyakov mechanism  
 941 for 1-form U(1) gauge theory in  $D = 3$  [66], which itself may be viewed as a higher-form  
 942 generalization of the Mermin-Wagner theorem for 0-form symmetries [4, 5]. In those marginal  
 943 cases, the bulk phase diagram should be qualitatively similar to that of the non-Abelian models  
 944 as in Fig. 5 [63, 67, 68].

#### 945 4.1.1 Gauss Law and Matter Symmetry

946 Before we introduce the Hamiltonian formulation and discuss matter symmetry, we point out  
 947 that the Higgs charges for  $k > 1$  behave slightly differently than for  $k = 1$ . When  $k = 1$ , the  
 948 zero-dimensional point charges must come in pairs at the two ends of oriented electric strings,  
 949 and are either positive or negative depending on which end of the string they sit. When  $k > 1$   
 950 the charges are extended oriented objects (e.g. strings when  $k = 2$ ) living on the edges of  
 951 electric  $k$ -branes. Such a brane for  $k > 1$  can have a single edge, meaning that it is perfectly  
 952 valid to have a single charged object in the system. As such the extended charged objects are  
 953 net-charge-neutral if they are contractible [54, 55]. It is only if they wrap around periodic  
 954 boundaries that they have non-trivial global charge.

955 The Hamiltonian formulation follows the exact arguments laid out in Section 2.1, with  
 956 conjugate operators  $[\hat{\theta}, \hat{n}] = i$  on all  $(k - 1)$ -cells and  $[\hat{A}, \hat{E}] = i$  on all  $k$ -cells. Invariance of  
 957 physical states under the gauge transformations, Eq. (83), enforces the Gauss law

$$-(d^\dagger \hat{E})_c \equiv -\sum_{c' \in \partial^\dagger c} \hat{E}_{c'} = \hat{n}_c \quad (c \in X_{k-1}), \quad (87)$$

958 where  $c$  is a  $(k - 1)$ -cell and the sum is over its coboundary, the set of  $k$ -cells  $c'$  containing  $c$   
 959 in their positively-oriented boundary. This simply says that the number of electric  $k$ -branes  
 960 emanating from  $c$  is equal to the amount of electric charge on  $c$ . For  $k > 1$ , the charges carry a  
 961 sense of orientation. For example, when  $k = 2$  the charges are nothing but the electric strings  
 962 of a 1-form gauge field. The “gauge-of-gauge” symmetry, Eq. (84), enforces the constraint

$$d^\dagger \hat{n} = 0, \quad (88)$$

963 which says that the charged objects are closed.<sup>7</sup>

964 In the  $k = 1$  theory discussed in Section 2 with 0-form Higgs field, the net charge of the  
 965 Higgs field generates a global 0-form symmetry, which is pure gauge with periodic boundaries

<sup>7</sup>This constraint obviously follows from the Gauss law Eq. (87) (following from  $d^2 = 0$ ), just as Eq. (84) is already implied by Eq. (83), but it is worth spelling out for those unfamiliar with this point.



966 but becomes physical with the choice of electric boundary conditions. The natural extension  
967 of this global matter symmetry for general  $k$  is a  $(k-1)$ -form symmetry,

$$\theta \rightarrow \theta + \lambda \quad \text{with} \quad d\lambda = 0. \quad (89)$$

968 Letting  $d = D - 1$  be the dimension of space, the generators of these transformations are  
969 Gukov-Witten operators [4] supported on  $(d - (k - 1))$ -dimensional closed surfaces  $\tilde{\Sigma}$  in the  
970 dual lattice

$$\hat{Q}(\tilde{\Sigma}) = \sum_{\tilde{c} \in \tilde{\Sigma}} \hat{n}_c \equiv \langle \hat{n}, \delta_{\tilde{\Sigma}} \rangle, \quad (90)$$

971 where  $c$  is the  $(k-1)$ -cell in the direct lattice corresponding to  $\tilde{c}$  in the dual lattice, and  $\delta_{\tilde{\Sigma}}$  is  
972 a  $(k-1)$ -form Poincaré dual to  $\tilde{\Sigma}$ .<sup>8</sup> These operators generate the symmetry, Eq. (89),

$$e^{-i\alpha\hat{Q}(\tilde{\Sigma})}|\theta\rangle = |\theta + \alpha\delta_{\tilde{\Sigma}}\rangle, \quad (91)$$

973 where  $\lambda \equiv \alpha\delta_{\tilde{\Sigma}}$  with  $\alpha$  a constant. Because  $\tilde{\Sigma}$  is a closed surface its Poincaré dual is a closed  
974 form,  $d\delta_{\tilde{\Sigma}} = \delta_{\partial\tilde{\Sigma}} = 0$ .

975 These operators are topological, i.e. they only depend on the homology class of  $\tilde{\Sigma}$ , ow-  
976 ing to the matter Gauss law Eq. (88). Consider replacing it with another surface such that  
977  $\tilde{\Sigma}' - \tilde{\Sigma} = \partial\tilde{V}$  for some  $(d - (k - 2))$ -volume  $\tilde{V}$ . Then  $\delta_{\tilde{\Sigma}'} = \delta_{\tilde{\Sigma}} + d\delta_{\tilde{V}}$ . Plugged into Eq. (90),  
978 we have

$$\hat{Q}(\tilde{\Sigma}') = \langle \hat{n}, \delta_{\tilde{\Sigma}} \rangle + \langle d^\dagger \hat{n}, \delta_{\tilde{V}} \rangle = \hat{Q}(\tilde{\Sigma}), \quad (92)$$

979 where we used the matter Gauss law, Eq. (88). Therefore there is one  $(k-1)$ -form charge  
980 generator for each homology class in  $H_{d-(k-1)}$ . Deforming  $\tilde{\Sigma}$  without changing its homology  
981 class corresponds to shifting  $\theta$  by an exact form, which are just the gauge transformations of  
982 Eq. (84).

983 The operators charged under  $\hat{Q}(\tilde{\Sigma})$  are the charge creation/annihilation operators, i.e.  
984 Wilson branes supported on open  $k$ -dimensional surfaces  $M$  which insert an electric membrane  
985 with charge on its boundary,

$$\begin{aligned} e^{i\alpha\hat{Q}(\tilde{\Sigma})} e^{i(d\hat{\theta}-A)(M)} e^{-i\alpha\hat{Q}(\tilde{\Sigma})} &= e^{-i\hat{A}(M)} e^{i\alpha\hat{Q}(\tilde{\Sigma})} e^{i\hat{\theta}(\partial M)} e^{-i\alpha\hat{Q}(\tilde{\Sigma})} \\ &= e^{-i\hat{A}(M)} e^{i(\hat{\theta}+\alpha\delta_{\tilde{\Sigma}})(\partial M)} \\ &= e^{i\alpha\#(\partial M, \tilde{\Sigma})} e^{i(d\hat{\theta}-\hat{A})(M)}, \end{aligned} \quad (93)$$

986 where we have defined the intersection number between the  $(k-1)$ -dimensional  $\partial M$  in the  
987 direct lattice and the  $(d - (k - 1))$ -dimensional  $\tilde{\Sigma}$  in the dual lattice,

$$\#(\partial M, \tilde{\Sigma}) = \delta_{\tilde{\Sigma}}(\partial M). \quad (94)$$

988 Thus the operator  $\hat{Q}(\tilde{\Sigma})$  simply counts the intersection number of the closed charged objects  
989 with  $\tilde{\Sigma}$ .

990 In the Maxwell case,  $k = 1$ , the matter charges are point particles,  $\tilde{\Sigma}$  is a closed  $d$ -dimensional  
991 volume in the dual lattice, and the only non-trivial choice is to take it to be all of space. The  
992 associated charge then simply counts the number of positive minus the number of negative  
993 charges. For a less trivial example, consider the case  $k = 2$  and  $d = 3$ , so that the matter  
994 charges are 1-dimensional strings and  $\tilde{\Sigma}$  is a closed two-dimensional surface in the dual lat-  
995 tice, intersecting a collection of links in the direct lattice. A choice of its Poincaré dual is a

<sup>8</sup>For our purposes, the defining property of the Poincaré dual of a  $(d-k)$ -dimensional closed surface  $\tilde{\Sigma}$  in the dual lattice is that it is a  $k$ -form in the direct lattice acting as a generalized delta function, for example the unit  $k$ -form supported on the direct lattice  $k$ -cells piercing  $\tilde{\Sigma}$  with the appropriate orientation. Note that  $\delta_{\tilde{\Sigma}}$  is only defined up to an exact form because  $\tilde{\Sigma}$  is closed, i.e. it is a cohomology class.

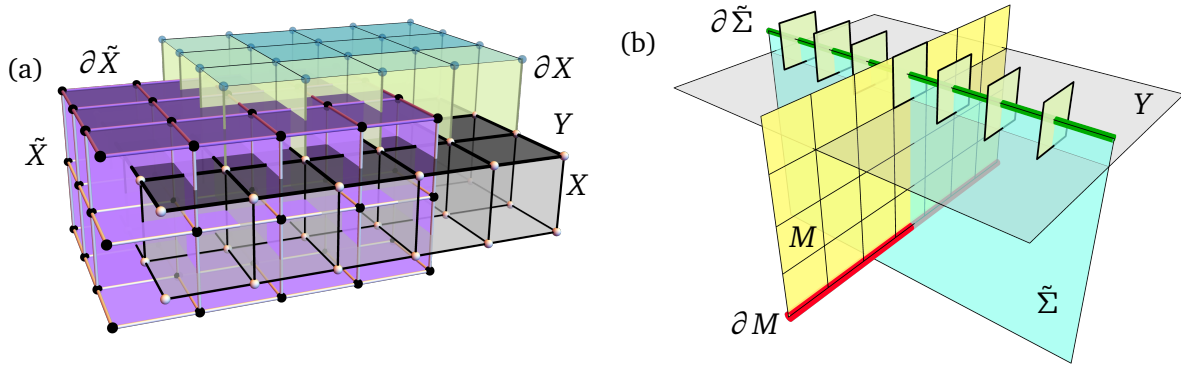


Figure 11: (a) An illustration of the relation between the direct lattice and dual lattice at the boundary of the system in  $d = 3$  spatial dimensions. The direct lattice is colored the same as in Fig. 2. The dual lattice is indicated by black dual sites, white dual edges, and purple dual plaquettes. Each  $k$ -cell of the direct lattice corresponds to a  $(d - k)$ -cell in the dual lattice. Because the boundary ( $\partial X$ ) of the direct lattice ( $X$ ) is open with cells “sticking out” (green), the dual boundary ( $\partial \tilde{X}$ ) is closed and has no protruding cells. We also color the  $(D - 1)$ -dimensional edge layer ( $Y$ ) dark gray, which is where the  $\kappa = \infty$  boundary action is defined, Eq. (102). (b) An illustration of a termination of  $\tilde{\Sigma}$  on the boundary for a 1-form Higgs field coupled to a 2-form gauge field in  $d = 3$  spatial dimensions.  $\tilde{\Sigma}$  is a two-dimensional surface (cyan) which terminates at the boundary along a 1-dimensional contour (green). The Gauss law makes  $\hat{Q}(\tilde{\Sigma})$  equal to the sum of the electric fluxes  $\hat{E}_p$  on the boundary plaquettes pierced by the edge of  $\tilde{\Sigma}$  (green squares with solid edges), Eq. (96). The edge  $\partial \tilde{\Sigma}$  then intersects the half-open Wilson membranes attached to a charged string (red curve) attached to an electric membrane (yellow) exiting the system through the open boundary.

1006 1-form which is zero everywhere except on the intersected links, on which it has unit value in  
 1007 the direction normal to the surface. The charge operator, Eq. (90), then counts (with signs,  
 1008 because  $\hat{n}_{-c} = -\hat{n}_c$ ) the number of strings piercing the surface  $\tilde{\Sigma}$ , i.e. the intersection number  
 1009 between closed strings and the surface. Because the charges are closed strings, this intersec-  
 1010 tion number must be zero unless  $\tilde{\Sigma}$  winds around a periodic boundary and intersects a charge  
 1011 which also winds around the periodic boundaries in the transverse direction.

1012 In a closed system, gauge invariance guarantees that the matter charge operators are  
 1013 exactly zero because of the Gauss law, Eq. (87), which when inserted into Eq. (90) yields  
 1014  $\langle \hat{E}, d\delta_{\tilde{\Sigma}} \rangle = 0$ . Equivalently, the intersection numbers, Eq. (94), are exactly zero because  $\partial M$   
 1015 has trivial homology class, i.e.  $\delta_{\tilde{\Sigma}}(\partial M) = d\delta_{\tilde{\Sigma}}(M) = 0$  since  $\tilde{\Sigma}$  is closed. Consider for exam-  
 1016 ple the case  $k = 2$ , where the charge operators count the number of charged strings wrapped  
 around a periodic boundary. We cannot, in a closed system, have a single non-contractible  
 charged string, because it is attached to an electric membrane which must end somewhere in-  
 side the system. The only possibility is that it ends on another non-contractible charged string  
 going the other direction, such that the two strings constitute the boundary of the electric  
 membrane. This is the sense in which a closed system is charge-neutral when  $k > 1$ .

#### 1012 4.1.2 Open Boundaries and Global Matter Symmetry

1013 To make the charge operators non-trivial, we must impose boundary conditions such that either  
 1014  $\tilde{\Sigma}$  can terminate on the boundary, and  $\delta_{\tilde{\Sigma}}$  is not a closed form, or such that the contour  $\partial M$   
 1015 can terminate at the surface and thus not be closed. The latter case, however, means that the  
 1016 charged objects can pass through the boundary, meaning charge is not conserved. Therefore,

1017 extending our results from Section 2, we take the former case. We consider open boundaries  
 1018 in the same form as Fig. 2. To be precise, the boundary consists of a layer of  $D$ -dimensional  
 1019 hypercubes, with all cells in the boundary layer which do *not* touch a bulk cell removed (or,  
 1020 equivalently,  $A = 0$  and  $\theta = 0$  on those cells). In other words, we remove the cells on the  
 1021 vacuum side, creating links missing one end, plaquettes missing one edge, cubic cells missing  
 1022 one face, etc. The boundary action is given by

$$S_{\text{bdry}} = -\beta \sum_{c \in \partial X_{k+1}} \cos(dA)_c, \quad (95)$$

1023 where  $\partial X_{k+1}$  denotes the set of  $(k+1)$ -cells in the boundary layer. As in Section 2, this  
 1024 boundary action does not allow the matter field  $\theta$  to tunnel through the boundary meaning  
 1025 that all the charged objects are closed and contained inside the bulk.

1026 In the presence of these boundary conditions, the matter charge operators, Eq. (90), can  
 1027 generate a physical symmetry. For  $k > 1$  we must take care to consider how the surfaces  $\tilde{\Sigma}$ ,  
 1028 which live in the dual lattice, can terminate at the boundary. Because we chose a “rough”  
 1029 boundary, as in Fig. 2, with a layer of cells sticking out from the edge of the system, the dual  
 1030 lattice boundary is flat. This is illustrated in Fig. 11(a) which shows the direct lattice bulk and  
 1031 boundary as in Fig. 2, along with the dual lattice in red and purple. The bulk part of the dual  
 1032 lattice is colored purple, while the boundary layer of the dual lattice is colored red and can  
 1033 be seen to form a flat surface without any protruding cells. The charge operators  $\hat{Q}(\tilde{\Sigma})$  can  
 1034 terminate on this flat dual boundary layer.

1035 For concreteness, consider the case  $k = 2$  in  $d = 3$ , in which case the matter charges are  
 1036 strings and  $\tilde{\Sigma}$  is a two-dimensional membrane in the dual lattice. Due to our boundary con-  
 1037 ditions the charge strings cannot terminate at the boundary, but the electric membranes can  
 1038 exit the system through the boundary. Referring to Fig. 11(b), consider a state with a single  
 1039 charged string wrapping around a periodic direction, as shown in Fig. 11(b) by the red line,  
 1040 attached to an electric membrane which exits through the boundary, illustrated by the yellow  
 1041 surface. This charged string is detected by taking the membrane  $\tilde{\Sigma}$  to intersect it transversely,  
 1042 as illustrated by the cyan surface. The charge associated to the surface, Eq. (90), is then related  
 1043 to the electric flux through the boundary via the Gauss law,

$$\hat{Q}(\tilde{\Sigma}) = \langle -d^\dagger \hat{E}, \delta_{\tilde{\Sigma}} \rangle = -\langle \hat{E}, d\delta_{\tilde{\Sigma}} \rangle = -\langle \hat{E}, \delta_{\partial \tilde{\Sigma}} \rangle \equiv \hat{Q}_{\text{bdry}}(\partial \tilde{\Sigma}). \quad (96)$$

1044 In the figure,  $\partial \tilde{\Sigma}$  is shown as a dark green line which pierces a collection of boundary plaque-  
 1045 ttes (green squares with black borders). According to Eq. (96), the amount of charge measured  
 1046 by  $\hat{Q}(\tilde{\Sigma})$  is equal to the number of electric branes exiting through the boundary measured by  
 1047 the set of plaquettes pierced by  $\partial \tilde{\Sigma}$ . In summary, the physical matter symmetry is generated  
 1048 by charge operators supported on  $\tilde{\Sigma}$  which terminate at the boundary and, by the Gauss law,  
 1049 acts on the gauge field  $A$  on the boundary elements pierced by  $\partial \tilde{\Sigma}$ .

### 1050 4.1.3 Boundary Symmetry Breaking

1051 Returning now to the higher-form gauge-Higgs action, Eq. (81), let us now see how the phys-  
 1052 ical charge symmetry is spontaneously broken at the boundary. In the limit  $\kappa \rightarrow \infty$  we have  
 1053 the constraint  $A = d\theta$  on every bulk  $k$ -cell. This completely freezes the bulk degrees of free-  
 1054 dom, as is seen by rotating to unitary gauge,  $\theta = 0$ , resulting in  $dA = 0$ . A covariant way to see  
 1055 this is that the gauge field operators  $A(M)$  for  $k$ -dimensional closed surfaces  $M$  trivialize—if  
 1056  $M$  is contained entirely within the bulk, then  $A(M) = d\theta(M) = \theta(\partial M) = 0$  since  $M$  is closed.  
 1057 This constraint is not imposed on the field variables on the cells touching the vacuum, how-  
 1058 ever. As a result, if  $M$  exist through the boundary, then we can decompose it into two pieces,  
 1059  $M = M|_X + M|_{\partial X}$ , where  $M|_X$  is the part of  $M$  supported on bulk cells and  $M|_{\partial X}$  is the part

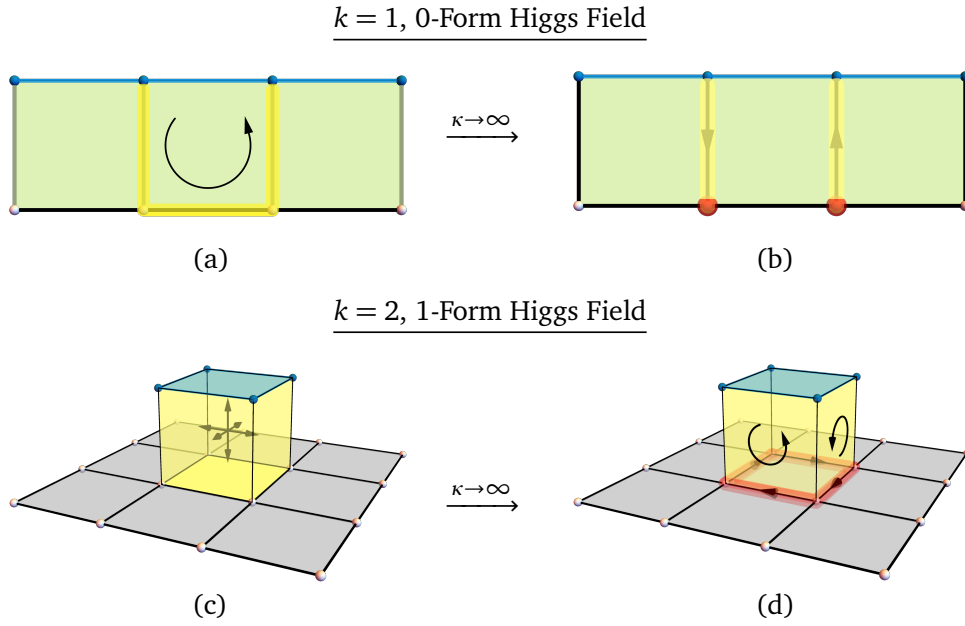


Figure 12: An illustration of how the  $\kappa \rightarrow \infty$  constraint  $A = d\theta$  turns closed membrane operators exiting through the boundary into open membrane operators terminating on a Higgs operator at the boundary. Each boundary  $(k+1)$ -cell  $c$  has one bulk  $k$ -cell  $c'$  in its boundary. The constraint turns  $A(c')$  on this  $k$ -cell into  $d\theta(c') = \theta(\partial c')$ . The end result is that all operators of the form  $A(M)$  where  $M$  exits the system through the boundary and is closed in the bulk are turned into open operators terminating on Higgs operators at the boundary, Eq. (98). We show (a,b) the case  $k = 1$  with a 0-form Higgs field, where (a) a string operator exiting the system at both ends (yellow), (b) turns into a pair of half-open string operators terminating on Higgs operators (red); and (c,d) the case  $k = 2$  with a 1-form Higgs field, where (c) a closed membrane operator exiting the system (yellow), (d) turns into a “half-open” membrane terminating on a Higgs string (red).

1060 supported on boundary cells. Since  $\partial M = 0$ , we have  $\partial M|_{\partial X} = -\partial M|_X$ . As a result, the gauge  
 1061 field operators decompose as

$$\begin{aligned} A(M) &\xrightarrow{\kappa \rightarrow \infty} A(M|_{\partial X}) + d\theta(M|_X) \\ &= A(M|_{\partial X}) + \theta(\partial M|_X) \\ &= A(M|_{\partial X}) - \theta(\partial M|_{\partial X}) \end{aligned} \tag{97}$$

$$= (A - d\theta)(M|_{\partial X}). \tag{98}$$

1062 In other words, for closed surfaces  $M$  exiting through the boundary, the  $\kappa \rightarrow \infty$  constraint  
 1063  $A = d\theta$  reduces  $A(M)$  to a half-open Wilson operator terminating on Higgs operators as soon  
 1064 as it touches the bulk. Similarly, longer half-open Wilson surfaces ending on the Higgs field  
 1065 in the bulk, e.g. Eq. (16), are reduced to short half-open Wilson surfaces ending on the Higgs  
 1066 field at the boundary.

1067 This is depicted in Fig. 12 for the cases  $k = 1$  and  $k = 2$ , where  $M$  is taken to be the  
 1068 smallest Wilson surfaces which are closed in the bulk,  $M = \partial c$  for  $c \in \partial X_{k+1}$ . In the case  
 1069  $k = 1$ , depicted in Fig. 12(a),  $c$  is an oriented boundary plaquette (green), and  $\partial c$  consists of  
 1070 three links (yellow), one of which is in the bulk. We decompose  $\partial c$  into the two links in the  
 1071 boundary, denoted  $\partial c|_{\partial X}$ , and the one link in the bulk, denoted  $\partial c|_X$ . The gauge field on the

1072 link in the bulk trivializes by the constraint  $A = d\theta$  into  $\theta$  evaluated at its two endpoints, i.e.  
 1073  $\theta(\partial(\partial c|_X))$ , depicted as red spheres in Fig. 12(b). These are the degrees of freedom appearing  
 1074 in the boundary action in Eq. (22). In the case  $k = 2$ , Fig. 12(c),  $c$  is a three-dimensional cube  
 1075 and  $\partial c$  is a set of five plaquettes (yellow). In Fig. 12(d), it decomposes into four plaquettes  
 1076 in the boundary (yellow),  $\partial c|_{\partial X}$ , and one plaquette in the bulk,  $\partial c|_X$ . The constraint turns  
 1077 the gauge field on this bulk plaquette into a Higgs string operator on its boundary (red). The  
 1078 extension to larger  $k$  is obvious, but can't be illustrated.

1079 Using this, we can see that the boundary action Eq. (95) contains precisely these minimal  
 1080 operators. In the general case, the action reduces in this limit to

$$\begin{aligned} S_{\kappa \rightarrow \infty}^{\text{bdry}} &= -\beta \sum_{c \in \partial X_{k+1}} \cos(dA)_c \quad (A_{\text{bulk}} = d\theta) \\ &= -\beta \sum_{c \in \partial X_{k+1}} \cos(A - d\theta)_{\partial c|_{\partial X}}. \end{aligned} \quad (99)$$

1081 We have already seen in Section 2 how in the case  $k = 1$  this can be recast as a 0-form XY  
 1082 model, Eq. (22), which we can now extend to the case  $k > 1$ . Note that every boundary  
 1083  $k$ -cell is associated to a unique bulk  $(k - 1)$ -cell (the one which trivializes under the  $A = d\theta$   
 1084 constraint). We define composite degrees of freedom for each such pair,

$$\vartheta(c) = A_{\partial X}(c) - \theta(c) \quad (c \in \partial X_{k-1}), \quad (100)$$

1085 where  $A_{\partial X}(c)$  is  $A$  evaluated on the unique boundary cell corresponding to  $c$ , which we treat as  
 1086 a  $(k - 1)$ -form rather than a  $k$ -form. Note that  $\vartheta$  are not gauge invariant when  $k > 1$ , because  
 1087 they would create open charged objects, but we can combine them to construct the gauge-  
 1088 invariant degrees of freedom appearing in Eq. (99). For example, in the case  $k = 2$ , each  $\vartheta$   
 1089 consists of  $A$  on a boundary plaquette and  $-\theta$  on the bulk link it touches, four of which combine  
 1090 to form the gauge-invariant composite object in Fig. 12(d). Let us denote the layer of bulk cells  
 1091 which touch the boundary layer, consisting of cells up to dimension  $d - 1$ , as  $Y$ , illustrated in  
 1092 Fig. 11 by the dark layer between  $X$  and  $\partial X$ . Each  $(k + 1)$ -cell  $c \in \partial X$  is associated to a unique  
 1093  $k$ -cell  $c_Y \in Y$ . We treat  $\vartheta$  as a  $(k - 1)$ -form gauge field in  $Y$ , so that its exterior derivative is  
 1094 given by

$$d\vartheta(c_Y \in Y_k) = (A_{\partial X} - \theta)(\partial c_Y) = (A - d\theta)(\partial c|_{\partial X}), \quad (101)$$

1095 where we identified  $\partial c_Y$  with  $\partial c|_{\partial X}$ . We can then write the boundary action Eq. (99) as

$$S_{\kappa \rightarrow \infty}^{\text{bdry}} = -\beta \sum_{c \in Y_{k-1}} \cos(d\vartheta). \quad (102)$$

1096 Equation (102) is precisely the action of a  $(k - 1)$ -form U(1) gauge theory defined at the  
 1097 boundary of the system in terms of composite half-open Wilson operators. In the case  $k = 1$  it  
 1098 reduces to the 0-form XY model identified in Section 2.

1099 We conclude that a  $k$ -form Abelian-Higgs model in  $D$  dimensions Higgses in the  $\kappa \rightarrow \infty$   
 1100 limit down to a  $(k - 1)$ -form gauge theory on the  $D - 1$  dimensional boundary. If  $D > k + 2$   
 1101 ( $k_m > 0$ ), this implies there will be a boundary phase transition. For  $k = 1$  this will be in the  
 1102  $(D - 1)$ -dimensional XY universality class, with a symmetry-broken phase at large  $\beta$ . For  $k > 1$   
 1103 it will be a confinement-deconfinement transition (expected to be first-order [7]), with a con-  
 1104 fined phase at small  $\beta$  and a deconfined phase at large  $\beta$ . This reduces to the results reported  
 1105 in Section 2 for  $k = 1$  and  $D = 4$ . The symmetry that is spontaneously broken at large  $\beta$  is  
 1106 the  $(k - 1)$ -form matter symmetry, corresponding to the electric symmetry of the boundary  
 1107 gauge theory when  $k > 1$ , under which  $d\vartheta$  (as a half-open Wilson operator) is charged. A  
 1108 summary of this result is given in the table Table 1 for  $k \leq 3$  and  $2 \leq D \leq 6$ , which may

1109 be extended straightforwardly to all  $k$  and  $D$ . In the cases where  $D = k + 2$  ( $k_m = 0$ ), a gen-  
 1110 eralized Mermin-Wagner theorem [5, 8] (equivalently, the Polyakov mechanism or magnetic  
 1111 instanton proliferation [66]) will prevent the symmetry from breaking. This may imply that  
 1112 the Higgs regimes of these marginal cases, which do not exhibit bulk higher-form symmetry  
 1113 breaking (deconfinement), are qualitatively distinct from the cases exhibiting boundary sym-  
 1114 metry breaking.

## 1115 4.2 Electric-Magnetic Dual Picture

1116 We can gain further insight into these Abelian models and the boundary symmetry breaking  
 1117 by reformulating them in terms of dual magnetic variables. We will do so for gauge group  
 1118  $U(1)$ . The duality transformation is well-established in a variety of forms [31–34]. We derive  
 1119 it here in the presence of our open boundary conditions, which provides a concrete picture of  
 1120 both the electric and magnetic sectors of the theory near the boundary.

### 1121 4.2.1 Open Boundary Duality Transformation

1122 The partition function of the original action for the  $k$ -form gauge theory is

$$Z = \int \mathcal{D}A \mathcal{D}\theta e^{-\beta \sum_{(x+\partial x)_{k+1}} \cos(dA) - \kappa \sum_{x_k} \cos(d\theta - A)}. \quad (103)$$

1123 This can be turned into a theory of electric strings and particles by utilizing the identity

$$e^{-x \cos(y)} = \sum_{n \in \mathbb{Z}} I_n(x) e^{iny},$$

1124 where  $I_n$  are Bessel functions. We introduce integer  $(k + 1)$ -form  $e$  coupled to  $dA$  and  $k$ -form  
 1125  $j_e$  coupled to  $d\theta - A$ , to rewrite the partition function exactly as

$$Z = \int \mathcal{D}A \mathcal{D}\theta \sum_e \sum_{j_e|_{\partial X} = 0} I_e(\beta) I_{j_e}(\kappa) e^{i\langle e, dA \rangle + i\langle j_e, d\theta - A \rangle}. \quad (104)$$

1126 The restriction  $j_e|_{\partial X} = 0$  arises from the fact that we did not include half-open Wilson strings  
 1127 coupling the bulk to the vacuum. Utilizing the adjointness relation  $\langle x, dy \rangle = \langle d^\dagger x, y \rangle$ , this  
 1128 reduces to

$$\begin{aligned} Z &= \sum_e \sum_{j_e|_{\partial=0}} I_e(\beta) I_{j_e}(\kappa) \int \mathcal{D}A e^{i\langle d^\dagger e - j_e, A \rangle} \int \mathcal{D}\theta e^{i\langle d^\dagger j_e, \theta \rangle} \\ &= \sum_e \sum_{j_e|_{\partial=0}} I_e(\beta) I_{j_e}(\kappa) \delta(d^\dagger e - j_e) \delta(d^\dagger j_e). \end{aligned} \quad (105)$$

1129 We interpret the  $k$ -form  $j_e$  as the worldlines swept out by the  $(k - 1)$ -dimensional Higgs ex-  
 1130 citations (carrying integer electric charge), and  $e$  as the worldsheets swept out by the  $k$ -form  
 1131 electric field. The first delta function is just the Gauss law—it tells us that the worldsheets of  
 1132 electric flux must terminate on the worldlines of the Higgs charges. The second delta function  
 1133 enforces that the the worldlines  $j_e$  are “divergence-free,” i.e. they form closed  $k$ -dimensional  
 1134 surfaces, corresponding to global conservation of charge. Note that, because the electric world-  
 1135 sheets can end, the electric 1-form symmetry  $d^\dagger e = 0$ , present when  $\kappa = 0$ , is explicitly broken,  
 1136 though it can be restored as an emergent symmetry at energies below the charge gap.

1137 With the choice of “electric” boundary conditions (Fig. 2), we have the constraint  $j_e = 0$   
 1138 on all links extending from the bulk to the vacuum in Eq. (105), because there is no  $d\theta$  term  
 1139 for these links, while  $e$  can be non-zero on the boundary plaquettes. This means that electric

1140 charge cannot enter or exit the system, but electric flux can. The fluxes in the bulk form closed  
 1141 surfaces unless they terminate on charges. In the presence of the boundary these fluxes may  
 1142 be cut off at the boundary without terminating on charges.

1143 We resolve the two constraints by writing<sup>9</sup>

$$j_e = d^\dagger h, \quad e = h + d^\dagger a_m, \quad (106)$$

1144 for integer  $(k + 1)$ -form  $h$  and  $(k + 2)$ -forms  $a_m$ , respectively. Note that these are not gauge-  
 1145 invariant and can be shifted by co-exact forms. We utilize the large-argument expansion of  
 1146 the Bessel functions,

$$I_n(z) \approx \frac{e^z}{\sqrt{2\pi z}} \left( 1 - \frac{4n^2 - 1}{8z} \right) \approx \frac{e^{z+1/8z}}{\sqrt{2\pi z}} e^{-n^2/2z},$$

1147 to approximate the partition function by<sup>10</sup>

$$Z \approx \sum_{a_m} \sum_h e^{-\frac{(d^\dagger a_m + h)^2}{2\beta}} e^{-\frac{(d^\dagger h)^2}{2\kappa}} \delta(d^\dagger h|_{\partial X}), \quad (107)$$

1148 where the delta function comes from the constraint  $j_e|_{\partial} = 0$  and we dropped the prefactor.  
 1149 Finally, we apply Poisson resummation to turn these into real-valued fields,

$$\sum_{n \in \mathbb{Z}} f(n) = \int_{\mathbb{R}} dx \sum_{m \in \mathbb{Z}} f(x) e^{-2\pi i m x}.$$

1150 We promote the integer fields to real fields,

$$h \rightarrow H \quad \text{and} \quad a_m \rightarrow A_m, \quad (108)$$

1151 coupled respectively to integer currents  $b$  and  $j_m$  via Poisson resummation. Lastly, we move  
 1152 to the dual lattice, replacing  $d^\dagger \alpha \leftrightarrow d\tilde{\alpha}$  for each  $p$ -form  $\alpha$ , where  $\tilde{\alpha}$  is a  $(D - p)$ -form in the  
 1153 dual lattice, the discrete Hodge dual of  $\alpha$  [34]. We thus obtain the dual partition function

$$Z_{\text{dual}} = \sum_{\tilde{j}_m, \tilde{b}} \int \frac{\mathcal{D}\tilde{H} \mathcal{D}\tilde{A}_m}{d\tilde{H}|_{\partial\tilde{X}=0}} e^{-\frac{(d\tilde{A}_m + \tilde{H})^2}{2\beta} - \frac{(d\tilde{H})^2}{2\kappa}} e^{-i2\pi[\langle \tilde{A}_m, \tilde{j}_m \rangle + \langle \tilde{H}, \tilde{b} \rangle]}, \quad (109)$$

1154 where  $\tilde{j}_m$  and  $\tilde{A}_m$  are  $(D - (k + 2))$ -forms, while  $\tilde{b}$  and  $\tilde{H}$  are  $(D - (k + 1))$ -forms, with the  
 1155 constraint that  $d\tilde{H}$  is zero within the dual boundary layer coming from the delta function in  
 1156 Eq. (107). Finally, let us rescale the fields by absorbing the  $2\pi$  into the definition of  $\tilde{A}_m$  and  
 1157  $\tilde{H}$ , to obtain the dual action

$$S_{\text{dual}} = -\frac{\beta'}{2} (d\tilde{A}_m + \tilde{H})^2 - \frac{\kappa'}{2} (d\tilde{H})^2 - i[\langle \tilde{A}_m, \tilde{j}_m \rangle + \langle \tilde{H}, \tilde{b} \rangle], \quad (110)$$

1158 with dual couplings  $\beta' = 1/4\pi^2\beta$  and  $\kappa' = 1/4\pi^2\kappa$ .

1159 The currents  $\tilde{j}_m$  and  $\tilde{b}$  correspond to the winding defects of the  $U(1)$  gauge field  $A$  and the  
 1160 Higgs field  $\theta$ , respectively. The former are the magnetic monopole worldlines, while the latter  
 1161 are the worldsheets of the vortices of the Higgs field. Under a gauge transformation of the  
 1162  $\mathbb{R}$ -valued gauge fields  $\tilde{A}_m \rightarrow \tilde{A}_m + \tilde{\lambda}$ ,  $\tilde{H} \rightarrow \tilde{H} - d\tilde{\lambda}$ , the action is shifted by

$$\delta S_{\text{dual}}^{\text{bulk}} = -i[\langle \tilde{\lambda}, \tilde{j}_m \rangle - \langle d\tilde{\lambda}, \tilde{b} \rangle] = -i[\langle \tilde{\lambda}, \tilde{j}_m - d^\dagger \tilde{b} \rangle]. \quad (111)$$

<sup>9</sup>Note that  $j_e$  and  $e$  can have a harmonic component corresponding to the electric winding sectors which we neglect. These give rise to ground state degeneracies in the topological Coulomb phase.

<sup>10</sup>We use the shorthand  $(\omega)^2$  to denote  $\langle \omega, \omega \rangle$ .

	1-Form U(1) Abelian-Higgs	2-Form U(1) Abelian-Higgs	3-Form U(1) Abelian-Higgs
$D = 2 + 1$	2D 0-Form U(1) BKT transition $k_m = 0$	$k_m = -1$	$k_m = -2$
$D = 3 + 1$	3D 0-Form U(1) continuous transition $k_m = 1$	3D 1-Form U(1) permanently confined $k_m = 0$	$k_m = -1$
$D = 4 + 1$	4D 0-Form U(1) continuous transition $k_m = 2$	4D 1-Form U(1) (de)confinement transition $k_m = 1$	4D 2-Form U(1) permanently confined $k_m = 0$
$D = 5 + 1$	5D 0-Form U(1) continuous transition $k_m = 3$	5D 1-Form U(1) (de)confinement transition $k_m = 2$	5D 2-Form U(1) (de)confinement transition $k_m = 1$

Table 1: The boundary theories of  $k$ -form U(1) Abelian-Higgs models in  $D$  spacetime dimensions in the  $\kappa \rightarrow \infty$  limit and their phase transitions. The pattern is that a  $k$ -form Abelian Higgs model Higgses down to a  $(k - 1)$ -form gauge theory on the boundary without matter. The number  $k_m = D - (k + 2)$  indicates the dimension of the magnetic worldlines of the bulk theory,  $\tilde{j}_m$  in Eq. (109). Note that in the  $\beta \rightarrow \infty$  limit the bulk has a corresponding  $k_m$ -form symmetry. Gray boxes indicates cases where the gauge field has no dynamics. The top non-trivial box of each column, which has  $D = k + 2$  ( $k_m = 0$ ), are affected by magnetic instanton proliferation (the Polyakov mechanism or a generalized Mermin-Wagner theorem forbidding boundary symmetry breaking) and do not exhibit a boundary phase transition, except in the case  $k = 1$  in  $D = 3$ , which can exhibit a BKT transition.

1163 If we integrate over all gauges, i.e. over all the generators  $\tilde{\lambda}$ , we obtain delta functions that  
 1164 yield the constraint

$$\tilde{j}_m = d^\dagger \tilde{b}. \quad (112)$$

1165 This says that the magnetic monopole worldlines form the boundaries of the Higgs vortex  
 1166 worldsheets. This is precisely the magnetic Gauss law, i.e. it says that magnetic monopoles are  
 1167 the sources of magnetic strings (compare to the electric Gauss law Eq. (105)). This is familiar  
 1168 from superconductor phenomenology—vortex cores carry magnetic flux. It also follows from  
 1169 this that  $d^\dagger \tilde{j}_m = 0$ , i.e. that the magnetic charge worldlines are closed and magnetic charge  
 1170 is conserved, which follows from the “gauge-of-gauge” invariance  $\tilde{A}_m \rightarrow \tilde{A}_m + d\tilde{\alpha}$  for arbitrary  
 1171  $\tilde{\alpha}$ .

1172 This theory can be recast as a U(1) gauge theory as follows. Summing over  $\tilde{b}$  undoes one  
 1173 of the Poisson resummations and forces  $\tilde{H} = 2\pi\tilde{h}$ , where the integer field  $\tilde{h}$  is the Hodge dual  
 1174 of  $h$  in Eq. (107). The residual gauge symmetry is  $\tilde{A}_m \rightarrow \tilde{A}_m + 2\pi\tilde{l}$  and  $\tilde{H} \rightarrow \tilde{H} - 2\pi d\tilde{l}$ , where  
 1175  $\tilde{l}$  is an integer shift, meaning that the gauge-invariant configuration space for  $\tilde{A}_m$  is actually  
 1176  $\mathbb{R}/2\pi\mathbb{Z}$  and for  $\tilde{H}$  is  $2\pi\mathbb{Z}$ . The resulting theory is therefore a Villainized  $k_m$ -form U(1) gauge  
 1177 theory [23, 69] (Eq. (86)) coupled to magnetic currents, the dual of the original Abelian Higgs  
 1178 model model, Eq. (103), which was coupled to electric currents. The integer gauge field  $\tilde{h}$   
 1179 measures the winding numbers of the compact  $\tilde{A}_m$ , and its fluxes  $d\tilde{H}$  are the homotopy defects  
 1180 of  $\tilde{A}_m$ , which are the electric charges of the original theory. They act as sources for the fluxes  
 1181  $d\tilde{A}_m$ , which are the electric strings in the direct lattice.

1182 Let us briefly review how the dual bulk behaves in the various limits in the Maxwell case,



1183  $D = 4$  and  $k = 1$ . First, consider the  $\beta \rightarrow \infty$  ( $\beta' \rightarrow 0$ ) limit: in the electric formulation the  
 1184 gauge field is turned off,  $dA = 0$ , and the remaining Higgs sector is a gauged  $4D$  XY model.  
 1185 In the dual theory the magnetic charges are turned off (integrating  $\tilde{A}_m$  sets  $\tilde{j}_m = 0$ ) and the  
 1186 magnetic 1-form symmetry is restored, resulting in a gas of closed membranes interacting via  
 1187 their coupling to the 2-form gauge field. Performing the Gaussian integration over  $\tilde{H}$  we obtain  
 1188 the action  $(\kappa'/2)\langle\omega, (d^\dagger d)^{-1}\omega\rangle$ , i.e. the gauge field  $\tilde{H}$  generates Coulomb interactions among  
 1189 the membranes.

1190 Next, consider the  $\kappa \rightarrow 0$  ( $\kappa' \rightarrow \infty$ ) limit. Electric charges are turned off, restoring the  
 1191 electric 1-form symmetry and reducing to a pure  $U(1)$  gauge theory. In the dual theory  
 1192 the gauge field  $\tilde{H}$  is turned off,  $d\tilde{H} = 0$ . The theory reduces to a Coulomb gas of magnetic  
 1193 monopole worldlines [31, 66], which has a phase transition separating the deconfined phase  
 1194 (low temperature condensate, 1-form symmetry spontaneously broken) and the confined phase  
 1195 (high temperature gas, 1-form symmetry unbroken).

1196 Lastly, consider the  $\beta \rightarrow 0$  ( $\beta' \rightarrow \infty$ ) limit, the strong coupling limit of the original theory.  
 1197 In the electric theory, we can fix unitary gauge to remove  $\theta$  and obtain the action  $-\kappa \cos(A)$  on  
 1198 every link independently, so the system is fully disordered. Equivalently, if we use Eq. (105),  
 1199 setting  $\beta = 0$  forces all of the Bessel functions to vanish except when  $e = j_e = 0$ , which reduces  
 1200 the partition function to  $\prod_\ell I_0(\kappa)$ . In the dual theory,  $\beta' \rightarrow \infty$ , the weak coupling limit, and  
 1201 we have the constraint  $\tilde{H} = -d\tilde{A}_m$ , which further implies  $d\tilde{H} = 0$ . The resulting theory then  
 1202 just has Lagrange multipliers that force the charge loops and membranes to vanish, so the  
 1203 theory trivializes completely.

#### 1204 4.2.2 Dual Boundary Symmetry Breaking

1205 We now consider setting  $\kappa' = 0$  in Eq. (110) ( $\kappa \rightarrow \infty$ ). The variables in play are  $\tilde{A}_m$  and  $\tilde{j}_m$ ,  
 1206 defined on all  $k_m$ -cells of the dual lattice, and  $\tilde{H}$  and  $\tilde{b}$  on all  $(k_m + 1)$ -cells. In the bulk, the  
 1207  $\kappa' = 0$  means that the kinetic term for  $\tilde{H}$  drops out and so the fluxes of  $\tilde{H}$  (corresponding to  
 1208 electric charges of the original action) are completely unconstrained. In other words, the bulk  
 1209  $\tilde{H}$  is in the strong coupling limit. We may integrate out  $\tilde{H}$ , to obtain

$$S_{\text{dual}}^{\text{bulk}} = -\frac{1}{2\beta'} \langle \tilde{b}, \tilde{b} \rangle - i \langle \tilde{A}_m, (\tilde{j}_m - d^\dagger \tilde{b})|_{\tilde{X}} \rangle. \quad (113)$$

1210 For a closed system, we can integrate out  $\tilde{A}_m$  and express the bulk partition function in the  
 1211 form

$$Z_{\text{dual}}^{\text{bulk}} \xrightarrow{\kappa \rightarrow \infty} \sum_{\tilde{b}} \sum_{\tilde{j}_m} e^{-\langle \tilde{b}, \tilde{b} \rangle / 2\beta'} \delta(d^\dagger \tilde{b} - \tilde{j}_m). \quad (114)$$

1212 The sum is over all possible configurations of the (open or closed) worldsheets  $\tilde{b}$  with a bare  
 1213 surface tension  $1/\beta' \propto \beta$ . An intuitive picture in the Maxwell case,  $k = 1$  and  $D = 4$ , is that  
 1214 in a time slice this corresponds to magnetic monopole pairs attached by a magnetic string with  
 1215 linearly rising potential, i.e. the magnetic charges are confined in this limit, as expected for a  
 1216 bulk electric condensate which collimates the magnetic field into flux tubes. The characteristic  
 1217 size (“Debye” screening length) of the neutral monopole pairs tends to zero as  $\beta$  tends to  $\infty$ .  
 1218 Alternatively, we may view this as monopole strings (worldlines)  $\tilde{j}_m$  interacting electrostatically  
 1219 through the membranes of the  $b$  field. For large  $\beta$  the membranes are short, meaning  
 1220 that the strings are bound into charge-neutral pairs. This phase persists to all  $\beta$  because the  
 1221 entropic gain of dipole strings outweighs their energetic cost at all effective temperatures.

1222 Now consider an open boundary. Recall that the boundary of the dual lattice is “flat”, as  
 1223 shown in Fig. 11, i.e. it has no cells extending into the vacuum. This means that no magnetic  
 1224 charge or magnetic flux can exit the system. More concretely, the constraint  $j_e|_{\partial X} = 0$ , in  
 1225 Eq. (104), in the electric variables is reflected in the dual constraint  $d\tilde{H}|_{\partial \tilde{X}} = 0$ , which enforces

1226 that  $\tilde{H}$  is pure gauge in the dual boundary layer. This means that the boundary action has no  
 1227  $\kappa$  dependence (it effectively has  $\kappa = 0$ ). We resolve the boundary constraint as  $\tilde{H} = d\tilde{f}$ , so  
 1228 that

$$S_{\text{dual}}^{\text{bdry}} = -\frac{\beta'}{2}(d(\tilde{A}_m + \tilde{f}))^2 - i\langle \tilde{A}_m, \tilde{j}_m |_{\partial\tilde{X}} \rangle - i\langle d\tilde{f}, b |_{\partial\tilde{X}} \rangle \quad (115)$$

1229 We then define a composite field  $\tilde{\chi} = \tilde{A}_m + \tilde{f}$ , which is gauge invariant under the gauge  
 1230 transformations  $\tilde{A}_m \rightarrow \tilde{A}_m + \tilde{\lambda}$  and  $f \rightarrow \tilde{f} - \tilde{\lambda}$ . This allows us to rewrite the boundary action  
 1231 as

$$S_{\text{dual}}^{\text{bdry}} = -\frac{\beta'}{2}(d\tilde{\chi})^2 - i\langle \tilde{\chi}, d^\dagger \tilde{b} |_{\partial\tilde{X}} \rangle - i\langle \tilde{A}_m, (\tilde{j}_m - d^\dagger \tilde{b}) |_{\partial\tilde{X}} \rangle. \quad (116)$$

1232 To proceed from here we need to be careful about how the  $\tilde{j}_m$  and  $\tilde{b}$  can move between the  
 1233 bulk and boundary layers. We do so in the  $\kappa \rightarrow \infty$  limit, by combining this with the bulk  
 1234 action Eq. (113). We can then integrate out  $\tilde{A}_m$  to generate the magnetic Gauss law, which is  
 1235 enforced on every link. This leaves us with the total action

$$S_{\text{dual}} \xrightarrow{\kappa \rightarrow \infty} -\frac{1}{2\beta'} \langle \tilde{b}, \tilde{b} \rangle_{\tilde{X}} - \frac{\beta'}{2} (d\tilde{\chi})_{\partial\tilde{X}}^2 - i\langle \tilde{\chi}, \tilde{j}_m |_{\partial\tilde{X}} \rangle. \quad (117)$$

1236 The boundary portion describes monopoles moving in the boundary layer interacting via a  
 1237 non-compact gauge field.

1238 One should be concerned here as to how the  $\tilde{j}_m$  from the bulk (edges of  $\tilde{b}$ ) couple to the  
 1239 boundary. The key to understand what happens here is that (i) the  $\tilde{b}$  membranes can lie in  
 1240 the boundary layer where they cost zero action, and (ii) for this action to be gauge-invariant  
 1241 under shifts of  $\tilde{\chi}$ , we must have an additional boundary Gauss law,

$$d^\dagger \tilde{j}_m |_{\partial\tilde{X}} = 0 \quad (118)$$

1242 This implies that, in the limit  $\kappa \rightarrow \infty$ , *magnetic monopoles cannot move between the boundary*  
 1243 *and the bulk*, i.e. there is a  $(k_m - 1)$ -form symmetry on the boundary (0-form in the Maxwell  
 1244 case) corresponding to conservation of boundary magnetic charge. The action Eq. (117) is  
 1245 precisely the dual of the  $\kappa = \infty$  boundary  $(k - 1)$ -form U(1) gauge theory Eq. (102), a 3D XY  
 1246 model in the Maxwell case.

1247 The  $\tilde{j}_m$  in the boundary layer must be coupled to  $\tilde{b}$  membranes by the magnetic Gauss law,  
 1248 but these have zero tension if they lie entirely within the boundary layer. This means that the  
 1249 Higgs vortices (magnetic field lines) are effectively not present within the boundary layer. This  
 1250 was by construction, since there were no  $d\theta$  terms in the original action which would allow  
 1251 for vortices of the Higgs field within the boundary layer. As a result, in the partition function  
 1252 to leading order the boundary and bulk are effectively decoupled from each other. Given any  
 1253 configuration of monopole worldlines  $\tilde{j}_m$ , which are closed in the boundary and closed in the  
 1254 bulk, the dominant contribution to the partition function will be for the boundary  $\tilde{j}_m$  to be  
 1255 connected to tensionless membranes in the boundary, rather than to be connected to a bulk  
 1256 monopole by a tensionful one. As a result, the monopoles on the boundary can condense  
 1257 at small  $\beta$ , which is the dual to the boundary symmetry breaking transition we found in the  
 1258 electric formulation.

1259 One can then consider turning on small  $\kappa'$  and doing a strong coupling expansion. This  
 1260 will have the effect of renormalizing the bulk length scale enabling boundary monopoles to  
 1261 extend further into the bulk by extending a magnetic flux tube while preserving the quasi-  
 1262  $(D - 1)$ -dimensional nature of the boundary.

### 1263 4.3 Summary and Discussion: Higher-Form Case

1264 In this section, we have generalized our results from Section 2 on 1-form Abelian-Higgs mod-  
 1265 els to higher form Abelian-Higgs models in  $D$  spacetime dimensions. In particular, we found

1266 that  $k$ -form gauge field coupled to a  $(k - 1)$ -form Higgs field reduces at infinite  $\kappa$  to a  $(k - 1)$ -  
 1267 form gauge theory on the boundary whose dynamical degrees of freedom are half-open Wilson  
 1268 branes terminating on the Higgs field as soon as they enter the bulk. This boundary theory ex-  
 1269 hibits a confinement-deconfinement transition when  $D > k + 2$  ( $k_m > 0$ ), which spontaneously  
 1270 breaks the  $(k - 1)$ -form global matter symmetry at large  $\beta$ . Table 1 summarizes this pattern  
 1271 of boundary symmetry breaking. In the marginal cases,  $D = k + 2$  ( $k_m = 0$ ), a generalized  
 1272 Mermin-Wagner theorem prevents the symmetry from breaking, except in the case  $D = 3$  and  
 1273  $k = 1$ , where we predict a BKT boundary transition. There are also precisely the cases where  
 1274 the same mechanism destabilizes the deconfined phase in the bulk [63, 64]. As in the 1-form  
 1275 Abelian and non-Abelian cases studied numerically in this paper, we expect that this boundary  
 1276 phase transition extends into the phase diagram when bulk fluctuations are restored and will  
 1277 end at a bulk critical point, demarcating a boundary between the Higgs and confining regimes.

1278 The general mechanism for this emergent boundary theory at large  $\kappa$  identified by con-  
 1279 sidering higher-form Abelian-Higgs models revolves around the constraint  $A = d\theta$  enforced  
 1280 exactly at infinite  $\kappa$ . This constraint implies that the Wilson operators which create electric  
 1281 charges attached to electric membranes,  $\exp[i(d\hat{\theta} - \hat{A})(M)]$  for open surfaces  $M$ , act as the  
 1282 identity. This naïvely indicates that the system is a condensate of electric charge in this limit,  
 1283 i.e. the ground state is a coherent state of the charge annihilation operators. As a consequence,  
 1284 the electric-brane insertion operators  $\exp[i\hat{A}(M)]$  for closed surfaces  $M$  trivialize in the bulk. In  
 1285 the presence of electric-flux-permeable open boundaries, however, operators inserting electric  
 1286 flux through the boundary are immediately screened as soon as they enter the bulk, terminat-  
 1287 ing on the Higgs field, as shown in Fig. 12, and become charged under the matter symmetry.  
 1288 These operators are the dynamical degrees of freedom at play at the boundary which exhibit  
 1289 the matter symmetry breaking. Presumably when  $\kappa$  is reduced the electric flux can penetrate  
 1290 further into the system before being screened by the electric charge condensate, forming a  
 1291 quasi- $(D - 1)$ -dimensional boundary. It would be interesting to explore whether this mech-  
 1292 anism can be extended to higher-form non-Abelian theories described by higher-categorical  
 1293 gauge groups [70–74].

1294 In the second part of this section, we studied the dualized version of these theories, iden-  
 1295 tifying the boundary degrees of freedom and accounting, in the 1-form case and  $D = 4$ , for  
 1296 the existence of the dual to the 3D XY model that we found in terms of direct variables. Mag-  
 1297 netic charge moves in the boundary layer, and there is an extra Gauss law in the  $\kappa \rightarrow \infty$  limit  
 1298 which originates from the constraint that electric charge cannot leave the system. This en-  
 1299 forces that magnetic charge cannot leave the boundary into the bulk, and thus the charges on  
 1300 the boundary can condense, leading to the dual phase transition. It would be of interest to  
 1301 study the dual theory in more detail, since it gives a clearer picture of the boundary symme-  
 1302 try breaking in the large- $\kappa$  (small  $\kappa'$ ) limit. In particular, it would be worthwhile to pursue  
 1303 Monte Carlo simulations in the dual representation, for which efficient algorithms have been  
 1304 developed [75–77]. It is also worth re-emphasising the importance of our choice of boundary  
 1305 conditions, which prevented electric charge from leaving the system while allowing electric  
 1306 flux to leave. In the dual theory this led to a flat dual boundary, meaning magnetic charge  
 1307 and flux is always contained in the system and cannot leave. It follows that if one started with  
 1308 flat boundaries, which keep all electric charge and flux inside the system, the dual boundaries  
 1309 would be open, i.e. magnetic charges are kept in the system but magnetic flux can leave. This  
 1310 implies a physical magnetic charge symmetry which can spontaneously break in the confined  
 1311 regime rather than the Higgs regime, with a phase transition on the  $\beta = 0$  axis instead of the  
 1312  $\kappa' = 0$  axis.<sup>11</sup>

<sup>11</sup>This was also discussed in the  $\mathbb{Z}_2$  1-form case in [22].

## 1313 5 Discussion and Conclusion

### 1314 5.1 Summary and Outlook

1315 In this work we have explored a variety of models of charged Higgs fields coupled to gauge  
 1316 fields in the fundamental representation, under the imposition of boundary conditions which  
 1317 allow electric flux, but not charge, to exit the system. In a closed system, the gauge field does  
 1318 not have a physical global charge symmetry which can spontaneously break, because a charge  
 1319 is always attached to electric flux, which must end inside the system on another charge. With  
 1320 the “electric-flux-permeable” boundary conditions we consider, the charge sectors and global  
 1321 symmetry become physical, as non-zero bulk charge can be compensated by non-zero bound-  
 1322 ary flux, and can in principle spontaneously break. This work, focusing on the boundary  
 1323 degrees of freedom, complements work exploring the interplay of global and gauge symme-  
 1324 tries in the bulk. See for example recent work in Refs. [78–82]. More broadly, the boundary  
 1325 perspective offers novel insight into the gauge-invariant description of Higgs phases and how  
 1326 they might be distinguished from confined phases, issues with a long history [13–15, 25, 26]  
 1327 which continue to generate interest to the present day [17–23, 37, 83–85].

1328 We have considered the Abelian-Higgs model, two types of non-Abelian Higgs models (with  
 1329 fundamental representation and group-valued Higgs fields), and higher-form Abelian-Higgs  
 1330 models. In terms of the inverse gauge coupling  $\beta$  and the matter coupling  $\kappa$ , all of these models  
 1331 share the common feature of a continuity between an electric-charge confining regime at small  
 1332  $\beta, \kappa$ , and a Higgs regime at large  $\beta, \kappa$ , which are two ends of one continuous thermodynamic  
 1333 phase, as proven by Fradkin and Shenker [14]. We have demonstrated through a combination  
 1334 of analytical argument and numerical investigation that, under all but a few marginal cases,  
 1335 there is a boundary phase transition which indicates the spontaneous breaking of the matter  
 1336 symmetry at large  $\beta, \kappa$ , i.e. in the Higgs regime, as illustrated in Fig. 1. Already in the seminal  
 1337 work of Fradkin and Shenker [14] it was understood that in gauge theories with fundamental  
 1338 Higgs matter, under most circumstances thermodynamic quantities exhibit no singularities  
 1339 along paths between Higgs and confined regimes, meaning that they form the same bulk phase  
 1340 of matter. The boundary spontaneous symmetry breaking investigated in this paper does not  
 1341 contradict this result, because it does not define a precise bulk phase boundary between the  
 1342 Higgs and confined regimes. Indeed, as we observed, one may tune the boundary coupling  
 1343 while preserving all the bulk properties to shift the location of the boundary phase transition.

1344 Ref. [22] predicted a boundary phase transition in the case of gauge group  $\mathbb{Z}_2$ , and verified  
 1345 it using DMRG in  $D = 2 + 1$  dimensions. Ref. [23] predicted the boundary transition for a mag-  
 1346 netic monopole-free Abelian U(1) Higgs model without numerics. Using lattice gauge theory  
 1347 Monte Carlo simulations, we have explored a wider range of models, both for Abelian and non-  
 1348 Abelian gauge groups. In Section 2, we have numerically verified and studied the boundary  
 1349 transition for gauge group U(1) (with monopoles) in  $D = 3 + 1$  dimensions, which exhibits a  
 1350 boundary XY transition. In Section 3, we extended this to non-Abelian gauge groups, perform-  
 1351 ing numerical simulations for both SU(2) and SU(3) gauge theories coupled to fundamental  
 1352 Higgs fields in  $D = 3 + 1$ , and considered generalizations to SU( $N$ ), SO( $N$ ), and general gauge  
 1353 groups. Lastly, in Section 4 we studied higher-form generalizations of Abelian-Higgs models,  
 1354 and demonstrated that the corresponding higher-form matter symmetry can spontaneously  
 1355 break at the boundary. In all of our numerical simulations, the nature of the boundary phase  
 1356 transitions deduced from the numerical data conforms to predictions obtained by studying the  
 1357  $\kappa \rightarrow \infty$  limit.

1358 We expect the considerations in this work to extend further to all gauge groups and dif-  
 1359 ferent Higgs representations [52]. Notably we have not discussed higher-rank gauge theories  
 1360 coupled to scalar matter that are connected to fractonic excitations [86–91], but here too one

1361 may preserve the Gauss law for tensor fields on the boundary and expect a  $U(1)$  global sym-  
1362 metry that, for certain classes of such models, can be broken spontaneously. It would also  
1363 be of interest to extend these results to discrete non-Abelian gauge groups, and non-Abelian  
1364 higher-form gauge theories with higher-categorical gauge groups [71–74].

1365 Before continuing, we comment briefly on some interesting connections between our work  
1366 and two other active areas of research: boundary criticality and asymptotic symmetries. “Tra-  
1367 ditional” boundary criticality has a long history [92, 93], and has recently received some new  
1368 insights [94, 95]. The central idea is that the boundary of a system may undergo a phase tran-  
1369 sition in a novel “extraordinary” universality class when coupled to a critical bulk, by tuning  
1370 the boundary coupling relative to the bulk. In this work we have only considered the behavior  
1371 of the boundary when the bulk is gapped, but it would be interesting to explore the boundary  
1372 criticality in more detail in the vicinity of the bulk critical point where the transition appears  
1373 to end for  $\alpha \geq 1$  (cf. Figs. 4 and 8), especially at the lower critical dimension [94]. Prior  
1374 boundary criticality studies have focused on criticality from the spontaneously breaking of 0-  
1375 form symmetries, but our work raises the possibility of novel boundary physics arising from  
1376 dynamical gauge fields and higher-form symmetries. On the one hand, such exploration may  
1377 yield novel boundary universality classes, and on the other it may yield some new insights into  
1378 the behavior of these enigmatic bulk critical points [96, 97].

1379 Another active area with some overlap with this work is the exploration of asymptotic sym-  
1380 metries in gauge theories and gravity on the boundary of compactified spacetime [98–107].  
1381 For example, in pure electromagnetism in Minkowski spacetime at null infinity it is well known  
1382 that there is an infinite dimensional symmetry generated by large gauge transformations with  
1383 conserved charges living on the boundary [100]. Indeed, Ref. [103] has already made some  
1384 direct connections between asymptotic (or “long-range gauge”) symmetries and the boundary  
1385 symmetries studied in this work. It would be interesting to deepen the connections between  
1386 Higgs boundary criticality on the lattice and asymptotic symmetries in the continuum.

## 1387 5.2 Higgs = SPT

1388 It would be remiss of us to conclude this paper without a description of some of the work  
1389 that motivated this study—namely the papers [21–23] discussing the relationship of Higgs  
1390 phases to symmetry-protected topological (SPT) phases. We briefly summarize the main find-  
1391 ings therein and comment on how our results bear on the generality of this relationship. For  
1392 more recent works related to this topic see Refs. [108–110]. An SPT phase is a state of mat-  
1393 ter that cannot be adiabatically connected to a trivial phase under local symmetry-preserving  
1394 perturbations without closing a gap. In general, a trivial phase can be reached without gap  
1395 closure only if those symmetries are broken. A classic example of an SPT phase in an inter-  
1396 acting lattice model is the spin one-half chain—the cluster model—whose nontrivial topology  
1397 is protected by  $\mathbb{Z}_2 \times \mathbb{Z}_2$  symmetry [111, 112]. A consequence of the topological nature of the  
1398 phase is the presence of gapless states localized at the boundary of an open chain.

### 1399 5.2.1 Review of Higgs=SPT

1400 The “Higgs=SPT” connection was first raised in Ref. [21], which considered gauging the  $\mathbb{Z}_2$   
1401 fermion parity symmetry of the Kitaev chain, which hosts an SPT phase. Gauging trivializes  
1402 the symmetry in the bulk, but by the same arguments we have discussed throughout this paper,  
1403 it is instead realized non-trivially on the boundary. In the Higgs regime a fermionic SPT order  
1404 emerges (that belongs to the same class as a stack of two Kitaev chains) protected by the  
1405  $\mathbb{Z}_2$  boundary fermion parity symmetry and the  $\mathbb{Z}_2$  0-form magnetic symmetry of the gauge  
1406 field. Allowing instantons (magnetic tunneling events) explicitly breaks the 0-form magnetic  
1407 symmetry and kills the SPT. In the similar spirit, it was argued that by gauging the  $\mathbb{Z}_2$  parity

1408 symmetry of the transverse field Ising model, in the Higgs phase one ends up with the cluster  
1409 SPT order.

1410 These 1D results were extended in Ref. [22] to the Higgs phases of  $\mathbb{Z}_2$  gauge theory with  
1411 matter in general dimensions with electric boundary conditions (Fig. 2). The phase diagram is  
1412 qualitatively the same as Fig. 1, with (within our notation) the deconfined phase at large  $\beta$  and  
1413 small  $\kappa$  exhibiting  $\mathbb{Z}_2$  toric code topological order (i.e. 1-form symmetry breaking) [22,28,97].  
1414 The  $\mathbb{Z}_2$  magnetic symmetry is a  $(d-1)$ -form symmetry.<sup>12</sup> The global  $\mathbb{Z}_2$  0-form Ising matter  
1415 symmetry is trivial in the bulk but is realized at the boundary. It was shown that on the  
1416 line  $\beta = \infty$  and in the large- $\kappa$  Higgs limit there is a cluster SPT order, protected by the  $\mathbb{Z}_2$   
1417 higher-form magnetic symmetry and the matter symmetry, hosting gapless surface states and  
1418 a boundary ground state degeneracy.<sup>13</sup> Going to finite  $\beta$  explicitly breaks the magnetic 1-form  
1419 symmetry, but as long as the magnetic symmetry is higher-form it is expected to survive in  
1420 the infrared as a low-energy emergent symmetry, because the magnetic defects are gapped at  
1421 large  $\beta$ .<sup>14</sup> Moreover, it was shown that in the  $\kappa = \infty$  limit the boundary degrees of freedom  
1422 are governed by an Ising model charged under the global matter symmetry, which is in the  
1423 spontaneously broken phase for large  $\beta$ . The boundary ground state degeneracy of the putative  
1424  $\beta = \infty$  SPT were directly identified with the Ising degeneracy of this phase. The boundary  
1425 symmetry breaking was verified numerically with a phase diagram qualitatively the same as  
1426 Fig. 1, and within the resolution of the DMRG numerics of Ref. [22] the phase boundary to  
1427 the boundary gapless phase extends from the critical endpoint. However, one cannot simply  
1428 identify the boundary-symmetry-broken regime with a bulk SPT, indeed Ref. [22] observed  
1429 that the position of the transition depends on microscopic details near the boundary (such as  
1430 the deformation  $\alpha$  which we have considered). Instead it was argued that certain properties  
1431 of SPT (such as edge modes and degeneracies of the entanglement spectrum) should be stable  
1432 in the Higgs regime in an open region of the phase diagram in the vicinity of the  $\beta \rightarrow \infty$   
1433 limit.<sup>15</sup> In particular, the mutual anomaly between the matter and magnetic symmetries at  
1434 the boundary is robust, and correspondingly the edge mode degeneracies should be as well  
1435 until a gap is closed.

1436 These ideas were extended in Ref. [23], which considers U(1) Higgs models with *exact*  
1437 magnetic symmetry, i.e. *without* magnetic monopoles. Starting from the continuum theory,  
1438 Eq. (1), the mutual anomaly can be exposed by coupling to background gauge fields for both  
1439 symmetries—1-form  $A_{\text{mat}}$  for the matter symmetry and  $(d-1)$ -form  $B_{\text{mag}}$  for the magnetic  
1440 symmetry. Deep in the Higgs regime, the bulk topological response was found to be

$$S_{\text{SPT}} = \frac{1}{2\pi} \int B_{\text{mag}} \wedge dA_{\text{mat}}. \quad (119)$$

1441 For a system with open boundaries this SPT response is not gauge invariant without adding  
1442 appropriate boundary degrees of freedom which cancel the anomaly. For the 3 + 1D Higgs  
1443 phase, the boundary theory takes the form

$$S_{\text{Boundary}} = \frac{1}{2\pi} \int d\varphi \wedge d\vartheta \quad (120)$$

<sup>12</sup>Note that the magnetic symmetry is  $(d-1)$ -form for discrete gauge group and  $(d-2)$ -form for U(1), where  $d$  is the dimension of space.

<sup>13</sup>For earlier work on SPTs protected by generalized symmetries see for example Refs. [74,113]

<sup>14</sup>The magnetic symmetry is equivalent to the closure of magnetic flux surfaces. The presence of magnetic defects allows the fluxes to end without closing, and thus explicitly breaks the symmetry. At large  $\beta$  the magnetic defects will have a large gap, and therefore at low energies magnetic fluxes will again be closed. Thus the symmetry is expected to be emergent in the infrared [114]. Indeed this argument explains why the deconfined phase, which spontaneously breaks the higher-form electric and magnetic symmetries, is stable in the presence of gapped magnetic and electric charges [4].

<sup>15</sup>The entanglement spectrum in this model was investigated recently in [115].

1444 for the conjugate pair: a compact scalar field  $\varphi$  and a compact  $U(1)$  gauge field  $\vartheta$ . This  
 1445 describes a boundary  $U(1)$  superfluid phase, which has the correct mixed anomaly to cure the  
 1446 bulk one [6]. This continuum discussion was supplemented with a lattice Villain formulation,  
 1447 where monopoles are under control and the magnetic 1-form symmetry is preserved.

1448 As it stands, we can summarize the Higgs=SPT situation as follows. For Abelian gauge  
 1449 fields coupled to fundamental matter with *exact* magnetic symmetry, the matter symmetry  
 1450 is realized at the boundary and shares a mutual anomaly with the bulk magnetic symmetry.  
 1451 The bulk of the system can be identified as an SPT protected by these two symmetries, and  
 1452 the SPT boundary modes originate from the spontaneously broken matter symmetry: for  $\mathbb{Z}_N$   
 1453 gauge group these are robust boundary discrete degeneracies, and for  $U(1)$  gauge group these  
 1454 are gapless edge modes identified with the boundary Goldstone modes. The authors of both  
 1455 Ref. [22] and Ref. [23] claim that some aspects of the SPT, in particular the edge modes and  
 1456 entanglement spectrum degeneracies, should be robust to explicit breaking of magnetic sym-  
 1457 metry (when it is a higher-form symmetry), even if the bulk is no longer strictly an SPT (and  
 1458 can indeed be continuously connected to the trivial confined phase).

### 1459 5.2.2 Insights, Challenges, and Future Directions

1460 Our work potentially extends the Higgs=SPT story, but also provides new challenges for it.  
 1461 Firstly, the general Higgs=SPT arguments generalize directly to the higher-form Abelian mod-  
 1462 els we considered in Section 4 if magnetic symmetry is enforced exactly. Secondly, we can  
 1463 say that spontaneous breaking of global charge conservation symmetry at the boundary is a  
 1464 universal feature of the Higgs regime, and that this statement applies to both Abelian and  
 1465 non-Abelian models. This could indicate that the Higgs-SPT relation holds in a much broader  
 1466 set of cases than originally envisioned. However, it may also be that the boundary symmetry  
 1467 breaking is a broader phenomenon than the Higgs=SPT relation, which happens to coincide  
 1468 with the SPT edge modes when the relation holds.

1469 We wish to point out an open issue for the Higgs=SPT connection with continuous gauge  
 1470 groups in the models we have considered here. In the Abelian-Higgs model, when the gauge  
 1471 group is discrete the gapped Higgs phase is continuously connected to the  $\beta = \infty$  limit where  
 1472 the magnetic symmetry is exact and the ground state is an SPT [22]. However, there is a  
 1473 subtlety about the large- $\beta$  limit in the  $U(1)$  case: the  $\beta = \infty$  limit of the Higgs regime is  
 1474 gapless, namely it is gauge-equivalent to a bulk superfluid. Therefore, if there is an SPT in  
 1475 the  $U(1)$  Fradkin-Shenker model at  $\beta = \infty$  where the magnetic symmetry is exact it must  
 1476 be gapless, and is therefore not adiabatically connected to the gapped Higgs phase when the  
 1477 gauge coupling is turned on.<sup>16</sup> Furthermore, the limiting point  $\beta = \kappa = \infty$  in the phase dia-  
 1478 gram is problematic, because the gap scales as  $\kappa/\beta$  as one approaches it [14]: approaching  
 1479 from  $\beta = \infty$  the bulk is gapless, while approaching from  $\kappa = \infty$  the bulk is gapped.<sup>17</sup> It is  
 1480 therefore unclear that the boundary edge modes of the gapped Higgs regime discussed in Sec-  
 1481 tion 2 and Section 4, particularly in the  $\kappa = \infty$  limit, can be identified with those of a putative  
 1482  $\beta = \infty$  SPT. Clearly this same issue holds for any continuous gauge group, in particular to the  
 1483 non-Abelian cases studied in Section 3.

1484 The physics of the non-Abelian gauge groups gives rise to a further puzzle. In Section 3 we  
 1485 have argued that in the limit  $\beta, \kappa \gg 1$  the boundary is generically expected to be gapless since  
 1486 it breaks a continuous symmetry. If the Higgs=SPT scenario is general enough to encompass  
 1487 the non-Abelian cases too, one should be able to identify the protecting (higher-form) bulk  
 1488 “magnetic” symmetry. Pure  $SU(N)$  gauge theory has no magnetic symmetry since the funda-

<sup>16</sup>This same problem with the  $\beta = \infty$  limit is also present in the Villainized model studied by Ref. [23] (in contrast to the Wilson model we have studied), but in that model one can effectively tune the magnetic monopole mass to infinity while holding  $\beta$  finite to obtain an exact magnetic symmetry.

<sup>17</sup>This limit was key to establishing the fixed-point SPT Hamiltonian in the  $\mathbb{Z}_2$  case in Ref. [22].

1489 mental group is trivial, and it is unclear whether there is a generalized symmetry present at  
 1490  $\beta = \infty$  for non-Abelian gauge groups that is an analog of the Abelian magnetic symmetry.

1491 Let us take a broader perspective and focus on the mutual anomaly which is key to the  
 1492 Higgs=SPT phenomenology. The core idea in the Abelian theories is as follows. Given an  
 1493 Abelian  $k$ -form symmetry  $\mathcal{G}$  there is a corresponding “dual”  $(d - k - n)$ -form  $\mathcal{G}$  symmetry cor-  
 1494 responding to suppressing defects in the ordered phase, where  $n = 0$  (1) if  $\mathcal{G}$  is discrete (con-  
 1495 tinuous), and these share a mutual anomaly [22, 23, 114].<sup>18</sup> When the symmetry is gauged,  
 1496 it is realized as a  $k$ -form symmetry on the  $(d - 1)$ -dimensional boundary, while the bulk has  
 1497 a new  $((d - 1) - k - n)$ -form magnetic symmetry, which we have emphasized has exactly the  
 1498 right degree to play the role of the dual symmetry on the boundary, and indeed shares the  
 1499 correct mutual anomaly [22, 23]. Some generalization of this mechanism should likely also  
 1500 hold true for gauging 0-form non-Abelian symmetries and spontaneously breaking them at the  
 1501 boundary. In general the emergent symmetries arising from spontaneously breaking a 0-form  
 1502  $\mathcal{G}$  symmetry do not form a group but rather a symmetry category, and these symmetries share  
 1503 a mixed anomaly with  $\mathcal{G}$  [114, 116]. Upon gauging the 0-form  $\mathcal{G}$  symmetry, forcing it to the  
 1504 boundary, one expects that the resulting gauge field has a “magnetic” symmetry category which  
 1505 preserves the correct anomaly structure at the boundary. The precise mathematical structure  
 1506 of the resulting mutual anomaly after gauging is likely complicated due to the fact that the  
 1507 boundary symmetry is generated by the *total* charge (gauge plus matter, cf. Section 3.1.3),  
 1508 rather than just the charge of the Higgs field. However, we believe that identifying the relevant  
 1509 generalized symmetries of the non-Abelian gauge field and matching the boundary anomaly  
 1510 are the required ingredients to extend the Higgs-SPT connection to the non-Abelian setting.

## 1511 Acknowledgements

1512 PM and PR acknowledge useful discussions with Pedro Bicudo and Nuno Cardoso as a part of  
 1513 a related collaboration. KTKC acknowledges Chris Hooley for useful discussion.

1514 **Funding information** S.M. is supported by Vetenskapsrådet (grant number 2021-03685),  
 1515 Nordita and STINT. This work was in part supported by the Deutsche Forschungsgemeinschaft  
 1516 under the cluster of excellence ct.qmat (EXC-2147, project number 390858490).

## 1517 A Discrete Differential Calculus for Abelian Fields

1518 We utilize notation which mimics continuum differential forms on a lattice, borrowed from  
 1519 algebraic topology [117] and used extensively in Section 4. Pedagogical treatments can be  
 1520 found in [34, 56]. Fields are described (locally) as differential forms (i.e. anti-symmetric  
 1521 tensors), whose primary property is that they can be integrated over surfaces. For our purposes  
 1522 we can think of them simply as functions of such surfaces, i.e. if  $\omega$  is a differential  $k$ -form and  
 1523  $U$  an oriented  $k$ -dimensional surface,  $\omega$  acts on  $U$  by integration

$$\omega(U) := \int_U \omega, \quad (\text{A.1})$$

<sup>18</sup>For example: a 0-form  $\mathbb{Z}_n$  symmetry has a corresponding  $d$ -form  $\mathbb{Z}_n$  symmetry associated to suppression of domains walls (conservation of symmetry breaking sector); a 0-form U(1) symmetry has a corresponding  $(d - 1)$ -form U(1) symmetry associated to suppression of vortices (conservation of winding number); and a 1-form U(1) symmetry has a corresponding  $(d - 2)$ -form U(1) symmetry associated to suppression of monopoles (i.e. magnetic symmetry, conservation of magnetic flux).



1524 which results in some number. There are two main properties that we wish to preserve on the  
 1525 lattice: reversing the orientation of  $U$  changes the sign of the integral, and if  $U$  is divided into  
 1526 a collection of smaller parts the total integral is the sum of the integrals over the parts, i.e.

$$\begin{aligned}\omega(-U) &= -\omega(U), \\ \omega(U_1 + U_2) &= \omega(U_1) + \omega(U_2),\end{aligned}\tag{A.2}$$

1527 where  $-U$  denotes the reversed orientation. Lastly, we can naturally define the derivative of a  
 1528  $k$ -form  $\omega$  to be a  $(k + 1)$ -form  $d\omega$  whose value on a  $(k + 1)$ -dimensional surface  $U$  is defined  
 1529 by Stoke's theorem,

$$\int_U d\omega := \int_{\partial U} \omega,\tag{A.3}$$

1530 where  $\partial U$  denotes the boundary of  $U$ .

1531 In this paper, our space(time) is a  $D$ -dimensional cubical cell complex—a collection of  $k$ -  
 1532 cells for  $k = 0, \dots, D$ , i.e. vertices, links, plaquettes, cubes, hypercubes, etc., where  $k$ -cells are  
 1533 glued along their  $(k - 1)$ -dimensional boundary cells. We denote the collection of all cells by  $X$   
 1534 and the collection of all  $k$ -cells by  $X_k$ . Because we also consider open boundaries in the form  
 1535 of Fig. 2, we let  $X_k$  denote just the bulk  $k$ -cells and  $\partial X_k$  denote the  $k$ -cells in the boundary  
 1536 layer which touch the vacuum.

1537 The cells naturally provide the integration surfaces once equipped with an orientation.  
 1538 It is natural to define the possible integration surfaces therefore as integer weighted linear  
 1539 combinations of oriented  $k$ -cells, call  $k$ -chains. The signs of the integer coefficients determine  
 1540 the orientations and their magnitudes determine how many times to integrate over each cell.  
 1541 Since we can formally add such chains together, they form an Abelian group,  $\mathcal{C}_k$ . The structure  
 1542 of the cell complex is contained in the boundary relation,

$$\partial : \mathcal{C}_k \rightarrow \mathcal{C}_{k-1},\tag{A.4}$$

1543 which distributes over the linear combinations on  $k$ -cells, and sends each oriented  $k$ -cell to  
 1544 the linear combination of its oriented boundary  $(k - 1)$ -cells.

1545 The sensible lattice analog of a differential form, i.e. a discrete  $k$ -form, also called a  $k$ -  
 1546 cochain, is a function which (i) maps chains to numbers, Eq. (A.1), and (ii) distributes over  
 1547 linear combinations, Eq. (A.2). In full generality, a discrete  $k$ -form  $\omega$  is a linear map from  
 1548 chains to elements of any Abelian group  $\mathcal{G}$ ,

$$\omega : \mathcal{C}_k \rightarrow \mathcal{G}.\tag{A.5}$$

1549 In practice what this means is that a discrete  $k$ -form is defined by its value on each oriented  
 1550  $k$ -cell  $c$ , and satisfies  $\omega(-c) = -\omega(c)$ , where  $-\omega$  is understood as the inverse operation in the  
 1551 Abelian group  $\mathcal{G}$ . The space of discrete  $k$ -forms is denoted  $\mathcal{C}^k(\mathcal{G})$ . Since we already have a  
 1552 natural notion of the boundary operation on chains, we can define a natural exterior derivative  
 1553 operation on cochains,  $d : \mathcal{C}^k \rightarrow \mathcal{C}^{k+1}$ , according to Stoke's theorem, i.e.

$$d\omega(U) := \omega(\partial U),\tag{A.6}$$

1554 where  $\omega$  is a  $k$ -form,  $d\omega$  is a  $(k + 1)$ -form, and  $U$  is a  $(k + 1)$ -chain.

1555 Denoting the coefficients in a  $k$ -chain  $u$  by

$$u = \sum_{c \in X_k} u_k c \quad (u_k \in \mathbb{Z}),\tag{A.7}$$

1556 where each  $k$ -cell is summed once with a fixed orientation, we can define a natural inner  
 1557 product on  $k$ -chains as

$$(u, w) = \sum_c u_c w_c.\tag{A.8}$$

1558 Using this, we can define an adjoint of the boundary operator, which we call the coboundary,<sup>19</sup>

$$(u, \partial v) = (\partial^\dagger u, v). \quad (\text{A.9})$$

1559 In particular, the coboundary of a single  $k$ -cell is

$$\partial^\dagger c = \sum_{c' \in X_{k+1}} (\partial^\dagger c)_{c'} c' = \sum_{c' \in X_{k+1}} (\partial^\dagger c, c') c' = \sum_{c' \in X_{k+1}} (c, \partial c') c' \quad (\text{A.10})$$

1560 By choosing to orient all the  $c'$  in the sum such that  $(c, \partial c') = +1$  or  $0$ , we can read this to  
 1561 say that *the coboundary of an oriented  $k$ -cell  $c$  is the sum of all oriented  $(k+1)$ -cells containing*  
 1562  *$+c$  in their positively oriented boundary.* For example, the coboundary of a point  $i$  is the set  
 1563 of oriented links which terminate at it, the coboundary of a link  $\ell$  is the set of plaquettes  $p$   
 1564 touching it, oriented so that  $\partial p$  circulates in the same direction as  $\ell$  is oriented, etc.

1565 The coboundary defines a co-exterior derivative, via a ‘‘co-Stoke’s theorem’’,

$$d^\dagger \omega(c) := \omega(\partial^\dagger c), \quad (\text{A.11})$$

1566 which reduces the degree of forms. In the case that  $\mathcal{G}$  is  $\mathbb{Z}$ ,  $\mathbb{R}$ , or  $\mathbb{C}$ , we can also define an  
 1567 inner product for  $k$ -forms,

$$\langle \alpha, \beta \rangle = \sum_{c \in X_k} \alpha(c)^* \beta(c) \quad (\text{A.12})$$

1568 where  $*$  denotes complex conjugation. It is easy to see that the codifferential is adjoint to the  
 1569 differential,

$$\begin{aligned} \langle \alpha, d\beta \rangle &= \sum_{c \in X_k} \alpha(c)^* \beta(\partial c) = \sum_c \alpha(c)^* \sum_{c' \in \partial c} \beta(c') \\ &= \sum_{\substack{c \in X_k \\ c' \in X_{k-1}}} \alpha(c)^* \beta(c') (\partial c, c') = \sum_{\substack{c \in X_k \\ c' \in X_{k-1}}} \alpha(c)^* \beta(c') (c, \partial^\dagger c') \\ &= \sum_{c' \in X_{k-1}} \alpha(\partial^\dagger c')^* \beta(c') = \langle d^\dagger \alpha, \beta \rangle. \end{aligned} \quad (\text{A.13})$$

1570 Qualitatively, one may think of the differential as a generalized gradient, describing how a  $k$ -  
 1571 form varies across  $(k+1)$ -cells, and the codifferential as a generalized divergence, describing  
 1572 how a  $k$ -form ‘‘flows into’’  $(k-1)$ -cells.

1573 Lastly, we review a bit of basic algebraic topology terminology used in Section 4. The  
 1574 boundary operation is nilpotent,  $\partial^2 = 0$ , and thus defines an exact sequence of maps,

$$0 \rightarrow \mathcal{C}_D \xrightarrow{\partial_D} \dots \mathcal{C}_1 \xrightarrow{\partial_1} \mathcal{C}_0 \rightarrow 0. \quad (\text{A.14})$$

1575 We can define the homology groups,  $H_k := \ker \partial_k / \text{im } \partial_{k+1}$ . The interpretation of these quotient  
 1576 groups is that they classify the non-contractible  $k$ -dimensional surfaces. Here,  $\ker \partial$  is gener-  
 1577 ated by the set of surfaces without boundaries (called cycles), while  $\text{im } \partial$  is generated by the  
 1578 set of surfaces which are boundaries of a  $(k+1)$ -dimensional volume, and are therefore con-  
 1579 tractible. The elements of  $H_k$  are equivalence classes of surfaces which differ by a boundary,  
 1580 i.e. homology classes.

1581 The dual of the homology classes on the differential form side are the cohomology classes,  
 1582 which are defined by the discrete equivalent of the de Rham complex:

$$0 \rightarrow \mathcal{C}^0 \xrightarrow{d_0} \mathcal{C}^1 \xrightarrow{d_1} \dots \xrightarrow{d_{D-1}} \mathcal{C}^D \rightarrow 0, \quad (\text{A.15})$$

<sup>19</sup>Note that this differs from the algebraic topology terminology, where the discrete exterior derivative is often called the coboundary.

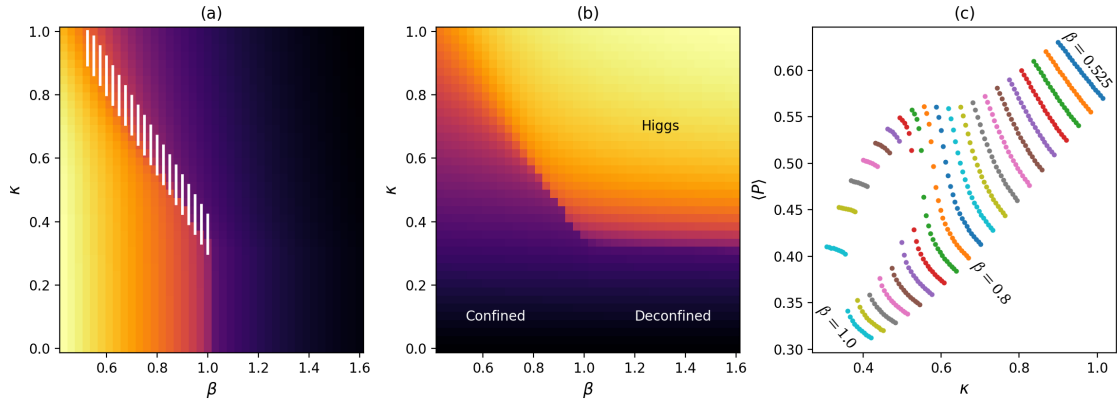


Figure 13: (a,b) Phase diagram of the 4D  $U(1)$  Abelian Higgs model for  $L = 16$  revealed through (a) expectation of the minimal Wilson loop,  $\langle 1 - \text{Re } W_p \rangle$ , and (b) expectation of the Wilson link,  $\langle \text{Re } \Lambda_\ell \rangle$ , averaged over all plaquettes and links, respectively. The color ranges from 0.1 (black) to 0.8 (yellow). (c) Cuts of  $\langle 1 - \text{Re } W_p \rangle$ , at constant  $\beta$  for different values of  $\beta$  from 0.525 to 1.000 in steps of 0.025 from right to left. The system is isotropic with  $L = 16$  and 50000 sweeps. The data shows a clear sign of a phase transition for larger  $\beta$  and a crossover for smaller  $\beta$ . The data is consistent with the presence of a first order transition with a critical endpoint at about  $\beta = 0.85$ .

1583 as  $H^k := \ker d_k / \text{im } d_{k-1}$ . Here  $\ker d_k$  is the set of locally-constant  $k$ -forms (called closed  
 1584 forms), and  $\text{im } d_{k-1}$  is the set of  $k$ -forms which are gradients of  $(k-1)$ -forms (called exact  
 1585 forms). Every exact form is closed, but there can exist closed forms which are not exact,  
 1586 which are classified by cohomology. Cohomology classes are equivalence classes of closed  
 1587 forms which differ by an exact form, just as homology classes are equivalence classes of closed  
 1588 surfaces which differ by a boundary. Note that exact forms integrate to zero by Stoke's theo-  
 1589 rem on any closed surface, while closed forms need only integrate to zero on closed surfaces  
 1590 that are boundaries. Forms with non-trivial cohomology class integrate non-trivially on non-  
 1591 contractible surfaces, defining a pairing between cohomology and homology classes.

## 1592 B $U(1)$ Bulk Phase Diagram: Limits, Symmetries and Monte Carlo

1593 Here we provide a brief review of the bulk phase diagram of the 4D  $U(1)$  Abelian-Higgs model,  
 1594 described by the action Eq. (8), the Hamiltonian Eq. (10), and dual action Eq. (110), by con-  
 1595 sidering the various limits and undertaking numerical Monte Carlo simulation in the action  
 1596 formulation. The phase diagram is sketched in Fig. 1, which conveniently summarizes the dis-  
 1597 cussion that follows. In particular, it is well-known that there are only two distinct phases [14],  
 1598 the Coulomb phase and the Higgs-confined phase. According to Eq. (104), this is a theory  
 1599 of electric strings terminating on electric point charges. The dual magnetic description is in  
 1600 terms of magnetic strings terminating on magnetic point charges (vortices and monopoles of  
 1601 the Higgs and gauge fields, respectively). The basic structure of the phase diagram can be  
 1602 deduced by consider each of the following four limits.

1603 *Pure gauge limit* ( $\kappa \ll 1$ ): In the limit  $\kappa = 0$  the gap of the electric point charges diverges,  
 1604 and the theory reduces to 4D  $U(1)$  gauge theory. In this limit, the system has a global 1-form  
 1605 symmetry,  $A \rightarrow A + \lambda$  with  $d\lambda = 0$ , called electric symmetry. This symmetry corresponds to  
 1606 electric strings forming closed loops, i.e. electric flux through closed surfaces is conserved.  
 1607 This theory has two phases, a confined phase at small  $\beta$  (strong coupling), where the sys-

tem is gapped and electric strings cost energy proportional to their length; and a deconfined phase at large  $\beta$  (weak coupling), where the electric strings condense, the electric symmetry is spontaneously broken, and the system has a gapless photon excitation. Turning on a small  $\kappa$  explicitly breaks the 1-form symmetry by introducing gapped electric point charges at which open electric strings end. Because the charges are strongly gapped, qualitatively speaking we expect the 1-form symmetry to re-emerge at low energies below the charge gap, thus allowing the deconfined phase to extend to finite  $\kappa$ .

*Frozen gauge limit ( $\beta \rightarrow \infty$ ):* In this limit the gauge fields are completely trivialized by the constraint  $dA = 0$ , and equivalently the mass of the magnetic monopoles diverges. We can choose a gauge where  $A = 0$  and the action turns into that of a 4D XY model, whose dual description is a gas of vortex strings with Coulomb interactions. This theory has a 1-form symmetry corresponding to the closure of these magnetic strings and the corresponding absence of magnetic monopoles, called magnetic symmetry. From the XY model we deduce a gapless superfluid phase at large  $\kappa$  and a gapped phase at small  $\kappa$  separated by a second-order phase transition, but this description is not gauge-invariant. The gauge-invariant statement is that at small  $\kappa$  the magnetic strings (disorder operators of the XY model) condense, spontaneously breaking the magnetic symmetry. For large but finite  $\beta$  the magnetic monopoles explicitly break the magnetic symmetry, though one expects it to be effectively restored at low energies below the monopole gap. The result is that the magnetic symmetry is spontaneously broken in the gapless Coulomb phase, while the superfluid at large  $\kappa$  is gapped out by the Higgs mechanism.

*Strong coupling (confining) limit ( $\beta = 0$ ):* In this limit the curvature of the gauge field  $A$  is not penalized, and we can say that the magnetic monopoles are maximally proliferated. If we fix to unitary gauge ( $\theta = \text{const.}$ ), the action becomes  $-\kappa \sum_{\ell} \cos(A_{\ell})$ , reducing to a set of completely disconnected link variables. Thus the system is in a trivial phase for all  $\kappa$ , and there is no bulk phase transition on this line. Strong coupling expansion (in  $\beta$ ) demonstrates that when  $\kappa = 0$  Wilson loops have an area law, indicating confinement of static charges by a tensionful electric string. This confinement extends to positive  $\kappa$ , though particle-anti-particle nucleation cuts off the area law of Wilson loops for large loops. Confinement may still be observed using the Fredenhagen-Marcu order parameter, however [27, 28].

*Infinite Higgs coupling limit ( $\kappa \rightarrow \infty$ ):* In this limit we have the constraint  $A = d\theta$ . This implies that the electric charge creation and annihilation operators, Eq. (14), act as the identity, and the system can be described as an electric condensate. The bulk has no dynamics and is completely frozen, which can be seen by fixing to unitary gauge ( $\theta = \text{const.}$ ), in which  $A = 0$  and the Higgs field is frozen. There is therefore no bulk phase transition along this line. For large but finite  $\kappa$  the bulk action can be roughly understood as the proca-type action, Eq. (23), describing a massive 1-form field, at least for large  $\beta$ .

This completes the general outline of the phase diagram in the vicinity of the edges in Fig. 1. The only question that remains is how the two transitions at small  $\kappa$  and large  $\beta$  reach each other to separate the Coulomb phase (in which the electric and magnetic symmetries are emergent and spontaneously broken) from the Higgs-confined phase. Figure 13 shows results from Monte Carlo simulations measuring the average Wilson plaquette and Wilson link, which fills in the remainder of the phase diagram schematically shown in Fig. 1. The two transitions extend as first-order transition lines and meet at a triple point in the vicinity of  $\beta \sim 1.0$  and  $\kappa \sim 0.4$ . A third first order line extends from this triple point towards smaller  $\beta$  and larger  $\kappa$  which ends at a critical endpoint. We show evidence for this first-order line in Fig. 13(c).

## References

1654

- 1655 [1] F. J. Wegner, *Duality in Generalized Ising Models and Phase Transitions without Local*  
1656 *Order Parameters*, J. Math. Phys. **12**(10), 2259 (1971), doi:[10.1063/1.1665530](https://doi.org/10.1063/1.1665530).
- 1657 [2] K. G. Wilson, *Confinement of quarks*, Phys. Rev. D **10**(8), 2445 (1974),  
1658 doi:[10.1103/PhysRevD.10.2445](https://doi.org/10.1103/PhysRevD.10.2445).
- 1659 [3] S. Elitzur, *Impossibility of spontaneously breaking local symmetries*, Phys. Rev. D **12**(12),  
1660 3978 (1975), doi:[10.1103/PhysRevD.12.3978](https://doi.org/10.1103/PhysRevD.12.3978).
- 1661 [4] D. Gaiotto, A. Kapustin, N. Seiberg and B. Willett, *Generalized global symmetries*, J.  
1662 High Energ. Phys. **2015**(2), 172 (2015), doi:[10.1007/JHEP02\(2015\)172](https://doi.org/10.1007/JHEP02(2015)172).
- 1663 [5] E. Lake, *Higher-form symmetries and spontaneous symmetry breaking*,  
1664 doi:[10.48550/arXiv.1802.07747](https://doi.org/10.48550/arXiv.1802.07747) (2018), [1802.07747](https://arxiv.org/abs/1802.07747).
- 1665 [6] L. V. Delacrétaz, D. M. Hofman and G. Mathys, *Superfluids as higher-form anomalies*,  
1666 SciPost Physics **8**(3), 047 (2020), doi:[10.21468/SciPostPhys.8.3.047](https://doi.org/10.21468/SciPostPhys.8.3.047).
- 1667 [7] N. Iqbal and J. McGreevy, *Mean string field theory: Landau-Ginzburg theory for 1-form*  
1668 *symmetries*, SciPost Physics **13**(5), 114 (2022), doi:[10.21468/SciPostPhys.13.5.114](https://doi.org/10.21468/SciPostPhys.13.5.114).
- 1669 [8] J. McGreevy, *Generalized Symmetries in Condensed Matter*, Annual Review of Condensed  
1670 Matter Physics **14**, 57 (2023), doi:[10.1146/annurev-conmatphys-040721-021029](https://doi.org/10.1146/annurev-conmatphys-040721-021029).
- 1671 [9] P. W. Anderson, *Plasmons, Gauge Invariance, and Mass*, Phys. Rev. **130**(1), 439 (1963),  
1672 doi:[10.1103/PhysRev.130.439](https://doi.org/10.1103/PhysRev.130.439).
- 1673 [10] F. Englert and R. Brout, *Broken Symmetry and the Mass of Gauge Vector Mesons*, Phys.  
1674 Rev. Lett. **13**(9), 321 (1964), doi:[10.1103/PhysRevLett.13.321](https://doi.org/10.1103/PhysRevLett.13.321).
- 1675 [11] P. W. Higgs, *Broken Symmetries and the Masses of Gauge Bosons*, Phys. Rev. Lett. **13**(16),  
1676 508 (1964), doi:[10.1103/PhysRevLett.13.508](https://doi.org/10.1103/PhysRevLett.13.508).
- 1677 [12] G. S. Guralnik, C. R. Hagen and T. W. B. Kibble, *Global Conservation Laws and Massless*  
1678 *Particles*, Phys. Rev. Lett. **13**(20), 585 (1964), doi:[10.1103/PhysRevLett.13.585](https://doi.org/10.1103/PhysRevLett.13.585).
- 1679 [13] J. Fröhlich, G. Morchio and F. Strocchi, *Higgs phenomenon without a symmetry*  
1680 *breaking order parameter*, Physics Letters B **97**(2), 249 (1980), doi:[10.1016/0370-](https://doi.org/10.1016/0370-2693(80)90594-8)  
1681 [2693\(80\)90594-8](https://doi.org/10.1016/0370-2693(80)90594-8).
- 1682 [14] E. Fradkin and S. H. Shenker, *Phase diagrams of lattice gauge theories with Higgs fields*,  
1683 Phys. Rev. D **19**(12), 3682 (1979), doi:[10.1103/PhysRevD.19.3682](https://doi.org/10.1103/PhysRevD.19.3682).
- 1684 [15] K. Osterwalder and E. Seiler, *Gauge field theories on a lattice*, Annals of Physics **110**(2),  
1685 440 (1978), doi:[10.1016/0003-4916\(78\)90039-8](https://doi.org/10.1016/0003-4916(78)90039-8).
- 1686 [16] J. Greensite, *An Introduction to the Confinement Problem*, Springer Cham, 2 edn., ISBN  
1687 978-3-030-51563-8 (1983).
- 1688 [17] W. Caudy and J. Greensite, *Ambiguity of spontaneously broken gauge symmetry*, Phys.  
1689 Rev. D **78**(2), 025018 (2008), doi:[10.1103/PhysRevD.78.025018](https://doi.org/10.1103/PhysRevD.78.025018).
- 1690 [18] A. Cherman, S. Sen and L. G. Yaffe, *Anyonic particle-vortex statistics and*  
1691 *the nature of dense quark matter*, Phys. Rev. D **100**(3), 034015 (2019),  
1692 doi:[10.1103/PhysRevD.100.034015](https://doi.org/10.1103/PhysRevD.100.034015).

- 1693 [19] A. Cherman, T. Jacobson, S. Sen and L. G. Yaffe, *Higgs-confinement phase transi-*  
1694 *tions with fundamental representation matter*, Phys. Rev. D **102**(10), 105021 (2020),  
1695 doi:[10.1103/PhysRevD.102.105021](https://doi.org/10.1103/PhysRevD.102.105021).
- 1696 [20] A. Cherman, T. Jacobson, S. Sen and L. G. Yaffe, *Line operators, vortex statis-*  
1697 *tics, and Higgs versus confinement dynamics*, doi:[10.48550/arXiv.2401.17489](https://doi.org/10.48550/arXiv.2401.17489) (2024),  
1698 [2401.17489](https://doi.org/10.48550/arXiv.2401.17489).
- 1699 [21] U. Borla, R. Verresen, J. Shah and S. Moroz, *Gauging the Kitaev chain*, SciPost Physics  
1700 **10**(6), 148 (2021), doi:[10.21468/SciPostPhys.10.6.148](https://doi.org/10.21468/SciPostPhys.10.6.148).
- 1701 [22] R. Verresen, U. Borla, A. Vishwanath, S. Moroz and R. Thorngren, *Higgs*  
1702 *Condensates are Symmetry-Protected Topological Phases: I. Discrete Symmetries*,  
1703 doi:[10.48550/arXiv.2211.01376](https://doi.org/10.48550/arXiv.2211.01376) (2022), [2211.01376](https://doi.org/10.48550/arXiv.2211.01376).
- 1704 [23] R. Thorngren, T. Rakovszky, R. Verresen and A. Vishwanath, *Higgs Condensates are*  
1705 *Symmetry-Protected Topological Phases: II. U(1) Gauge Theory and Superconductors*,  
1706 doi:[10.48550/arXiv.2303.08136](https://doi.org/10.48550/arXiv.2303.08136) (2023), [2303.08136](https://doi.org/10.48550/arXiv.2303.08136).
- 1707 [24] P. A. M. Dirac, *Gauge-invariant formulation of quantum electrodynamics*, Can. J. Phys.  
1708 **33**(11), 650 (1955), doi:[10.1139/p55-081](https://doi.org/10.1139/p55-081).
- 1709 [25] T. Kennedy and C. King, *Symmetry Breaking in the Lattice Abelian Higgs Model*, Phys.  
1710 Rev. Lett. **55**(8), 776 (1985), doi:[10.1103/PhysRevLett.55.776](https://doi.org/10.1103/PhysRevLett.55.776).
- 1711 [26] T. Kennedy and C. King, *Spontaneous Symmetry Breakdown in the Abelian Higgs Model*,  
1712 Commun.Math. Phys. **104**(2), 327 (1986), doi:[10.1007/BF01211599](https://doi.org/10.1007/BF01211599).
- 1713 [27] K. Fredenhagen and M. Marcu, *Confinement criterion for QCD with dynamical quarks*,  
1714 Phys. Rev. Lett. **56**(3), 223 (1986), doi:[10.1103/PhysRevLett.56.223](https://doi.org/10.1103/PhysRevLett.56.223).
- 1715 [28] K. Gregor, D. A. Huse, R. Moessner and S. L. Sondhi, *Diagnosing deconfinement*  
1716 *and topological order*, New J. Phys. **13**(2), 025009 (2011), doi:[10.1088/1367-](https://doi.org/10.1088/1367-2630/13/2/025009)  
1717 [2630/13/2/025009](https://doi.org/10.1088/1367-2630/13/2/025009).
- 1718 [29] J. B. Kogut, *An introduction to lattice gauge theory and spin systems*, Rev. Mod. Phys.  
1719 **51**(4), 659 (1979), doi:[10.1103/RevModPhys.51.659](https://doi.org/10.1103/RevModPhys.51.659).
- 1720 [30] M. Creutz, *Quarks, Gluons and Lattices*, Cambridge University Press, Cambridge (1984).
- 1721 [31] T. Banks, R. Myerson and J. Kogut, *Phase transitions in Abelian lattice gauge theories*,  
1722 Nuclear Physics B **129**(3), 493 (1977), doi:[10.1016/0550-3213\(77\)90129-8](https://doi.org/10.1016/0550-3213(77)90129-8).
- 1723 [32] R. Savit, *Duality in field theory and statistical systems*, Rev. Mod. Phys. **52**(2), 453  
1724 (1980), doi:[10.1103/RevModPhys.52.453](https://doi.org/10.1103/RevModPhys.52.453).
- 1725 [33] R. Savit, *Duality transformations for general abelian systems*, Nuclear Physics B **200**(2),  
1726 233 (1982), doi:[10.1016/0550-3213\(82\)90085-2](https://doi.org/10.1016/0550-3213(82)90085-2).
- 1727 [34] K. Drühl and H. Wagner, *Algebraic formulation of duality transformations for abelian lat-*  
1728 *tice models*, Annals of Physics **141**(2), 225 (1982), doi:[10.1016/0003-4916\(82\)90286-](https://doi.org/10.1016/0003-4916(82)90286-X)  
1729 [X](https://doi.org/10.1016/0003-4916(82)90286-X).
- 1730 [35] J. Ranft, J. Kripfganz and G. Ranft, *Phase structure, magnetic monopoles, and*  
1731 *vortices in the lattice Abelian Higgs model*, Phys. Rev. D **28**(2), 360 (1983),  
1732 doi:[10.1103/PhysRevD.28.360](https://doi.org/10.1103/PhysRevD.28.360).

- 1733 [36] A. P. Gottlob and M. Hasenbusch, *Critical behaviour of the 3D XY-model: A Monte*  
1734 *Carlo study*, Physica A: Statistical Mechanics and its Applications **201**(4), 593 (1993),  
1735 doi:[10.1016/0378-4371\(93\)90131-M](https://doi.org/10.1016/0378-4371(93)90131-M).
- 1736 [37] T. H. Hansson, V. Oganesyan and S. L. Sondhi, *Superconductors are topologically ordered*,  
1737 Annals of Physics **313**(2), 497 (2004), doi:[10.1016/j.aop.2004.05.006](https://doi.org/10.1016/j.aop.2004.05.006).
- 1738 [38] A. M. Polyakov, *Gauge Fields and Strings*, Routledge, London, ISBN 978-0-203-75508-2,  
1739 doi:[10.1201/9780203755082](https://doi.org/10.1201/9780203755082) (2017).
- 1740 [39] J. Kogut and L. Susskind, *Hamiltonian formulation of Wilson's lattice gauge theories*,  
1741 Phys. Rev. D **11**(2), 395 (1975), doi:[10.1103/PhysRevD.11.395](https://doi.org/10.1103/PhysRevD.11.395).
- 1742 [40] L. Susskind and J. Kogut, *XIV. New ideas about confinement*, Physics Reports **23**(3), 348  
1743 (1976), doi:[10.1016/0370-1573\(76\)90055-7](https://doi.org/10.1016/0370-1573(76)90055-7).
- 1744 [41] R. Oeckl and H. Pfeiffer, *The dual of pure non-Abelian lattice gauge theory as a spin foam*  
1745 *model*, Nuclear Physics B **598**(1), 400 (2001), doi:[10.1016/S0550-3213\(00\)00770-7](https://doi.org/10.1016/S0550-3213(00)00770-7).
- 1746 [42] C. Bonati, G. Cossu, M. D'Elia and A. Di Giacomo, *Phase diagram of*  
1747 *the lattice SU(2) Higgs model*, Nuclear Physics B **828**(1), 390 (2010),  
1748 doi:[10.1016/j.nuclphysb.2009.12.003](https://doi.org/10.1016/j.nuclphysb.2009.12.003).
- 1749 [43] K. Kanaya and S. Kaya, *Critical exponents of a three-dimensional O(4) spin model*, Phys.  
1750 Rev. D **51**(5), 2404 (1995), doi:[10.1103/PhysRevD.51.2404](https://doi.org/10.1103/PhysRevD.51.2404).
- 1751 [44] A. D. Kennedy and B. J. Pendleton, *Improved heatbath method for Monte Carlo calcula-*  
1752 *tions in lattice gauge theories*, Physics Letters B **156**(5), 393 (1985), doi:[10.1016/0370-](https://doi.org/10.1016/0370-2693(85)91632-6)  
1753 [2693\(85\)91632-6](https://doi.org/10.1016/0370-2693(85)91632-6).
- 1754 [45] M. Creutz, *Overrelaxation and Monte Carlo simulation*, Phys. Rev. D **36**(2), 515 (1987),  
1755 doi:[10.1103/PhysRevD.36.515](https://doi.org/10.1103/PhysRevD.36.515).
- 1756 [46] G. Sordi and A.-M. S. Tremblay, *Introducing the concept of Widom line in the QCD phase*  
1757 *diagram*, doi:[10.48550/arXiv.2312.12401](https://doi.org/10.48550/arXiv.2312.12401) (2023), [2312.12401](https://arxiv.org/abs/2312.12401).
- 1758 [47] S. Chandrasekharan and U. J. Wiese, *An introduction to chiral symmetry*  
1759 *on the lattice*, Progress in Particle and Nuclear Physics **53**(2), 373 (2004),  
1760 doi:[10.1016/j.pnpnp.2004.05.003](https://doi.org/10.1016/j.pnpnp.2004.05.003).
- 1761 [48] J. B. Kogut, M. Snow and M. Stone, *Mean field and Monte Carlo studies of SU(N) chiral*  
1762 *models in three dimensions*, Nuclear Physics B **200**(1), 211 (1982), doi:[10.1016/0550-](https://doi.org/10.1016/0550-3213(82)90065-7)  
1763 [3213\(82\)90065-7](https://doi.org/10.1016/0550-3213(82)90065-7).
- 1764 [49] L. D. Faddeev and N. Y. Reshetikhin, *Integrability of the principal chiral field model*  
1765 *in 1 + 1 dimension*, Annals of Physics **167**(2), 227 (1986), doi:[10.1016/0003-](https://doi.org/10.1016/0003-4916(86)90201-0)  
1766 [4916\(86\)90201-0](https://doi.org/10.1016/0003-4916(86)90201-0).
- 1767 [50] J. J. Binney, N. J. Dowrick, A. J. Fisher and M. E. J. Newman, *The Theory of Critical*  
1768 *Phenomena: An Introduction to the Renormalization Group*, Oxford University Press,  
1769 Oxford, New York, ISBN 978-0-19-851393-3 (1992).
- 1770 [51] F. Kos, D. Poland and D. Simmons-Duffin, *Bootstrapping the O(N) Vector Models*, J. High  
1771 Energ. Phys. **2014**(6), 91 (2014), doi:[10.1007/JHEP06\(2014\)091](https://doi.org/10.1007/JHEP06(2014)091).
- 1772 [52] L.-F. Li, *Group theory of the spontaneously broken gauge symmetries*, Phys. Rev. D **9**(6),  
1773 1723 (1974), doi:[10.1103/PhysRevD.9.1723](https://doi.org/10.1103/PhysRevD.9.1723).

- 1774 [53] L. Zou, Y.-C. He and C. Wang, *Stiefel Liquids: Possible Non-Lagrangian Quantum Criticality from Intertwined Orders*, Phys. Rev. X **11**(3), 031043 (2021),  
1775 doi:[10.1103/PhysRevX.11.031043](https://doi.org/10.1103/PhysRevX.11.031043).  
1776
- 1777 [54] M. Henneaux and C. Teitelboim, *P-Form electrodynamics*, Foundations of Physics **16**(7),  
1778 593 (1986), doi:[10.1007/BF01889624](https://doi.org/10.1007/BF01889624).
- 1779 [55] C. Teitelboim, *Gauge invariance for extended objects*, Physics Letters B **167**(1), 63  
1780 (1986), doi:[10.1016/0370-2693\(86\)90546-0](https://doi.org/10.1016/0370-2693(86)90546-0).
- 1781 [56] D. K. Wise, *P-form electromagnetism on discrete spacetimes*, Class. Quantum Grav.  
1782 **23**(17), 5129 (2006), doi:[10.1088/0264-9381/23/17/004](https://doi.org/10.1088/0264-9381/23/17/004).
- 1783 [57] C. Omero, P. A. Marchetti and A. Maritan, *Gauge differential form theories on the lattice*,  
1784 J. Phys. A: Math. Gen. **16**(7), 1465 (1983), doi:[10.1088/0305-4470/16/7/022](https://doi.org/10.1088/0305-4470/16/7/022).
- 1785 [58] M. Kalb and P. Ramond, *Classical direct interstring action*, Phys. Rev. D **9**(8), 2273  
1786 (1974), doi:[10.1103/PhysRevD.9.2273](https://doi.org/10.1103/PhysRevD.9.2273).
- 1787 [59] R. L. Davis and E. P. S. Shellard, *Global strings and superfluid vortices*, Phys. Rev. Lett.  
1788 **63**(19), 2021 (1989), doi:[10.1103/PhysRevLett.63.2021](https://doi.org/10.1103/PhysRevLett.63.2021).
- 1789 [60] M. Franz, *Vortex-boson duality in four space-time dimensions*, EPL **77**(4), 47005 (2007),  
1790 doi:[10.1209/0295-5075/77/47005](https://doi.org/10.1209/0295-5075/77/47005).
- 1791 [61] K. T. K. Chung and M. J. P. Gingras, *2-Form  $U(1)$  Spin Liquids: Classical Model and  
1792 Quantum Aspects*, doi:[10.48550/arXiv.2310.17607](https://doi.org/10.48550/arXiv.2310.17607) (2023), [2310.17607](https://arxiv.org/abs/2310.17607).
- 1793 [62] R. I. Nepomechie, *Magnetic monopoles from antisymmetric tensor gauge fields*, Phys.  
1794 Rev. D **31**(8), 1921 (1985), doi:[10.1103/PhysRevD.31.1921](https://doi.org/10.1103/PhysRevD.31.1921).
- 1795 [63] S.-J. Rey, *Higgs mechanism for Kalb-Ramond gauge field*, Phys. Rev. D **40**(10), 3396  
1796 (1989), doi:[10.1103/PhysRevD.40.3396](https://doi.org/10.1103/PhysRevD.40.3396).
- 1797 [64] P. Orland, *Instantons and disorder in antisymmetric tensor gauge fields*, Nuclear Physics  
1798 B **205**(1), 107 (1982), doi:[10.1016/0550-3213\(82\)90468-0](https://doi.org/10.1016/0550-3213(82)90468-0).
- 1799 [65] R. B. Pearson, *Phase structure of antisymmetric tensor gauge fields*, Phys. Rev. D **26**(8),  
1800 2013 (1982), doi:[10.1103/PhysRevD.26.2013](https://doi.org/10.1103/PhysRevD.26.2013).
- 1801 [66] A. M. Polyakov, *Compact gauge fields and the infrared catastrophe*, Physics Letters B  
1802 **59**(1), 82 (1975), doi:[10.1016/0370-2693\(75\)90162-8](https://doi.org/10.1016/0370-2693(75)90162-8).
- 1803 [67] F. Quevedo and C. A. Trugenberger, *Condensation of p-Branes and General-  
1804 ized Higgs/Confinement Duality*, Int. J. Mod. Phys. A **12**(06), 1227 (1997),  
1805 doi:[10.1142/S0217751X97000955](https://doi.org/10.1142/S0217751X97000955).
- 1806 [68] F. Quevedo and C. A. Trugenberger, *Phases of antisymmetric tensor field theories*, Nuclear  
1807 Physics B **501**(1), 143 (1997), doi:[10.1016/S0550-3213\(97\)00337-4](https://doi.org/10.1016/S0550-3213(97)00337-4).
- 1808 [69] T. Sulejmanpasic and C. Gattringer, *Abelian gauge theories on the lattice: Theta-terms  
1809 and compact gauge theory with(out) monopoles*, Nuclear Physics B **943**, 114616 (2019),  
1810 doi:[10.1016/j.nuclphysb.2019.114616](https://doi.org/10.1016/j.nuclphysb.2019.114616).
- 1811 [70] H. Pfeiffer, *Higher gauge theory and a non-Abelian generalization of 2-form electrody-  
1812 namics*, Annals of Physics **308**(2), 447 (2003), doi:[10.1016/S0003-4916\(03\)00147-7](https://doi.org/10.1016/S0003-4916(03)00147-7).



- 1813 [71] J. C. Baez and J. Huerta, *An invitation to higher gauge theory*, Gen Relativ Gravit **43**(9),  
1814 2335 (2011), doi:[10.1007/s10714-010-1070-9](https://doi.org/10.1007/s10714-010-1070-9).
- 1815 [72] S.-J. Rey and F. Sugino, *A Nonperturbative Proposal for Nonabelian Tensor Gauge Theory*  
1816 *and Dynamical Quantum Yang-Baxter Maps*, doi:[10.48550/arXiv.1002.4636](https://doi.org/10.48550/arXiv.1002.4636) (2010),  
1817 [1002.4636](https://doi.org/10.48550/arXiv.1002.4636).
- 1818 [73] A. E. Lipstein and R. A. Reid-Edwards, *Lattice gerbe theory*, J. High Energ. Phys.  
1819 **2014**(9), 34 (2014), doi:[10.1007/JHEP09\(2014\)034](https://doi.org/10.1007/JHEP09(2014)034).
- 1820 [74] A. Kapustin and R. Thorngren, *Higher Symmetry and Gapped Phases of Gauge Theo-*  
1821 *ries*, In D. Auroux, L. Katzarkov, T. Pantev, Y. Soibelman and Y. Tschinkel, eds., *Algebra,*  
1822 *Geometry, and Physics in the 21st Century: Kontsevich Festschrift*, Progress in Mathemat-  
1823 ics, pp. 177–202. Springer International Publishing, Cham, ISBN 978-3-319-59939-7,  
1824 doi:[10.1007/978-3-319-59939-7\\_5](https://doi.org/10.1007/978-3-319-59939-7_5) (2017).
- 1825 [75] Y. D. Mercado, C. Gattringer and A. Schmidt, *Surface worm algorithm for abelian Gauge-*  
1826 *Higgs systems on the lattice*, Computer Physics Communications **184**(6), 1535 (2013),  
1827 doi:[10.1016/j.cpc.2013.02.001](https://doi.org/10.1016/j.cpc.2013.02.001).
- 1828 [76] Y. D. Mercado, C. Gattringer and A. Schmidt, *Dual Lattice Simulation of the Abelian*  
1829 *Gauge-Higgs Model at Finite Density: An Exploratory Proof of Concept Study*, Phys. Rev.  
1830 Lett. **111**(14), 141601 (2013), doi:[10.1103/PhysRevLett.111.141601](https://doi.org/10.1103/PhysRevLett.111.141601).
- 1831 [77] A. Schmidt, Y. D. Mercado and C. Gattringer, *Monte Carlo simulation of abelian gauge-*  
1832 *Higgs lattice models using dual representation*, doi:[10.48550/arXiv.1211.1573](https://doi.org/10.48550/arXiv.1211.1573) (2012),  
1833 [1211.1573](https://doi.org/10.48550/arXiv.1211.1573).
- 1834 [78] A. Pelissetto and E. Vicari, *Multicomponent compact Abelian-Higgs lattice models*, Phys.  
1835 Rev. E **100**(4), 042134 (2019), doi:[10.1103/PhysRevE.100.042134](https://doi.org/10.1103/PhysRevE.100.042134).
- 1836 [79] C. Bonati, A. Pelissetto and E. Vicari, *Global symmetry breaking in gauge theories: The*  
1837 *case of multiflavor scalar chromodynamics*, doi:[10.48550/arXiv.2110.05341](https://doi.org/10.48550/arXiv.2110.05341) (2021),  
1838 [2110.05341](https://doi.org/10.48550/arXiv.2110.05341).
- 1839 [80] C. Bonati, A. Pelissetto and E. Vicari, *Breaking of the gauge symmetry in lattice gauge the-*  
1840 *ories*, Phys. Rev. Lett. **127**(9), 091601 (2021), doi:[10.1103/PhysRevLett.127.091601](https://doi.org/10.1103/PhysRevLett.127.091601).
- 1841 [81] C. Bonati, A. Pelissetto and E. Vicari, *Critical behaviors of lattice  $U(1)$  gauge models and*  
1842 *three-dimensional Abelian-Higgs gauge field theory*, Phys. Rev. B **105**(8), 085112 (2022),  
1843 doi:[10.1103/PhysRevB.105.085112](https://doi.org/10.1103/PhysRevB.105.085112).
- 1844 [82] C. Bonati, A. Pelissetto and E. Vicari, *Scalar gauge-Higgs models with dis-*  
1845 *crete Abelian symmetry groups*, Phys. Rev. E **105**(5), 054132 (2022),  
1846 doi:[10.1103/PhysRevE.105.054132](https://doi.org/10.1103/PhysRevE.105.054132).
- 1847 [83] J. Greensite and K. Matsuyama, *Symmetry, Confinement, and the Higgs Phase*, Symmetry  
1848 **14**(1), 177 (2022), doi:[10.3390/sym14010177](https://doi.org/10.3390/sym14010177).
- 1849 [84] M. P. Hertzberg and M. Jain, *Counting of states in Higgs theories*, Phys. Rev. D **99**(6),  
1850 065015 (2019), doi:[10.1103/PhysRevD.99.065015](https://doi.org/10.1103/PhysRevD.99.065015).
- 1851 [85] M. P. Hertzberg and M. Jain, *Ground state wave function overlap in superconductors and*  
1852 *superfluids*, Zeitschrift für Naturforschung A **75**(12), 1063 (2020), doi:[10.1515/zna-](https://doi.org/10.1515/zna-2020-0277)  
1853 [2020-0277](https://doi.org/10.1515/zna-2020-0277).

- 1854 [86] M. Pretko, *Subdimensional particle structure of higher rank  $U(1)$  spin liquids*, Phys. Rev.  
1855 B **95**(11), 115139 (2017), doi:[10.1103/PhysRevB.95.115139](https://doi.org/10.1103/PhysRevB.95.115139).
- 1856 [87] R. M. Nandkishore and M. Hermele, *Fractons*, Annual Review of Condensed Matter  
1857 Physics **10**(1), 295 (2019), doi:[10.1146/annurev-conmatphys-031218-013604](https://doi.org/10.1146/annurev-conmatphys-031218-013604).
- 1858 [88] D. Bulmash and M. Barkeshli, *Higgs mechanism in higher-rank symmetric  $U(1)$  gauge  
1859 theories*, Phys. Rev. B **97**(23), 235112 (2018), doi:[10.1103/PhysRevB.97.235112](https://doi.org/10.1103/PhysRevB.97.235112).
- 1860 [89] P. Gorantla, H. T. Lam, N. Seiberg and S.-H. Shao, *A modified Villain formulation of  
1861 fractons and other exotic theories*, Journal of Mathematical Physics **62**(10), 102301  
1862 (2021), doi:[10.1063/5.0060808](https://doi.org/10.1063/5.0060808).
- 1863 [90] R. Banerjee, *Hamiltonian formulation of higher rank symmetric gauge theories*, Eur.  
1864 Phys. J. C **82**(1), 22 (2022), doi:[10.1140/epjc/s10052-021-09964-2](https://doi.org/10.1140/epjc/s10052-021-09964-2).
- 1865 [91] Y. Hirono, M. You, S. Angus and G. Y. Cho, *A symmetry principle for gauge theories with  
1866 fractons*, SciPost Physics **16**(2), 050 (2024), doi:[10.21468/SciPostPhys.16.2.050](https://doi.org/10.21468/SciPostPhys.16.2.050).
- 1867 [92] J. Cardy, *Surface critical behaviour*, In *Scaling and Renormalization in Statistical Physics*,  
1868 Cambridge Lecture Notes in Physics, pp. 133–144. Cambridge University Press, Cam-  
1869 bridge, ISBN 978-0-521-49959-0, doi:[10.1017/CBO9781316036440.008](https://doi.org/10.1017/CBO9781316036440.008) (1996).
- 1870 [93] H. W. Diehl, *The Theory of Boundary Critical Phenomena*, Int. J. Mod. Phys. B **11**(30),  
1871 3503 (1997), doi:[10.1142/S0217979297001751](https://doi.org/10.1142/S0217979297001751).
- 1872 [94] M. A. Metlitski, *Boundary criticality of the  $O(N)$  model in  $d=3$  critically revisited*,  
1873 doi:[10.48550/arXiv.2009.05119](https://doi.org/10.48550/arXiv.2009.05119) (2021), [2009.05119](https://arxiv.org/abs/2009.05119).
- 1874 [95] A. Krishnan and M. A. Metlitski, *A plane defect in the 3D  $O(N)$  model*,  
1875 doi:[10.48550/arXiv.2301.05728](https://doi.org/10.48550/arXiv.2301.05728) (2023), [2301.05728](https://arxiv.org/abs/2301.05728).
- 1876 [96] A. M. Somoza, P. Serna and A. Nahum, *Self-Dual Criticality in Three-  
1877 Dimensional  $Z_2$  Gauge Theory with Matter*, Phys. Rev. X **11**(4), 041008 (2021),  
1878 doi:[10.1103/PhysRevX.11.041008](https://doi.org/10.1103/PhysRevX.11.041008).
- 1879 [97] W.-T. Xu, F. Pollmann and M. Knap, *Critical behavior of the Fredenhagen-Marcu or-  
1880 der parameter at topological phase transitions*, doi:[10.48550/arXiv.2402.00127](https://doi.org/10.48550/arXiv.2402.00127) (2024),  
1881 [2402.00127](https://arxiv.org/abs/2402.00127).
- 1882 [98] R. Sachs, *Asymptotic Symmetries in Gravitational Theory*, Phys. Rev. **128**(6), 2851  
1883 (1962), doi:[10.1103/PhysRev.128.2851](https://doi.org/10.1103/PhysRev.128.2851).
- 1884 [99] A. Strominger, *Asymptotic symmetries of Yang-Mills theory*, J. High Energ. Phys. **2014**(7),  
1885 151 (2014), doi:[10.1007/JHEP07\(2014\)151](https://doi.org/10.1007/JHEP07(2014)151).
- 1886 [100] A. Strominger, *Lectures on the Infrared Structure of Gravity and Gauge Theory*,  
1887 doi:[10.48550/arXiv.1703.05448](https://doi.org/10.48550/arXiv.1703.05448) (2018), [1703.05448](https://arxiv.org/abs/1703.05448).
- 1888 [101] M. Henneaux and C. Troessaert, *Asymptotic symmetries of electromagnetism at spatial  
1889 infinity*, J. High Energ. Phys. **2018**(5), 137 (2018), doi:[10.1007/JHEP05\(2018\)137](https://doi.org/10.1007/JHEP05(2018)137).
- 1890 [102] E. Esmaeili, *Asymptotic symmetries of Maxwell theory in arbitrary dimensions at spatial  
1891 infinity*, J. High Energ. Phys. **2019**(10), 224 (2019), doi:[10.1007/JHEP10\(2019\)224](https://doi.org/10.1007/JHEP10(2019)224).
- 1892 [103] D. Harlow and H. Ooguri, *Symmetries in quantum field theory and quantum gravity*,  
1893 doi:[10.48550/arXiv.1810.05338](https://doi.org/10.48550/arXiv.1810.05338) (2019), [1810.05338](https://arxiv.org/abs/1810.05338).

- 1894 [104] M. Henneaux and C. Troessaert, *Asymptotic structure of a massless scalar field and*  
1895 *its dual two-form field at spatial infinity*, J. High Energ. Phys. **2019**(5), 147 (2019),  
1896 doi:[10.1007/JHEP05\(2019\)147](https://doi.org/10.1007/JHEP05(2019)147).
- 1897 [105] K. Prabhu and I. Shehzad, *Asymptotic symmetries and charges at spatial infinity in*  
1898 *general relativity*, Class. Quantum Grav. **37**(16), 165008 (2020), doi:[10.1088/1361-](https://doi.org/10.1088/1361-6382/ab954a)  
1899 [6382/ab954a](https://doi.org/10.1088/1361-6382/ab954a).
- 1900 [106] R. Tanzi and D. Giulini, *Asymptotic symmetries of scalar electrodynamics and of the*  
1901 *abelian Higgs model in Hamiltonian formulation*, J. High Energ. Phys. **2021**(8), 117  
1902 (2021), doi:[10.1007/JHEP08\(2021\)117](https://doi.org/10.1007/JHEP08(2021)117).
- 1903 [107] R. Tanzi, *Hamiltonian study of the asymptotic symmetries of gauge theories*,  
1904 doi:[10.48550/arXiv.2109.02350](https://doi.org/10.48550/arXiv.2109.02350) (2021), [2109.02350](https://arxiv.org/abs/2109.02350).
- 1905 [108] T. T. Dumitrescu and P.-S. Hsin, *Higgs-Confinement Transitions in QCD from Symmetry*  
1906 *Protected Topological Phases*, doi:[10.48550/arXiv.2312.16898](https://doi.org/10.48550/arXiv.2312.16898) (2024), [2312.16898](https://arxiv.org/abs/2312.16898).
- 1907 [109] H. Sueno, K. Ikeda and T.-C. Wei, *Bulk and boundary entanglement transitions in the*  
1908 *projective gauge-Higgs model*, doi:[10.48550/arXiv.2402.11738](https://doi.org/10.48550/arXiv.2402.11738) (2024), [2402.11738](https://arxiv.org/abs/2402.11738).
- 1909 [110] Y. Choi, Y. Sanghavi, S.-H. Shao and Y. Zheng, *Non-invertible and higher-form symmetries*  
1910 *in 2+1d lattice gauge theories*, doi:[10.48550/arXiv.2405.13105](https://doi.org/10.48550/arXiv.2405.13105) (2024), [2405.13105](https://arxiv.org/abs/2405.13105).
- 1911 [111] H. J. Briegel and R. Raussendorf, *Persistent Entanglement in Arrays of Interacting Parti-*  
1912 *cles*, Phys. Rev. Lett. **86**(5), 910 (2001), doi:[10.1103/PhysRevLett.86.910](https://doi.org/10.1103/PhysRevLett.86.910).
- 1913 [112] W. Son, L. Amico and V. Vedral, *Topological order in 1D Cluster state protected by sym-*  
1914 *metry*, Quantum Inf Process **11**(6), 1961 (2012), doi:[10.1007/s11128-011-0346-7](https://doi.org/10.1007/s11128-011-0346-7).
- 1915 [113] B. Yoshida, *Topological phases with generalized global symmetries*, Phys. Rev. B **93**(15),  
1916 155131 (2016), doi:[10.1103/PhysRevB.93.155131](https://doi.org/10.1103/PhysRevB.93.155131).
- 1917 [114] S. D. Pace, *Emergent generalized symmetries in ordered phases*,  
1918 doi:[10.48550/arXiv.2308.05730](https://doi.org/10.48550/arXiv.2308.05730) (2023), [2308.05730](https://arxiv.org/abs/2308.05730).
- 1919 [115] W.-T. Xu, M. Knap and F. Pollmann, *Entanglement of Gauge Theories: From the Toric Code*  
1920 *to the Z2 Lattice Gauge Higgs Model*, doi:[10.48550/arXiv.2311.16235](https://doi.org/10.48550/arXiv.2311.16235) (2023), [2311.](https://arxiv.org/abs/2311.16235)  
1921 [16235](https://arxiv.org/abs/2311.16235).
- 1922 [116] L. Bhardwaj, M. Bullimore, A. E. V. Ferrari and S. Schäfer-Nameki, *Anomalies of*  
1923 *generalized symmetries from solitonic defects*, SciPost Physics **16**(3), 087 (2024),  
1924 doi:[10.21468/SciPostPhys.16.3.087](https://doi.org/10.21468/SciPostPhys.16.3.087).
- 1925 [117] A. Hatcher, *Algebraic Topology*, Cambridge University Press (2002).